In presenting the dissertation as a partial fulfillment of the requirements for an advanced degree from the Georgia Institute of Technology, I agree that the Library of the Institute shall make it available for inspection and circulation in accordance with its regulations governing materials of this type. I agree that permission to copy from, or to publish from, this dissertation may be granted by the professor under whose direction it was written, or, in his absence, by the Dean of the Graduate Division when such copying or publication is solely for scholarly purposes and does not involve potential financial gain. It is understood that any copying from, or publication of, this dissertation which involves potential financial gain will not be allowed without written permission.

_____

3/17/65
b

NEEDLE CONTROL SYSTEM

FOR TUFTING MACHINERY

A THESIS

Presented to

The Faculty of the Graduate Division

by

Stanley Frederick Petry

In Partial Fulfillment

of the Requirements for the Degree

Doctor of Philosophy

in the School of Mechanical Engineering

Georgia Institute of Technology

November, 1966

NEEDLE CONTROL SYSTEM

FOR TUFTING MACHINERY

Approved:

Date approved by Chairman: Nov. 3, 1966

ACKNOWLEDGMENTS

The author dedicates this thesis to his wife, Toni, whose sacrifices and encouragement made it possible.

To Dr. Eugene Harrison, faculty advisor, the author expresses sincere gratitude for invaluable help. Through the efforts of Dr. Harrison, the project was begun; and with his creative guidance, the work progressed smoothly to a successful conclusion.

The author thanks Mr. Lewis Card for sponsoring the project. The advice and experience of Mr. Card and Mr. Joe Milburn were of particular value.

Recognition is certainly due a fellow student, Charles E. Willbanks, for his assistance during several phases of the project, and James G. Wright and Frank H. Speckhart were likewise helpful. Also, members of the staff of the School of Mechanical Engineering at Georgia Tech were very generous with their time and effort to help the author, especially Mrs. Whitt and Mr. Doyal. Others were Miss Wright, Mrs. Campbell, Mr. Cavalli, Mr. Davis, Mr. Grim, Professor Harrelson, Professor Foster, Mr. Kiebel, and Mr. Stokes.

Thanks also to the DuPont Company and its representative, Mr. Herrmann, for donating patterns used in several experiments.

And finally, the author expresses his appreciation to Dr. Roger P. Webb and Dr. John H. Murphy for their efforts as members of the thesis committee.

TABLE OF CONTENTS

Page

Page

LIST OF ILLUSTRATIONS

Page

Page

SUMMARY

The major objective of the reported research was the development of an improved needle control system for tufting machinery as used in the manufacture of bedspreads, rugs, and carpets.

Most current controlled-needle tufting machines impart a reciprocating motion to a bar in which many spring-loaded needle holders are contained. In various ways a pattern signal is converted into a means by which a needle holder is latched to the bar causing the corresponding needle(s) to sew. The contrast of sewing and not sewing through a backing material fashions a pattern in a piece of tufted goods.

The research was directed toward a class of machinery termed cut-pile, with a pattern attachment of the scroll type. The control system concept was to include single needle control, a feature which has been found relatively difficult to achieve and sustain at desirable speeds in the tufting industry. A nominal speed of 1,000 strokes per minute was to be achieved, a rate considerably higher than most comparable machines currently in use. Other factors taken into consideration during the project were such matters as

pattern cost, needle control system cost, average maintenance capability in tufting mills, yarn feed location, accommodation of existing cutting mechanism, and use of existing pattern design.

The initial phase of the study was concerned with evaluating the relative merit of pattern sensing concepts with regard to economic considerations and design restrictions imposed by existing equipment. Methods which were electrical, mechanical, hydraulic, vacuous, and pneumatic in nature were considered and the advantages and disadvantages of each were compared. The conclusion was reached that, of these, the pneumatic approach offered the greatest number of significant advantages despite attendant disadvantages. Air sensing systems are relatively inexpensive to manufacture, inexpensive to operate, and reliable. Minimum wear and low maintenance requirements are assets as well. Also, the disadvantages of pneumatic systems are generally less inherent and offer greater opportunity to minimize than the liabilities of most other systems adjudged.

Having elected to develop a pneumatic needle control system, concepts for specific components were considered. In view of the heavy suspension of lint particles in the atmosphere inside most tufting mills, methods were sought in which air intake from the

surroundings was avoided in order to minimize potential pluggage. Accordingly, a row of nozzles flowing air from a manifold was conceived as a means to sense a pattern. Each nozzle is tapped transversely such that blocking the mouth of the nozzle with a pattern creates a signal at the tap in the form of raised back-pressure. Such patterns can be formed by alternate raised and recessed areas of material passing in very close proximity to the mouths of the sensing nozzles.

Several means of pattern signal amplification were considered, including a type of ball amplifier and several fluidic devices such as the bistable, turbulence, and vortex amplifiers. A spool valve amplifier was chosen largely because the amount of amplification is relatively flexible, and the long and successful usage of spool valves in fluid systems provides a high degree of confidence for their use in the needle control system.

Latching the needle holders by converting the air power signals from the spool valves presented the final problem of conceptual evaluation. Cam action was rejected in favor of direct latching by means of small spring-loaded pistons which engage notches in the needle holders.

A mathematical model was derived to describe the behavior of

the control system for purposes of analysis. Separate sections of the system were defined and individual differential equations were written for each section.

One equation describes the behavior of the tap pressure in terms of the pattern position relative to the mouth of the sensing nozzle. Assuming a reversible adiabatic process, an expression was derived from the gas law, fundamental orifice equations for compressible flow, and geometrical relationships at the nozzle, resulting in a first order nonlinear differential equation.

In like manner, appropriate expressions were found for the spool valve pressure transfer function, transmission of pneumatic signals through small lines, and the movement of a spring-loaded spool and piston. The composite of these equations, in state variable representation, was used to formulate an overall mathematical model for the control system.

A computer program was written to solve the equations, permitting the variation of each significant pressure signal to be studied. Major purposes of mathematical modeling were to evaluate the time responses within the system as well as to study the effect of changing system parameters.

Initial experimental investigations were primarily concerned

with development of an optimum sensing nozzle configuration. An ordinary drilled hole was studied but the tap backpressure was found very sensitive to tap location, exit conditions, etc., making it difficult to produce numerous nozzles with essentially identical characteristics. This difficulty was overcome by placing an orifice at the entrance to the hole, and final tests were run to select the best base hole and orifice hole combination.

A commercial product was found from which patterns could readily be made by exposing a photosensitive material to ultraviolet light passing through a film negative of the chosen design.

Response measurements were made with the aid of a simulated pattern glued to the side of a gear which was driven at the proper speed. A micrometer nozzle adjustment permitted the test nozzles to be accurately positioned. Response measurements were initiated using a photocell pickup which triggered an oscilloscope signal, thus registering the output of a strain gauge pressure transducer upon a memory screen. In this manner the reliability of the response equations for system components was evaluated. The same physical arrangement was also used for experimentation to determine the sensitivity of the system with regard to pattern resolution.

In order to examine the effects of the continuous flexing of

tubing such as would occur at the connection of the latching pistons in the reciprocating drive bar, a cam action device was constructed and several kinds of tubing were subjected to multimillion cycle tests at more than 1,000 strokes per minute. Both nylon and vinyl tubing appeared entirely satisfactory in this service.

Finally, a machine was constructed to simulate the movement of an actual tufting machine using an eccentric and push rod from an existing machine. By adapting to this machine the various components conceived in the needle control system as developed during this research project, the operability of the complex was conclusively demonstrated.

NOMENCLATURE

A	amplitude of machine stroke, ft
A_o	orifice area, general
A1	cross-sectional area of transmission line, sq ft
A2	area of spool face, sq ft
A3	area of piston face, sq ft
AO1	area of orifice between manifold and base hole of sensing nozzle, sq ft
AO2	variable area of orifice at mouth of sensing nozzle, sq ft
AO3	variable area of orifice at manifold entrance to spool valve, sq ft
B1	spool damping coefficient, lb-sec/ft
B2	piston damping coefficient, lb-sec/ft
C	speed of sound, fps
C'	constant, general
C''	constant
C'''	constant
Cd	coefficient of discharge, general
C1	2.06 ^{o}R/sec
CD1	coefficient of discharge, orifice at manifold entrance to sensing nozzle
CD2	coefficient of discharge, orifice at mouth of sensing nozzle

CD3 coefficient of discharge, orifice at manifold entrance to spool valve

d displacement of needle holder from center of machine

$\ddot{d}$ $\frac{d^2d}{dt^2}$

DE density of air, slugs/ft-sec

f coefficient of friction

Ff static force of friction, lb

Fh force of retaining spring on needle holder, lb

Fn normal component of force on piston tip, lb

G gap between raised pattern surface and mouth of sensing nozzle, ft

g force of gravity, ft/sec^2

k polytropic exponent (i.e., for air)

K1 spool spring constant, lb/ft

K2 piston spring constant, lb/ft

Kh needle holder spring constant, lb/ft

L1 length of transmission line from sensing nozzle to spool valve, ft

L2 length of transmission line from spool valve to piston, ft

m mass, lb

$\dot{m}$ $\frac{dm}{dt}$

M1 mass of spool, slugs

M2	mass of piston, slugs
Mh	mass of needle holder, slugs
φ	angle of piston tip
ρ	density of air, slugs/ft-sec
P	force exerted by piston spring, lb
ΔP	pressure drop across orifice, general, psf
P(u)	signal input pressure at sensing nozzle, psfg*
$\dot{P}(u)$	$\frac{dP(u)}{dt}$
P(i)	initial pressure of P(u), psfg*
P(B)	pressure outside of sensing nozzle mouth, psfg*
P(1)	supply manifold pressure to sensing nozzles, psfg*
P(2)	pressure at end of transmission line to spool valve, psfg*
$\dot{P}(2)$	$\frac{dP(2)}{dt}$
$\ddot{P}(2)$	$\frac{d^2P(2)}{dt^2}$
P(3)	manifold supply pressure to spool valve, psfg*
P(4)	pressure downstream of spool valve, psfg*

*Depending on particular context, pressures may appear as gauge or absolute values as noted; however, for purposes of calculation in Appendix C, all pressure values are gauge.

$\dot{P}(4)$ $\frac{dP(4)}{dt}$

P(5) pressure at piston face, psfg*

$\dot{P}(5)$ $\frac{dP(5)}{dt}$

$\ddot{P}(5)$ $\frac{d^2P(5)}{dt^2}$

Q flow through orifice, general

R gas constant, ft/^{o}R

R frictional resistance of transmission line, lb-sec/ft^4

RN radius of base hole of sensing nozzle, ft

RO radius of supply pressure hole to spool valve, ft

S1 damping ratio of first transmission line

S2 damping ratio of second transmission line

t independent variable time, sec

T temperature, ^{o}R

T(i) initial temperature, ^{o}R

U dynamic viscosity of air, slugs/ft-sec

v specific volume, general, cu ft/lb

V volume, general, cu ft

VF volume of second transmission line plus entrance to piston, cu ft

---

*See footnote on previous page.

VP	variable terminal volume at piston, cu ft
VS	variable terminal volume at spool, cu ft
VT	volume of first transmission line plus entrance to piston, cu ft
ω	frequency, radians/sec
W	weight rate of flow, general, lb/sec
ΔW	difference in flow rates W1 and W2, lb/sec
W1	weight rate of flow through orifice at manifold entrance to sensing nozzle, lb/sec
W2	weight rate of flow through mouth of sensing nozzle, lb/sec
WN1	undamped natural frequency, first transmission line
WN2	undamped natural frequency, second transmission line
x	pattern displacement, ft
$\dot{x}$	$\frac{dx}{dt}$
X( )	state variable
$\dot{X}$( )	$\frac{dX(\ )}{dt}$
y	piston displacement, ft
$\dot{y}$	$\frac{dy}{dt}$
$\ddot{y}$	$\frac{d^2y}{dt^2}$
y(0)	initial piston spring compression, ft
y(t)	piston spring compression as a function of time, ft

Y	orifice expansion factor, general
z	spool displacement, ft
$\dot{z}$	$\frac{dz}{dt}$
$\ddot{z}$	$\frac{d^2z}{dt^2}$

CHAPTER I

INTRODUCTION

History and Background

The tufting industry has expanded rapidly in recent years to meet demands for such tufted products as bedspreads, rugs, and carpets. Beasley (1) describes the phenomenal growth of this industry.

For some thirty-five years until the early 1930's, tufting was accomplished entirely by hand in a so-called "cottage industry." Hand tufted bedspreads, gowns and housecoats were sold to southeastern tourists at roadside stands and shipped to department stores throughout the country.

Early tufting machines essentially were modified sewing machines, followed by multiple needle equipment to add versatility. Just prior to World War II, the first coarse-gauge machines were created to produce a complete tufted bedspread in a single pass. After considerable evolution the highly significant controlled-needle bedspread machine was invented. In 1950 and 1951, machines were introduced which could produce broadloom carpet, ushering in a tufted carpet industry which has progressed very rapidly.

In much tufting machinery now in use, an eccentric drive imparts reciprocating motion to a bar which spans the entire width of the tufted article being produced. Many needle holders are housed through the bar, and each can be separately latched to move with the bar and cause the corresponding needle(s) to sew through a moving backing material. Springs restrain unlatched needle holders to prevent sewing. By exercising control over the latching mechanisms, patterns can be created in a backing material from the contrast between areas sewn and not sewn.

Tufting machines may be divided into two broad categories, cut-pile and loop-pile machines, the obvious difference being that the loops are cut in the first-named machine. A cross section of a cut-pile tufting machine is shown in Figure 1. Controlled-needle machines may be further classified according to the pattern attachment used, some of which are called the roll type, the universal-type, the scroll-type, and the slat-type. (This research project is concerned only with cut-pile controlled-needle machines having a scroll pattern attachment. In context, a scroll refers to the surface of a drum upon which a pattern is created such that a machine can interpret and reproduce it.)

Among cut-pile, scroll-pattern tufting machines developed by

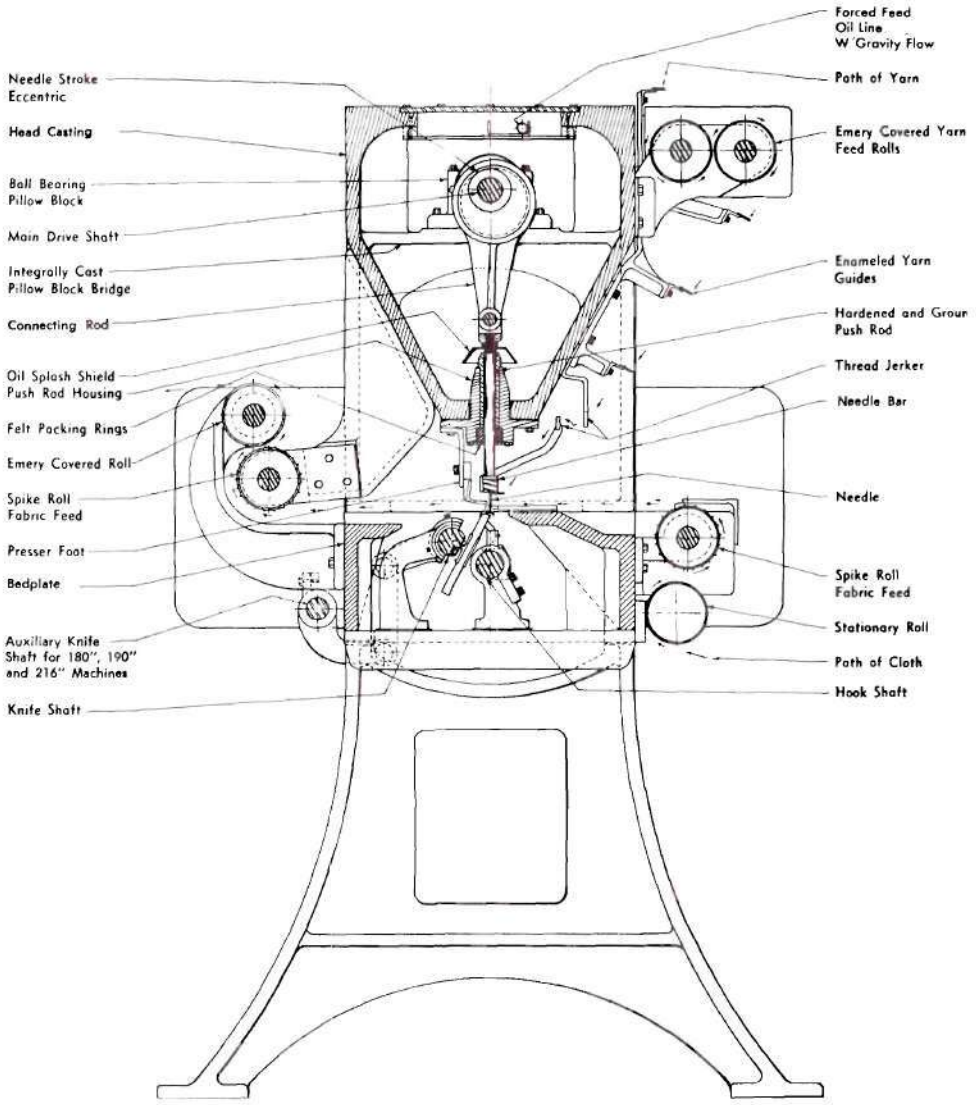

Figure 1. Cross Section of a Cut-pile Tufting Machine (1).

1966, two concepts have gained prominence in use. The pattern used in the first of these concepts is a phenolic drum into which grooves have been machined. High and low places in each groove correspond to a given pattern design. Fingers--one for each groove--ride on the rotating drum to close and open electrical contacts. The contacts actuate solenoids which move latch pins to engage or release needle holders as described above. Patterns are ordinarily symmetrical such that one pattern groove will exercise control over two or more needle holders. A ratchet device enables each needle to draw an appropriate length of yarn for each stitch.

The second kind of cut-pile, scroll-pattern tufting machine now in favor operates in similar fashion except that the drum is made of transparent material with a light source inside. The pattern is a photographic positive (or direct drawing) wrapped around the drum. The opaque sections of the positive prevent the internal light from shining through to photocell sensors, which serve the same function as the pattern fingers in the first machine. The very low current generated by the photocells is greatly amplified in order to control relay contacts which actuate solenoids as before.

Each of the machines described has distinct disadvantages. Phenolic drum patterns are expensive in the case of the first

machine, and the electrical contacts are difficult to maintain. Amplification problems occur in the other machine due to low level signals from the photocells. Also the second machine is relatively expensive and specialized maintenance personnel are necessary. Solenoid space limitations are a problem common to both machines. A need exists to examine avenues of potential improvement in order to develop tufting machinery in which such undesirable features are minimized.

Project Definition

The research effort for this project was confined to that area of a cut-pile, scroll-pattern tufting machine that is concerned with the pattern itself, pattern detection, pattern signal amplification and needle holder engagement--an area hereafter called the needle control system. Existing machine framework, feed drives, power drives and eccentrics, tuft cutting facilities, and the like are expressly excluded from consideration herein, except as it is necessary for innovations in the area of concern to accommodate restrictions imposed by existing equipment not specifically within the scope of study.

The project objectives included not only the development of a needle control system which minimizes certain disadvantages of

existing tufting machines but also the provision of another feature, that of individual needle control. Previous efforts at single needle control have not proven entirely satisfactory, such that most existing machines exercise control over individual needle holders (see Figure 2) containing two needles normally spaced on 3/16 in.

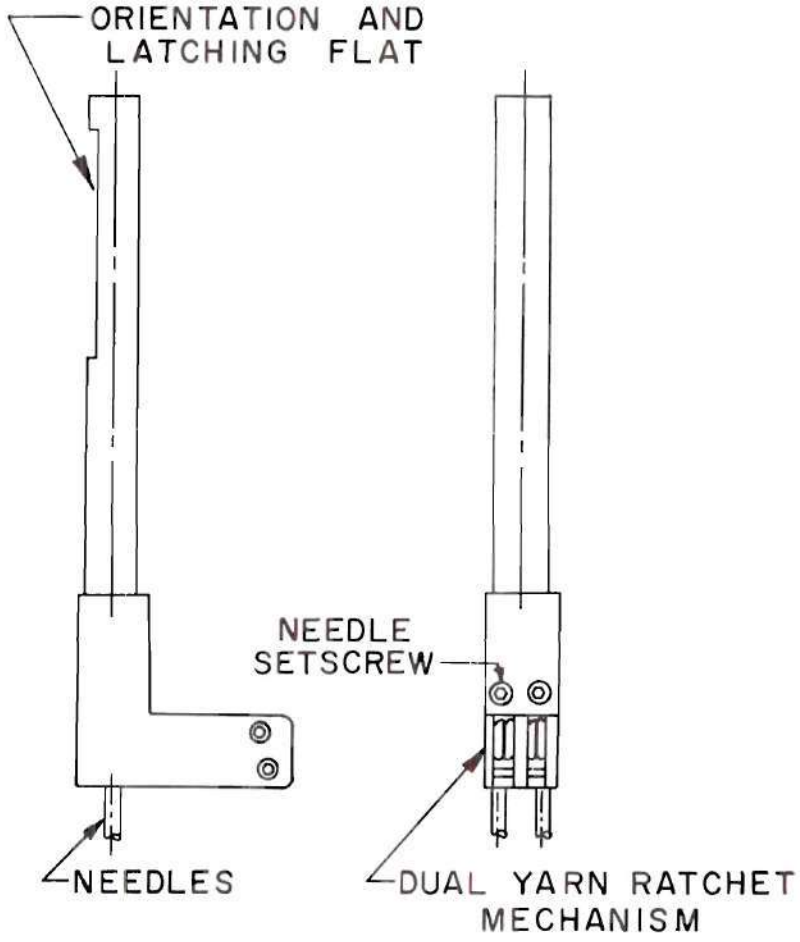

Figure 2. Needle Holder.

centers. Thus, if a pattern design were to call for tufting a diagonal line, the best approximation that could be achieved would be a "staircase" with a run of 3/8 in. By controlling each needle individually--that is, by housing only one needle in each holder--a machine can produce a tufting pattern with much finer design resolution. Of course, physical limitations severely restrict the size of the needle holder and latching mechanism and pose a difficult orientation problem; however, the objective of this work was to provide individual needle holders and to retain the present 3/16 in. needle spacing if possible (7/32 in. maximum).

Other physical criteria also constrained the needle control system development. The needles could not be staggered in order to gain space, because the existing cutting facilities could only accommodate needles in a straight row. For similar reasons, yarn could be fed to needles from one side of the machine only. The amplitude of the needle stroke remained 7/8 in., but the nominal machine speed was to be increased to 1,000 strokes per minute, more than doubling that of one machine now used extensively. Ten stitches per inch was a design guide, and no less than three consecutive tufts was considered in possible pattern designs.

Factors of an economic and commercial nature also influenced the research, although absolute cost criteria naturally depended

upon performance in several areas. In general it was desirable to limit the separate cost of the needle control system as previously described to approximately $30,000 in order that the machine would be favorably competitive with most recent machines. Also, the cost of an individual pattern was to be well below that of a grooved phenolic drum (about $300).

Other less tangible considerations influenced various decisions throughout the project. For example, previous unfavorable experience with a concept already tried unsuccessfully in the industry would obviously limit the marketability of a similar concept, regardless of its merit otherwise. An arrangement necessitating synchronization of the pattern position with the machine drive would normally be much less desirable than a scheme without such a restriction. Also, in view of the relatively unskilled technicians available, particularly in some tufting mills, advantages that might accrue from more complex approaches can easily be outweighed by the resulting change in maintenance requirements.

Finally, in order that the myriad of pattern designs now in existence could be readily converted for use with the new control system, the conventional (half) choice of pattern scale was specified. In addition, only pattern designs which were symmetrical

about the center of the machine were to be used. The significance of the latter specification is found in the need to sense a folded pattern (i.e., half of a pattern) and to convert one pattern signal into a means of controlling two symmetrically placed needles.

CHAPTER II

EVALUATION OF CONCEPTS

Pattern Sensing

A good measure of the potential success of the project depended upon the initial approach. In order to select the most advantageous concept for a needle control system within the restrictions imposed by the project definition, a number of alternative methods were considered. Early studies were largely confined to examination of various pattern sensing techniques (2), because the means for sensing a pattern determines the course of development of other elements in the control system.

Electric Sensing

In view of widespread utilization of electrical methods for pattern sensing in other fields, several electrical concepts were evaluated.

Direct Contact Sensing. One means of electrical sensing is shown in Figure 3. A grounded metal drum is covered with a perforated pattern of insulating material. As the drum turns the spring-loaded brushes make contact through perforations, completing

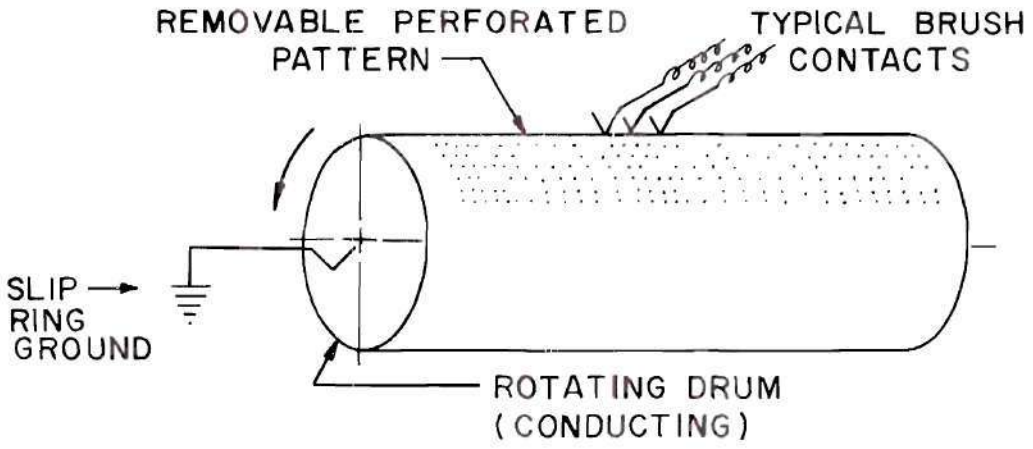

Figure 3. Direct Contact Sensing.

electrical circuits.

Direct contact sensing is very simple and relatively inexpensive. Pattern costs are also small; however, pattern life is short from friction wear as well as destruction from arcing. This concept has already been tried in the tufting industry, leaving unfavorable experience particularly with regard to maintaining electrical contact between the brushes and the drum.

Photoelectric Sensing. Another method of electrical sensing makes use of photocells as shown in Figure 4. In fact, this form of sensing is one of the two described in Chapter I that are now extensively in use. Even so, the concept was reconsidered with the idea of improving the existing systems by using light sensitive resistivity elements in circuits containing silicon controlled rectifiers.

Photoelectric sensing is now familiar in the industry, and the

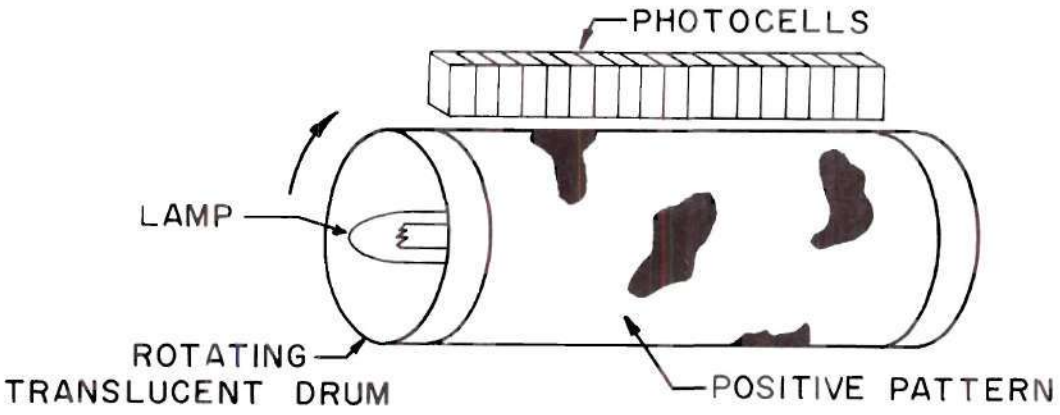

Figure 4. Photoelectric Sensing.

positive patterns are relatively inexpensive and not subject to wear. Conversely, a photoelectric sensing system is expensive, requiring low level signal amplification and specialized service attention.

Hot Wire Anemometer Sensing. A hot wire anemometer (3) means of electrical sensing appears in Figure 5. Here, air is pulled (or forced) through a given pattern perforation past a resistance wire heated by an electric current, causing a change in current through the wire. This, of course, is the same principle used in measuring air flow through ducts except the calibration requirements are much less stringent.

Advantages of hot wire anemometer sensing are high frequency response and an inexpensive pattern subject to very little wear. Disadvantages are the delicate circuitry in confined spaces, the need to

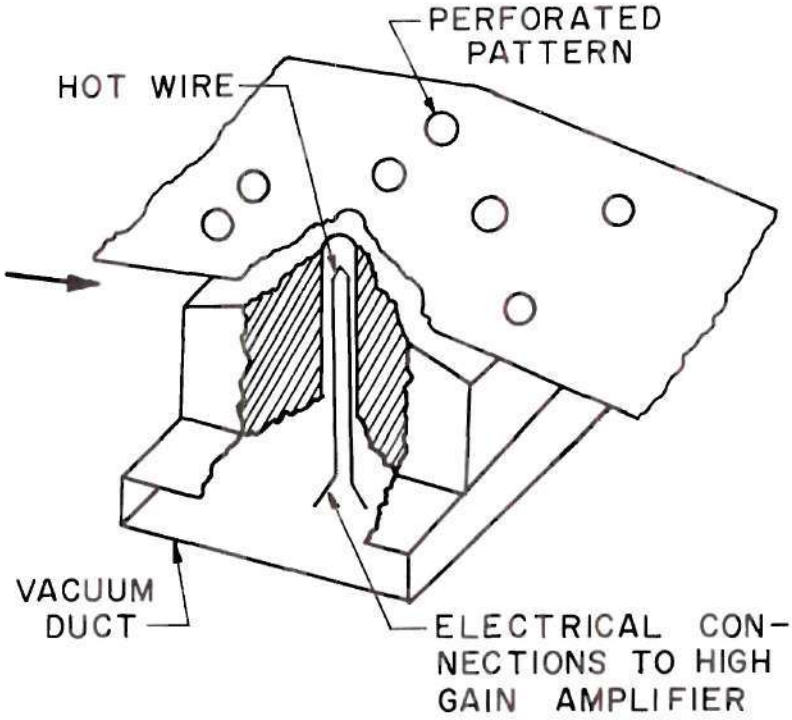

Figure 5. Hot Wire Anemometer Sensing.

amplify low level signals, the expensiveness of the system, the specialized maintenance requirement, and the necessity to provide both pneumatic and electrical circuitry.

Hydraulic Sensing

A partially hydraulic means of pattern sensing is sketched in Figure 6. Again a pattern perforated according to design passes over a sensing block in which spring-loaded plungers are placed in correspondence to the rows of pattern holes. The ends of lengths of fluid-filled tubing are aligned with the plungers in very close proximity to the moving pattern. The plungers can pass through the

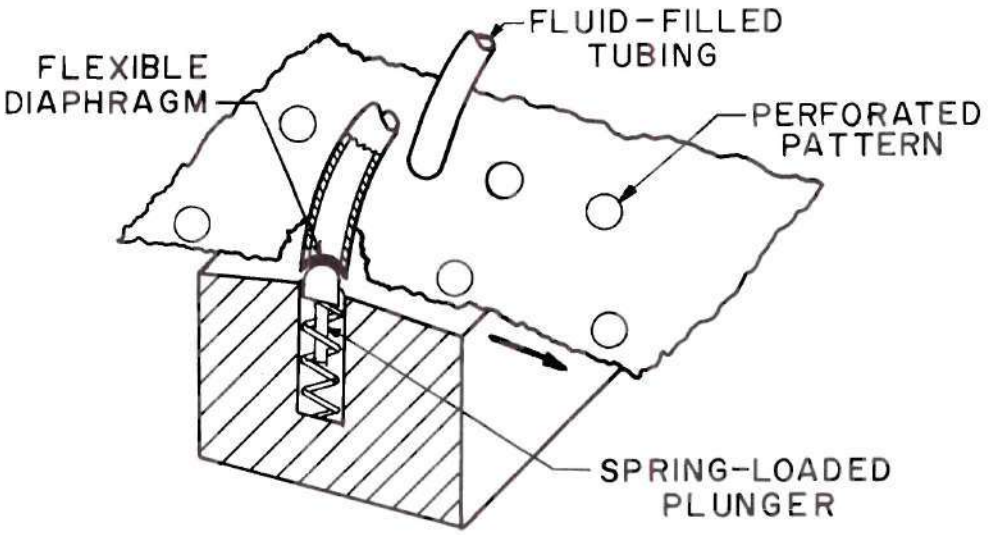

Figure 6. Hydraulic Sensing.

pattern holes and depress the diaphragms covering the tubing ends, causing the corresponding diaphragms at the tubing ends not shown to project outward in a manner that could be converted to some form of mechanical needle control.

The benefits of the semihydraulic sensing arrangement outlined above are the moderate cost both for the system and the pattern, the direct transmission of pattern signals, and the unskilled maintenance requirements. Liabilities envisioned are the sealing and containment of fluid in the lines, potentially troublesome temperature effects from tubing expansion, excessive pattern wear, and possible diaphragm problems.

Mechanical Sensing

A mechanical linkage form of pattern sensing is pictured in Figure 7. The principle employed is very similar to that in the

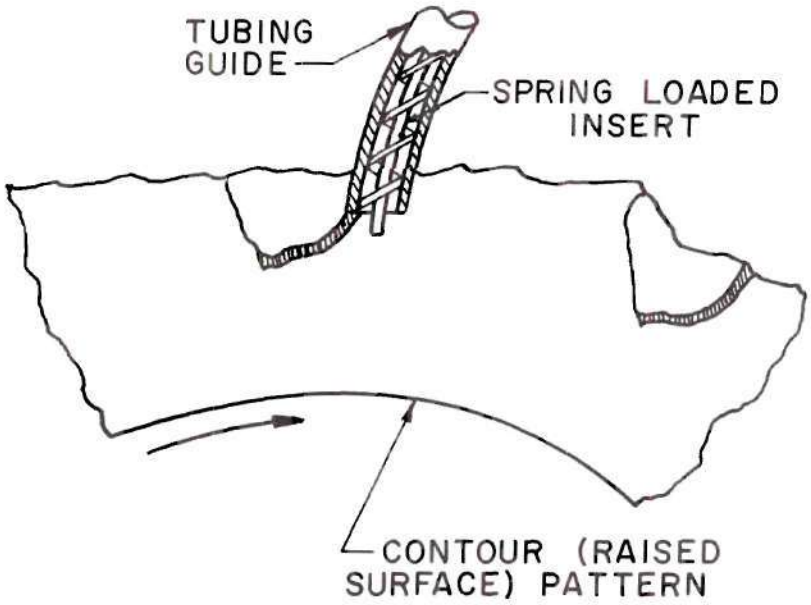

Figure 7. Mechanical Sensing.

hydraulic technique. In this case flexible inserts are spring-loaded in the tubing run with the tapered tip (taper not shown) positioned very near the recessed surface of a contour pattern. As a raised pattern surface passes the mouth of a sensing tube, the insert is forced to retract such that it will extend at the opposite end of the tube to effect needle control through some form of cam action.

Although such a mechanical system is direct, simple, and

relatively inexpensive, using a comparatively inexpensive pattern and demanding inexpert service attention only; synchronization of the pattern travel with needle movement would be almost mandatory, pattern wear could be excessive, and precise tolerances would be necessary and difficult to sustain.

Vacuum Sensing

A typical pattern sensor applying a vacuum source is illustrated in Figure 8. The drawing may be recognized as the design

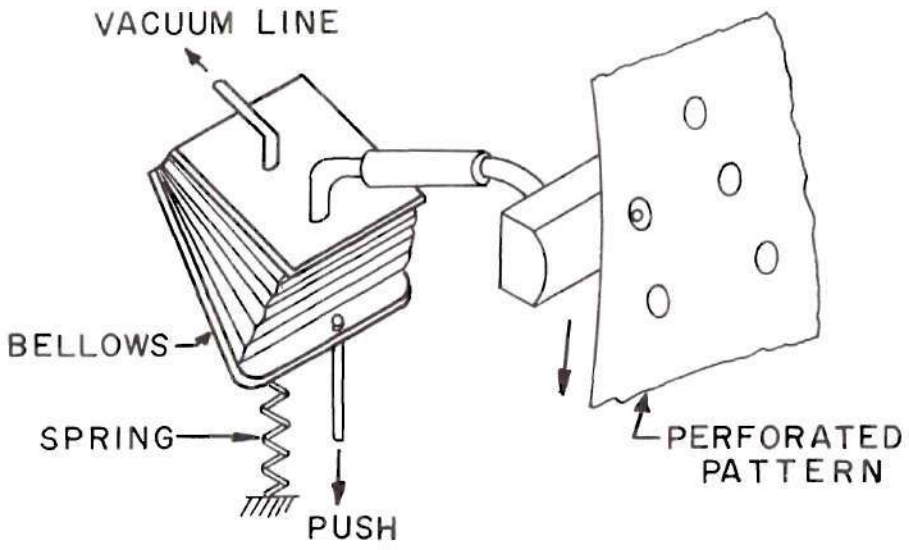

Figure 8. Vacuum Sensing.

commonly used in the player piano. A perforated pattern traverses the mouths of a row of tubes upon which a vacuum is being drawn through bellows. A hole in the pattern vents a given line and

causes the bellows to expand and physically displace a push rod. The rod movement can be transformed into a latching operation.

A vacuum design of this kind is very simple, making use of a low cost pattern subjected to slight wear. The response of the system is relatively slow, however, and the nature of a vacuum scheme introduces additional potential of fouling from an atmosphere heavily laden with lint particles. In addition, effective location of the bellows would be difficult within the space limitations defined in this project.

Pneumatic Sensing

Several direct ways to sense patterns pneumatically were considered and dismissed in favor of an indirect approach represented in Figure 9. The major determinant in the selection was elimination of system fouling from the air intake. As shown in the sketch, air from a pressure manifold flows out of a drilled hole nozzle which has been tapped transversely. As a raised surface of the pattern passes close to the mouth of the nozzle (4, 5), flow is restricted and the backpressure rises in the side tap, thus creating a pattern signal. Since air flows continually out of the sensing configuration, potential pluggage is minimized. Several pattern structures were conceived for possible use with the system

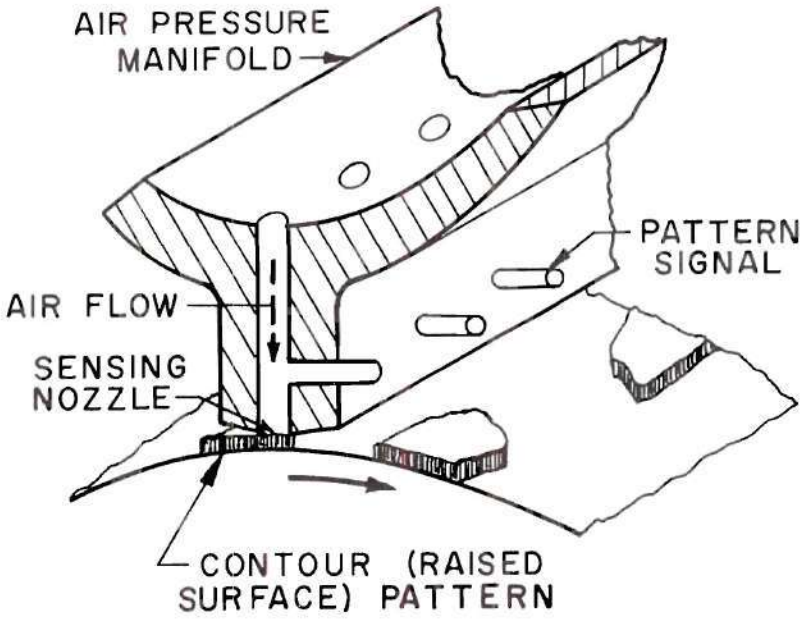

Figure 9. Pneumatic Sensing.

shown--one being a screen material with a pattern formed by blocking or filling appropriate areas of screen mesh--but considerations of pattern wear made the contour pattern preferable.

Plus factors of the choice of pneumatic pattern sensing are low cost patterns, inexpensive system components, absence of appreciable wear of either the system or the pattern, and of particular importance, the adaptability of this scheme to reliable and inexpensive signal amplification techniques. Negative factors are the close tolerances required between the pattern and nozzles, possible high consumption of air, and potential signal transient troubles.

Judicious comparison of the foregoing methods of pattern

sensing within the prescribed project framework led to the conclusion that the economic advantages and versatility promised by development of a pneumatic needle control system clearly outweighed the merits of the other concepts. Furthermore, the disadvantages of the air pressure approach also appeared less inherent and therefore more likely to be alleviated. Accordingly, investigation was begun to evaluate possible avenues for amplifying the pneumatic pattern signals.

Signal Amplification

Fluid Amplifiers

Since the 1960 announcements by the Diamond Ordnance Fuze Laboratories regarding fluid amplification, interest in fluid amplifiers has grown very rapidly. As a result, considerable research is now taking place in this area. A survey of the literature concerning fluidic devices (6, 7, 8, 9, 10, 11) revealed a number of plausible approaches to amplification of pneumatic signals. A brief description and evaluation of several of these devices is given in Appendix A.

In general, a control system using fluid amplifiers would be relatively inexpensive to manufacture, would be virtually free of wear, and would utilize inexpensive patterns which in turn would

be subjected to little or no wear. Potential liabilities of such a system are possible high air consumption, fouling from the atmosphere, and transient problems (particularly in staging concepts).

Use of fluid amplifiers in this project as a first approach was rejected for the following reasons:

1. Although a great deal of research has already been conducted toward the development of amplifiers which might well be useful in this application, proprietary interests apparently have resulted in specific design specifications and related information being omitted in the literature. Therefore considerable experimentation would be necessary just to achieve reasonable duplication of existing knowledge.
2. There is no assurance that a fluid amplifier unit is the best choice of pneumatic system, particularly in view of other potential solutions that have not been investigated.

Ball Amplifier

A very simple device which can be used for air signal amplification is the ball amplifier (12) shown in Figure 10. An unbalanced force will cause the balls to shift in the confined space.

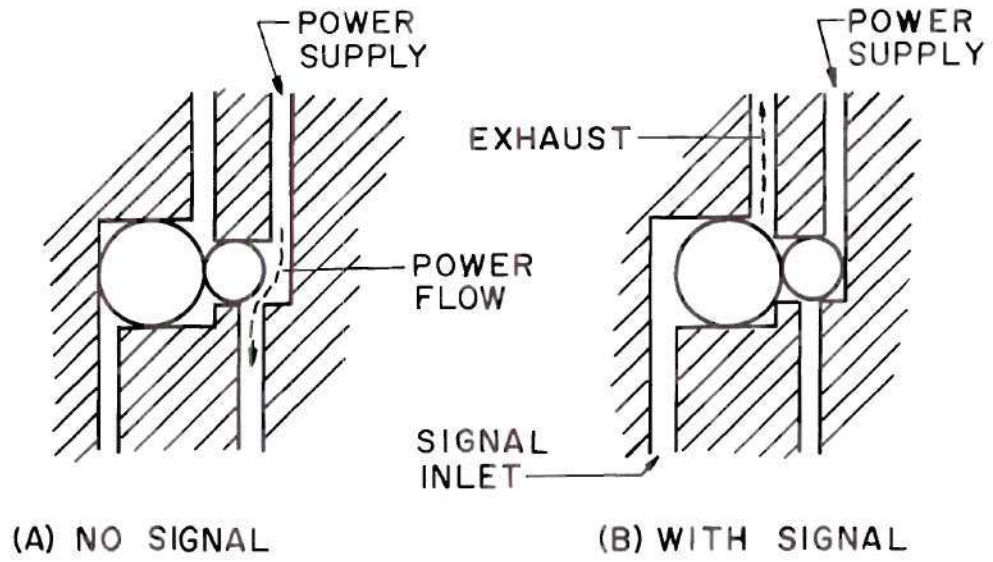

Figure 10. Ball Amplifier.

With no signal applied as in (A), the power supply is transmitted past the smaller ball into the lower port. A signal pressure somewhat smaller than the power supply will, when applied to the projected area of the larger ball, cause the balls to shift into the position (B), thus blocking the power supply and venting any trapped pressure at the same time.

Such an amplifier is easy to manufacture and inexpensive. Ball diameters of from 1/16 to 3/8 in. can readily be used with supply pressures from fractions of 1 psig to 100 psig. Response frequencies above 500 switches per second have been observed. Yet physical limitations make it difficult to use a ratio of ball diameters greater than two to one, meaning that a maximum amplifica-

tion of four is obtainable from the device (unless the air power supply is cycled). While this degree of amplification may be adequate for the pneumatic control system, very little safety factor could be incorporated in the design.

Spool Valve

Another way to amplify a pneumatic signal makes use of a conventional spool valve construction as drawn in Figure 11. Here, an air pressure signal will displace the spool to the right against the spring force until the supply pressure ports are uncovered (and the exhaust ports are blocked), allowing the supply air to flow through the valve and out of the transmission ports. In most applications, spool valves (13) must be very accurately made in order to limit leakage, and close tolerances result in expensive manufacturing costs. But for use in the control system for a tufting machine, where minor air leakage is not of great concern as long as the valve functions properly, a spool valve of less than ordinary tolerance specifications would be entirely satisfactory.

An important asset of the spool valve is found in the variable amplification ratio that can be achieved if desired. Except for the indirect flow force exerted by the supply air, the mass of the spool and the spring constant (and friction) are all

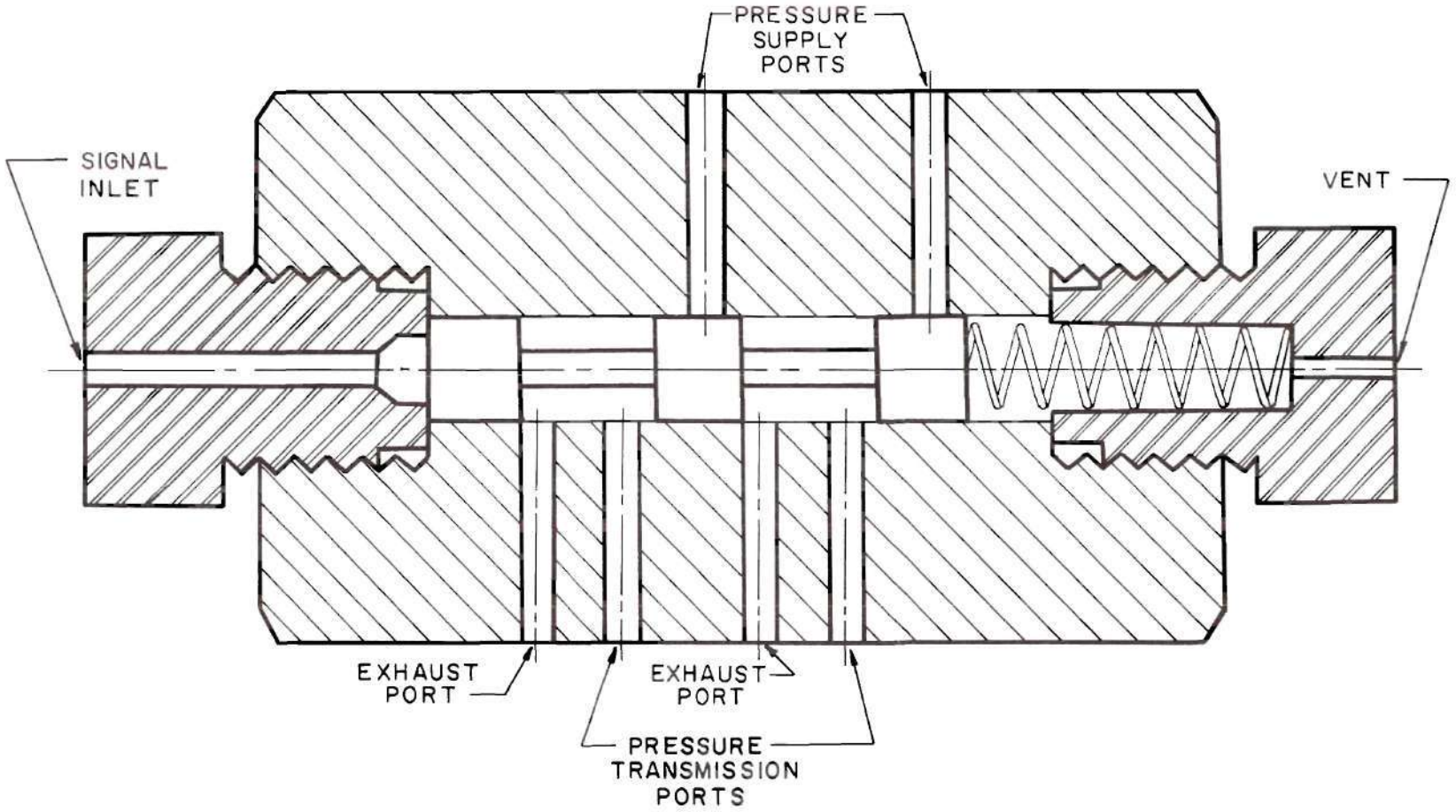

Figure 11. Spool Valve Assembly.

that limit the pressure level that can be accommodated at the supply ports, even though the signal pressure may be relatively small. As a result of this versatile feature, a safety factor could automatically be incorporated in a system which uses spool valve amplification, because the supply pressure can be increased if needed. Also, as illustrated in Figure 11, the spool valve lends itself readily to division of one pattern signal into several power signals with which to accomplish needle control. Chiefly for the reasons just given, the spool valve approach was selected over the other methods of signal amplification described. When comparing other characteristics the spool valve consumes less air than all except the ball amplifier, is less subject to transients, receives more wear although not a great deal, and is more expensive but still relatively low in cost.

At this point of the evaluation procedure, it was decided to pursue development of a control system for tufting machinery which employed a pneumatic pattern sensing scheme with a spool valve signal amplifier. There remained the means of needle engagement to be conceived.

Needle Engagement

In order to fully comprehend the context in which arrange-

ments for controlling the tufting needles were analyzed, it is helpful to understand that the orientation of the needles is critical and that deviation from proper orientation will result in needle and/or cutting hook destruction. In the tufting machine using the needle holder pictured in Figure 2, a metal edge riding in the flat maintains the orientation of the holder and needles. The lower recess lip of the same flat serves to latch the needle holder to the drive bar by means of a pin thrust against the flat by solenoid action.

In view of the single needle control feature to be included in the system as well as the restriction preventing staggering of needles, a scale-down version of the holder of Figure 2 would not be satisfactory, because not enough flat surface could be machined on the smaller diameter shank for orientation purposes and the edge of the flat would not be deep enough for latching. So, the decision was reached to make the needle holders rectangular in cross section to pass in a conforming slot, eliminating the problem of orientation and providing bulk for latching reasons. Of course, holes are easier to drill than slots are to machine, but it was believed that the rectangular holder and slot arrangement would have less critical wear restrictions than the flat on existing holders and that longer

life would be a fortunate consequence.

Before deciding upon a specific mechanism with which to engage the needle holder, attention should also be given to the timing aspect of engagement. It is imperative that the needle travel the full stroke of the drive bar, or not enter the cutting zone at all, because--as with misoriented needles--needles at improper elevation also cause breakage. In effect, this restriction means that needle engagement can only be effected near the top of the drive bar stroke. Also, if a positive method of engagement such as direct cam action were employed, some means of synchronization of the pattern signals with the position of the drive bar would be necessitated. It is desirable, of course, to avoid such timing constraints if feasible.

Several pursuits to the problem of latching a needle holder to the drive bar were considered in which various forms of indirect cam action produced the engagement. Still, such approaches required conversion of the pneumatic power signal from the spool valve into some means of cam actuation. The possibility of directly converting the pneumatic signal to a latching operation by means of a spring-loaded piston was then considered, which emphasized problems associated with the 3/16 in. needle spacing.

For the advantages of simplicity, the approach finally selected was direct as illustrated by Figure 12. The inlet power signal from the spool valve displaces the spring-loaded plunger into a notch in the needle holder in order to latch the holder to the drive bar. The piston tip is also notched in conformance with the needle holder recess to prevent disengagement during a tufting stroke. A restraining spring on the holder insures that contact is maintained at the notch. A cast iron striking bar stops the holder near the top of the stroke to allow the piston tip to be released or inserted into the notch. Aside from being inexpensive and long-lasting, cast iron was chosen for the striking bar primarily because of its high damping capacity (14) in order to minimize the potential bouncing action as the needle holder hits the bar. The spacing problem is solved by staggering the piston assemblies (and corresponding needle holder notches) on 3/8 in. centers. Note that no synchronization restrictions are placed on the pattern signal with the arrangement employed in Figure 12. A signal may begin or end at any time during a stroke, but the engagement or release of a needle holder can take place only once during a stroke cycle--at the top position of the drive bar.

Finally, after examining and evaluating a number of alterna-

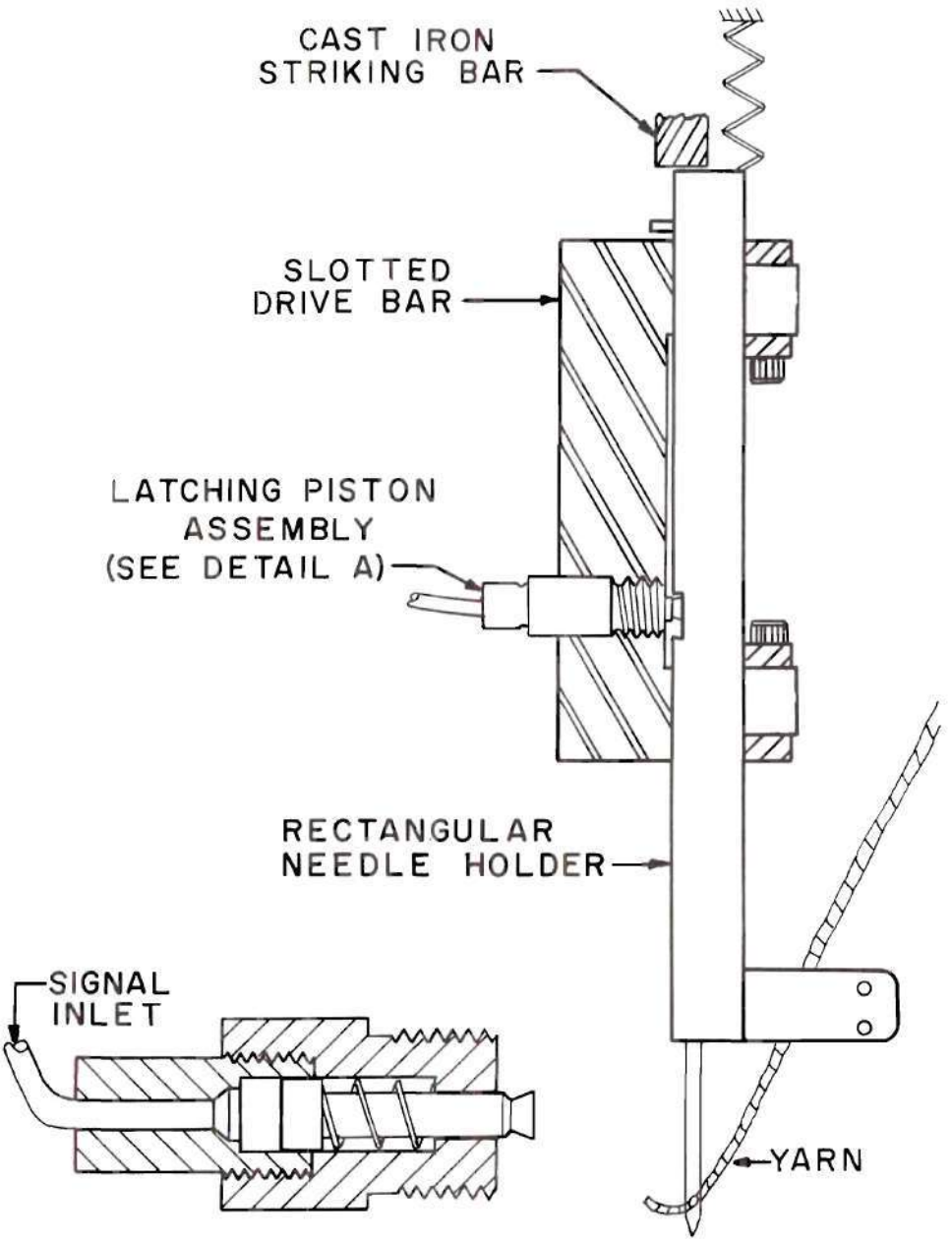

Figure 12. Needle Engagement.

tive approaches to pattern sensing, signal amplification and needle engagement, an overall concept for a needle control system emerged as represented in Figure 13. A raised-surface contour pattern creates a pressure signal as it restricts the mouth of a sensing nozzle. The transmitted pressure signal opens a spool valve admitting two power signals to latching pistons positioned symmetrically from the center of the needle drive bar.

There remained the analytical and experimental investigations needed to develop a specific system within the framework of Figure 13 and to substantiate the success of the development.

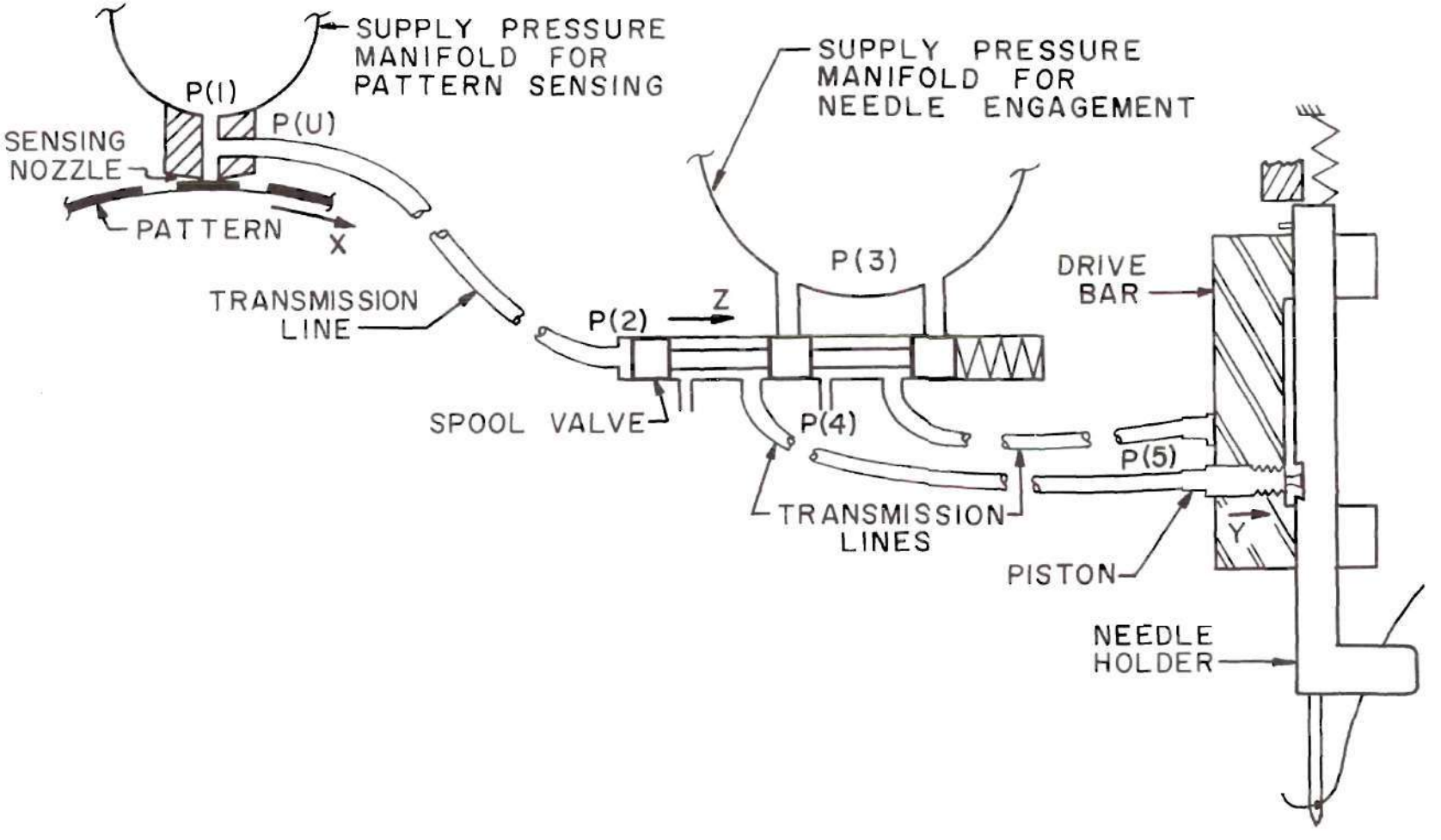

Figure 13. Schematic Diagram of Needle Control System.

CHAPTER III

EXPERIMENTAL INVESTIGATIONS

Nozzle Development

Most experimental testing for the project was intended to verify some phase of mathematical analysis or to confirm the functional success of a concept. However, mathematical analysis of the sensing nozzle (see Chapter IV) took place concurrently with the experimental work. In fact, nozzle testing was largely guided by a study of parameter effects during development of a mathematical model for the system. Thus, the selective tests made during nozzle development were an integral part of the analysis leading to the final nozzle choice.

In the beginning the nozzle concept was that of a simple drilled hole tapped transversely as shown in Figure 9. The obvious points of question concerned the diameter and length of the base hole and the position of the tap. Neglecting for the moment less fundamental factors, the basic criteria upon which to judge nozzle performance were the extent that signals to sew and not to sew were distinguishable and the reproducibility of results. With these

essential requirements in mind, experiments to examine nozzle characteristics were begun.

The basic manifold used for most of the static nozzle tests is illustrated in Figure 14. Air is supplied into the trunk of the manifold which opens into a plenum behind a removable face plate. Test holes can then be drilled around the periphery of the face plate as desired. An adjustable blocking bar is positioned a known distance away from the mouth of a test nozzle by shim washers as shown. In this manner the blocking bar simulates a stationary pattern. In practice, it was necessary to verify the gap at the nozzle mouth with a feeler gauge and to make shim adjustments accordingly. A picture of the nozzle testing apparatus used is shown in Figure 15.

The first series of tests were made simply to measure the tap backpressure characteristics for seven distinct nozzle configurations as the gap between a nozzle mouth and the blocking bar increases from closed to 0.010 in. The different nozzle arrangements and their resulting characteristic curves are drawn in Figure 16. A gauge manifold pressure of 4 in. Hg was chosen for convenience. The first three nozzles shown were compared in the initial test. Tapping close to the mouth as in nozzle 1 produces a sig-

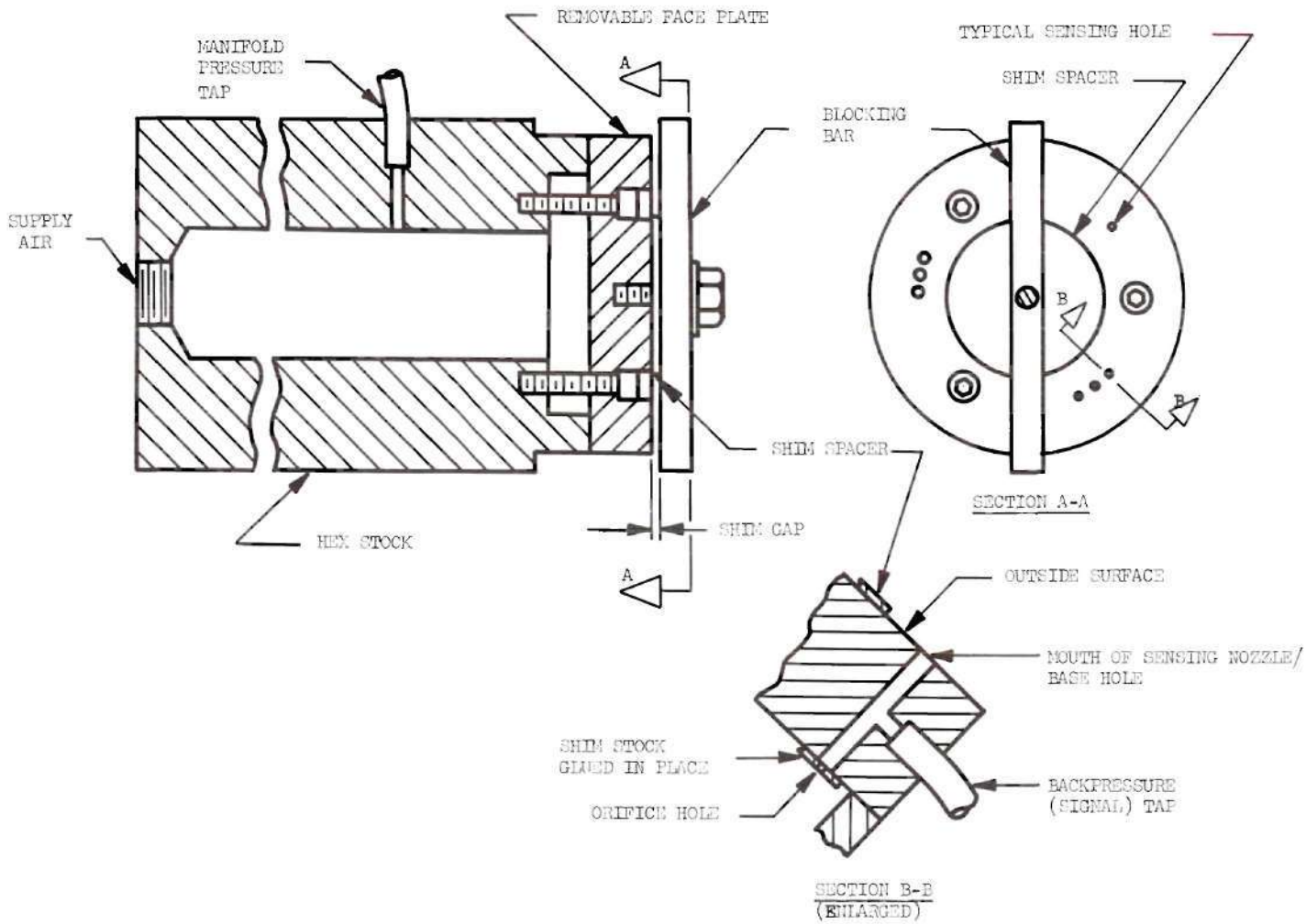

Figure 14. Test Manifold.

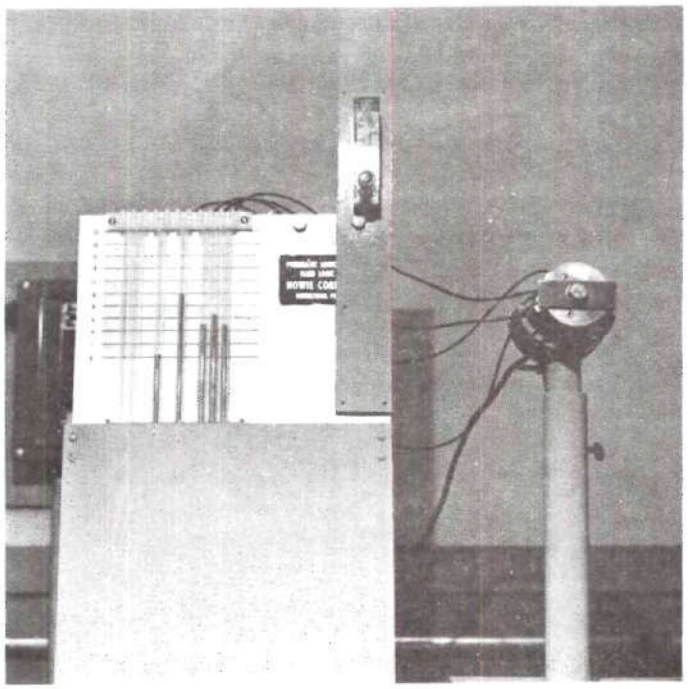

Figure 15. Nozzle Testing Apparatus.

nificantly greater contrast between a blocked (i.e., small gap) and an open nozzle than does tapping near the manifold plenum as in nozzle 3. From Figure 16 it is apparent that the smaller 0.031 in. base hole of nozzle 2 is better yet. A factor (not shown) that became evident in several early efforts to make the first three nozzles was the effect of the drill sharpness on the performance curves. This variation together with the critical tap location foretold problems in manufacturing numerous nozzles of this general type having essentially the same behavior in use. In addition, test results not given demonstrated that base hole exit conditions also affect the characteristic curves of nozzles made as in examples 1, 2,

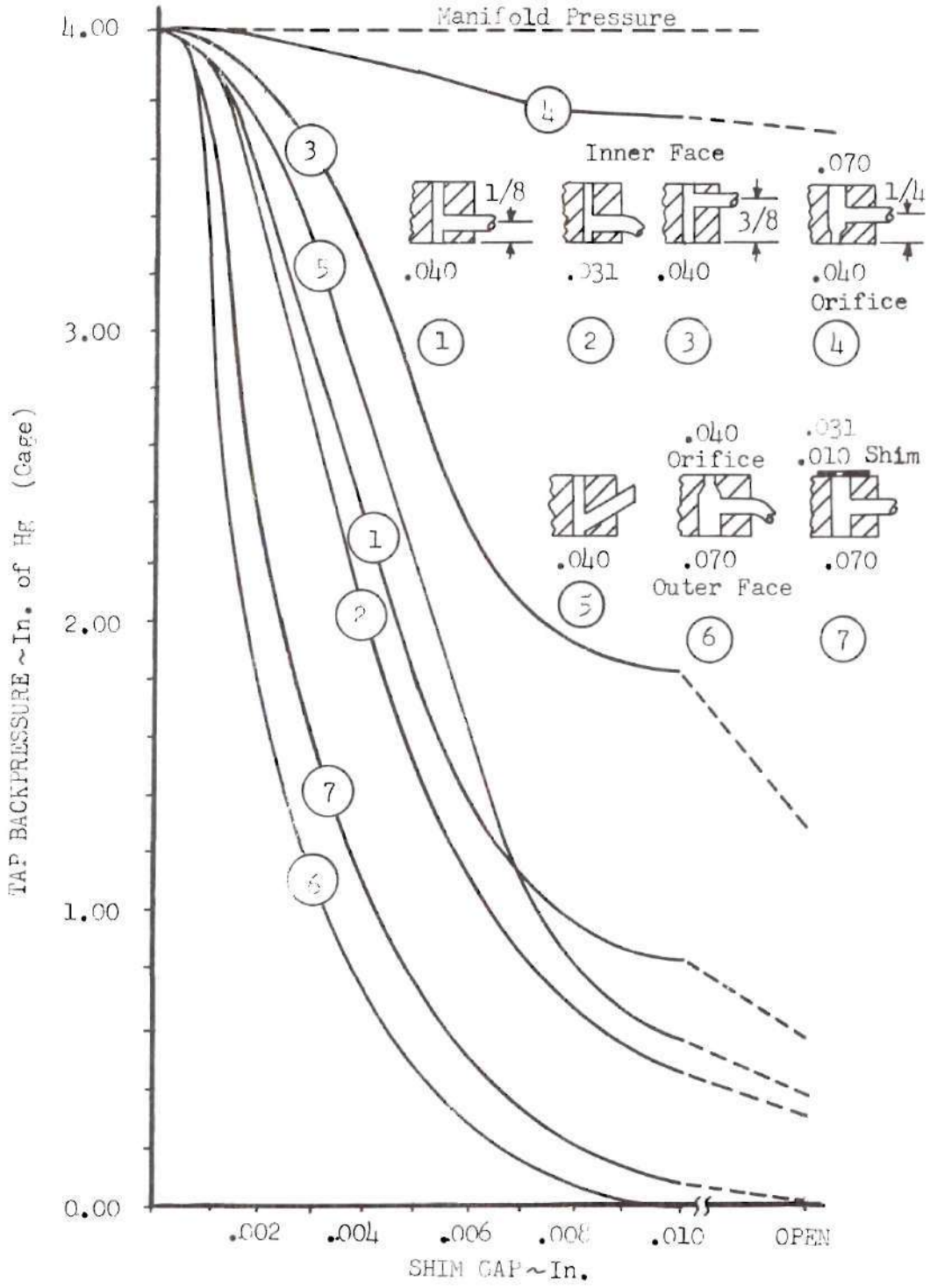

Figure 16. Comparison of Sensing Nozzles.

and 3.

A second test was designed to compare nozzles 4, 5, and 6. Nozzle 4 was checked for possible reference purposes only. The intent in testing nozzle 5 was to determine the outcome of tapping the base hole as close to the mouth as possible. This was accomplished by drilling angularly to intercept the base hole. The decrease in tap backpressure with the nozzle open appeared insufficient to justify angular drilling in mass scale. Even more than expected, nozzle 6 succeeded in maximizing the contrast between an open and closed nozzle. This nozzle was constructed by stopping a 0.070 in. base hole drill just short of the inside of the face plate and completing the nozzle by drilling through with a 0.040 in. drill, thus creating an orifice. As seen in Figure 16 for the open nozzle 6, virtually all of the pressure drop between the manifold and atmosphere takes place before the 0.070 in. base hole is tapped--that is, across the orifice.

Having concluded then that an orificed configuration as in nozzle 6 was the logical choice, the last preliminary test was conducted for nozzle 7, which is essentially the same nozzle using a sharp-edged orifice. This two-pieced arrangement is much more practical both to manufacture and to reproduce. As evidenced by

the characteristic curve, the latter nozzle produces the sharp contrast desired between a blocked and open mouth. In addition, since almost all of the pressure drop occurs across the orifice, factors such as the location of the backpressure tap or the sharpness of the drill are no longer critical to the successful performance of the nozzle.

The next stage of nozzle development tests were needed to tentatively bracket the optimum size range for the base and orifice holes. The mathematical relationship derived to describe the behavior of the nozzle in use (see Chapter IV) revealed that these two parameters were--with the exception of the manifold pressure and the shim gap--the most dominant factors in determining nozzle behavior. At this point it was necessary to amplify the definition of performance being sought. If the nozzle mouth were to be fully closed by the pattern to create a signal to sew, maximum contrast between signals to sew versus not to sew could be achieved. However, in order to insure full nozzle closure at one extreme of manufacturing tolerances, some pressure would need to be applied to the pattern at the opposite extreme.

Thus, provision to completely close a nozzle mouth immediately introduces the undesirable feature of pattern wear into the over-

all picture. A good deal of unfortunate experience has accumulated in small tufting mills with patterns of light construction wearing out, a factor which in part explains the continued use of the expensive but sturdy phenolic drum patterns. From this standpoint an arrangement whereby the pattern does not touch the nozzle mouth is preferable as in the case of the photocell sensing technique of Figure 4.

A folded half-scale pattern for a conventional ten feet square bedspread could encircle a drum 19 in. in diameter and 30 in. long. Careful machining of the drum could produce a surface round within a tolerance of 0.001 in., and the transverse diametral dimension can be held within 0.0005 in. Allowing for wear adjustments and slight pattern thickness variations, it was decided that a nominal distance between the pattern surface and the face of the piece containing the sensing nozzle should be about 0.002 in. in order to prevent pattern wear. To provide a still greater factor of safety, a distance of 0.003 in. was chosen for purposes of design and evaluation. Therefore--remembering the 0.001 in. roundness tolerance--to select the desired nozzle, the contrast in tap back-pressure between a shim gap of 0.004 in. and open (i.e., near 0.010 in.) should be used as the prime criterion.

The characteristic curves resulting from tests to select the best choice of base and orifice holes for the sensing nozzle are given in Figure 17. An orifice hole of 0.0135 in. diameter is seen to be too small regardless of base hole size, because virtually the entire range of backpressure variation is completed within a gap spacing of less than 0.004 in. Although the 0.025 in. diameter orifice tests yielded the desired backpressure contrasts between a 0.004 in. gap and a 0.010 in. gap, the relatively high backpressure remaining at the 0.010 in. gap is not desirable, because a threshold of signal pressure at which the spool valve would not actuate could thus become as important a control standard as that which would actuate the valve. The same objection is found with regard to the nozzle having a 0.031 in. base hole and a 0.020 in. diameter orifice. From Figure 20 the conclusion was reached that the optimum choice of orifice hole was 0.020 in. with a base hole of about 0.052 in. or 0.040 in., depending on the amount of signal contrast necessary. In view of the 3/32 in. (half-scale) spacing of nozzles, a base hole much larger than 0.052 in. would be physically impractical.

Now that the choice of nozzle was reasonably well bracketed, more specific information was needed regarding the possible inter-

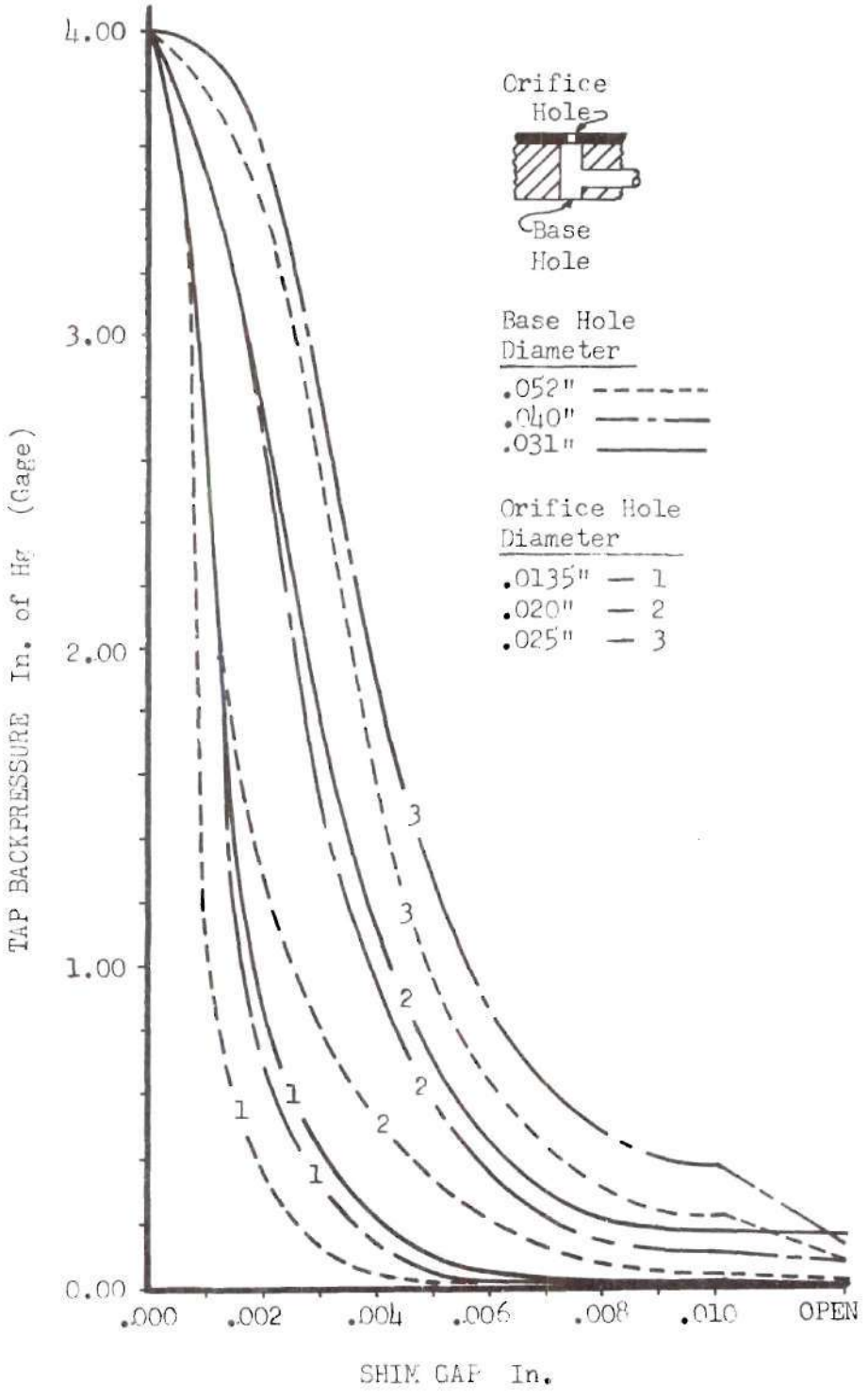

Figure 17. Effect of Nozzle and Orifice Hole Variation.

action of adjacent nozzles. First a simple test was run to compare the backpressure of three adjacent nozzles to learn what effect, if any, one nozzle has upon another. The curves of Figure 18 were obtained using three nozzles spaced 3/32 in. apart and having a 0.040 in. diameter base hole and a 0.021 in. diameter orifice hole. The difference in tap backpressure of the center hole was relatively small as shown, but was definitely significant from the standpoint of measuring thresholds. For this reason all further tests were made with three properly spaced nozzles flowing, and data was always taken from the center nozzle tap.

The next nozzle test was conducted to demonstrate an inherent safety factor in the pneumatic concept being developed. As seen in Figure 19, the simple expedient of raising the manifold pressure supplying the nozzles also raises the backpressure signal strength at a gap below 0.004 in. much more than the strength is raised at a 0.010 in. gap. Thus, if a control system began operating poorly due to wear, pluggage, or the like, it would be entirely possible that a temporary solution would be to raise the pattern sensing manifold pressure until a convenient period for cleaning or repairs could be scheduled.

The curves of Figure 19 apply to a nozzle having a 0.052 in.

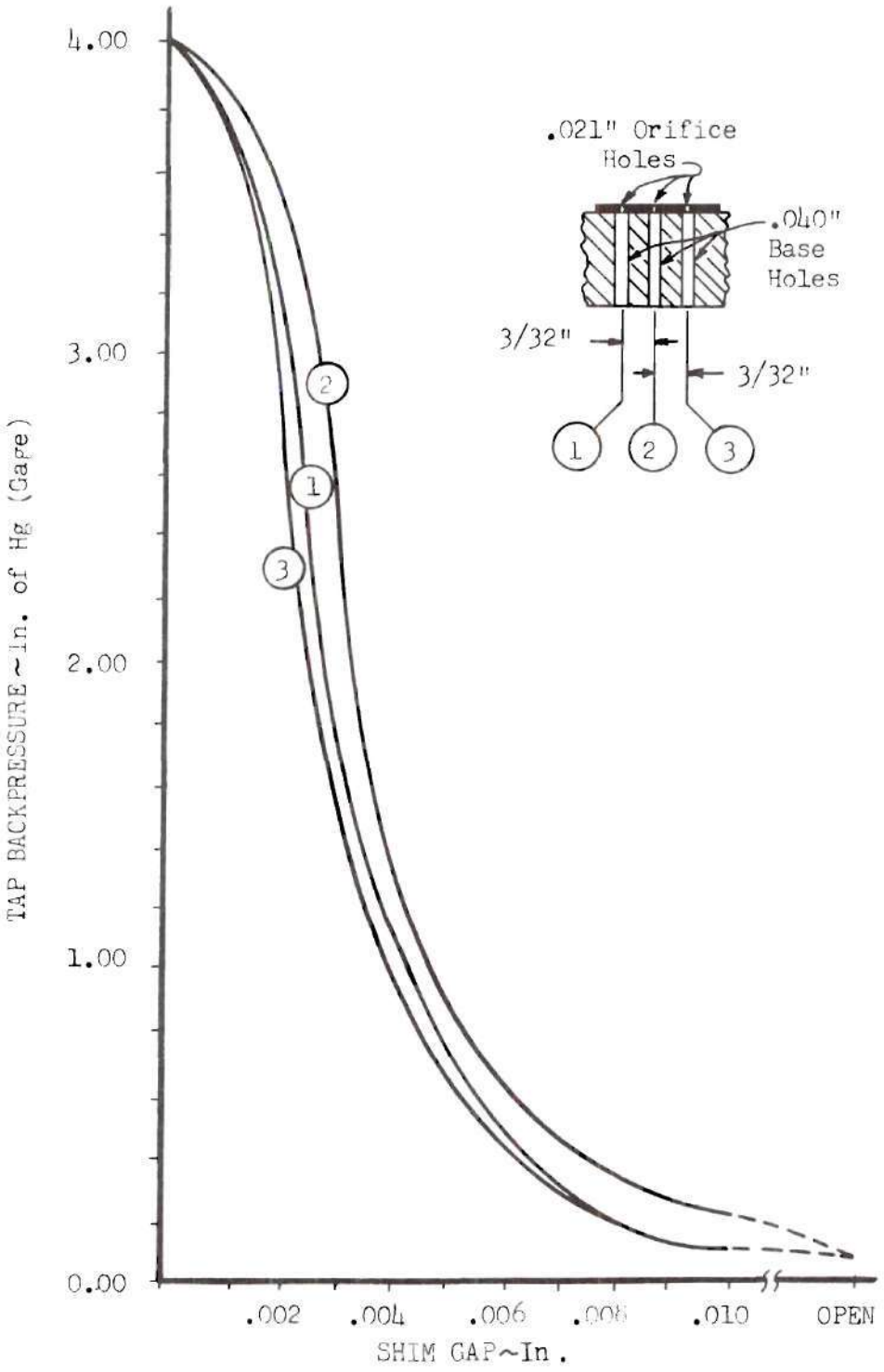

Figure 18. Interaction of Adjacent Nozzles.

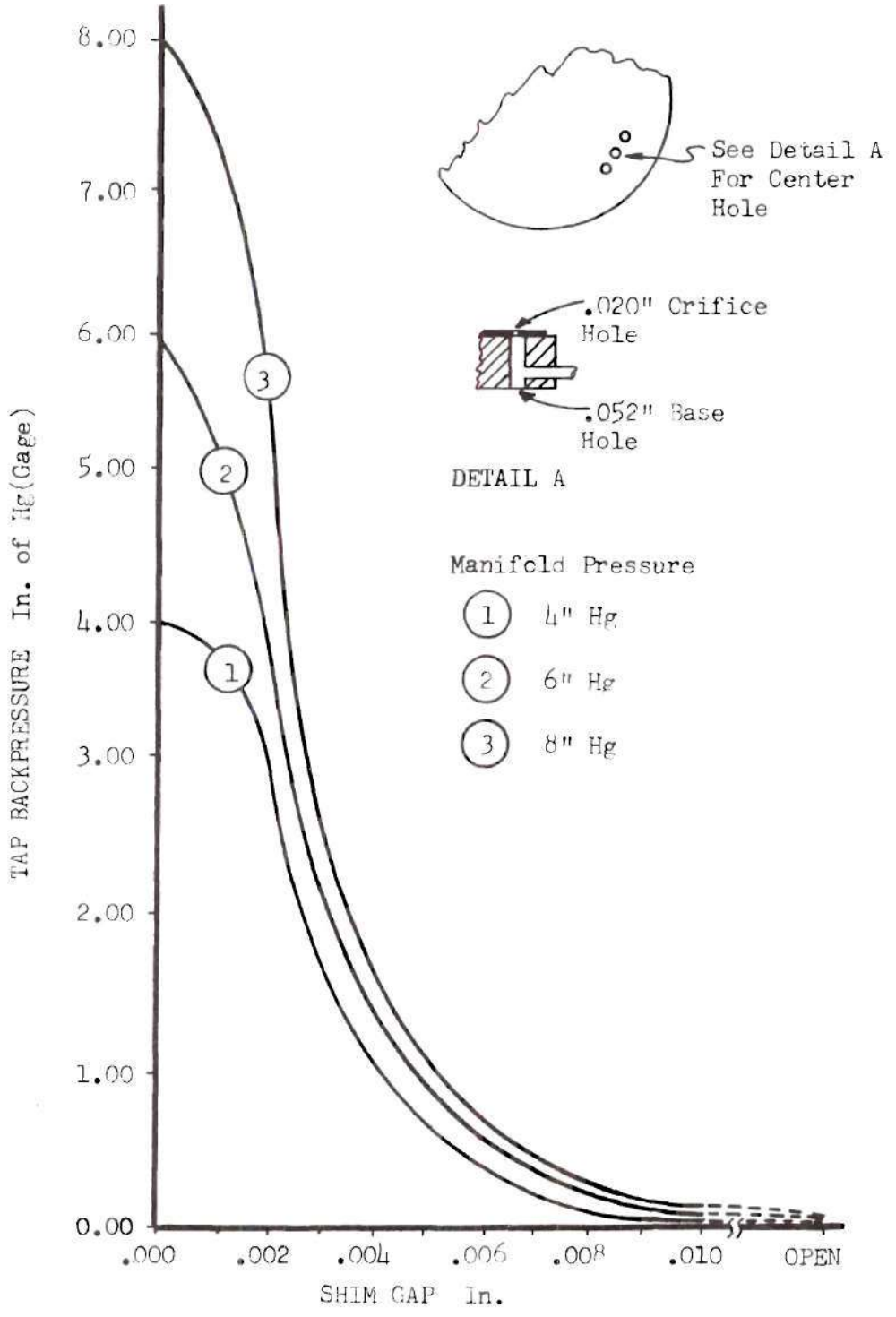

Figure 19. Effect of Manifold Pressure Variation.

base hole. Those for a 0.040 in. base hole were similar, but the pressure at a gap of 0.010 in. was found significantly less for the 0.052 in. hole as also evidenced in Figure 17. The difference is probably a result of the greater area of air escape of a larger hole versus a smaller hole if both are blocked the same distance from the mouth. As previously explained, the low pressure at a 0.010 in. gap is desirable to avoid involvement with a second signal pressure threshold.

The last series of static* experiments for nozzle development were concerned with the signal threshold between adjacent nozzles as a raised pattern surface blocks the mouth of one nozzle and not the other. One reason for making these tests was to determine how accurately a pattern edge would have to pass between two adjacent nozzles in order that a straight line is sewn parallel to the side of a bedspread. Several tests were run having this general purpose, and some basic results are presented in Figure 20. The A series of curves presents the tap backpressure characteristics with the edge of the raised surface of the special blocking bar just covering a

---

*Note that the slow (less than one in. per second) travel of the pattern past the sensing nozzles gave no cause to anticipate transient problems which might change the conclusions reached from static evaluation of nozzle performance.

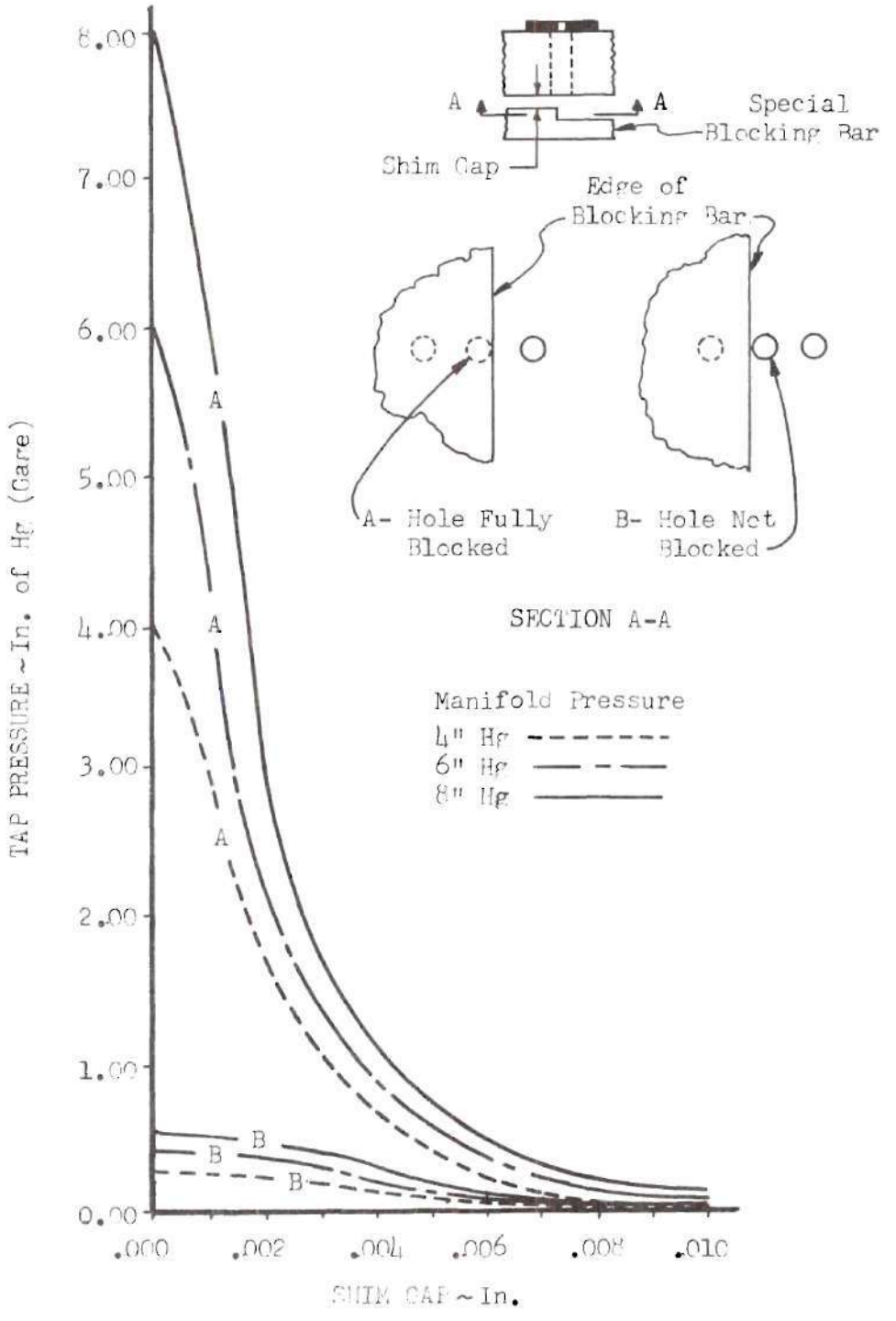

Figure 20. Evaluation of Signal Threshold.

nozzle mouth completely. The B series of characteristic curves were measured with the blocking bar edge just before covering a portion of the mouth of the adjacent nozzle. For a given manifold pressure at a shim gap below 0.004 in., it is seen that a distinct contrast exists between positions A and B of the blocking bar. For example, if the manifold pressure supplying the sensing nozzles is 6 in. Hg at a shim gap of .003 in., any signal threshold between 0.3 and 1.5 in. Hg would permit a pattern edge to vary at least over the distance between adjacent holes (corresponding to blocking bar positions A and B of Figure 20), 0.042 in., without causing an edge stitch either to be added or missed. Further test results indicated that partial overlapping of the sensing holes can even occur without interrupting the sewing edge.

In Chapter IV the nozzle behavior is described analytically, and the specific effect of changing physical parameters is explained with regard to a balance of several design objectives.

Pattern Material

Having decided to employ a raised surface contour style of pattern for reasons already explained, a search was conducted to find a way to produce such a pattern. After consulting several manufacturers seeking suitable materials, it was learned that products

ideally suited for the purpose were commercially available. One range of products (called either Dycril or Templex as trade names) by the DuPont Company was selected for the tests.

A sketch of the pattern material during and after processing is given in Figure 21. A photosensitive material is laminated to a

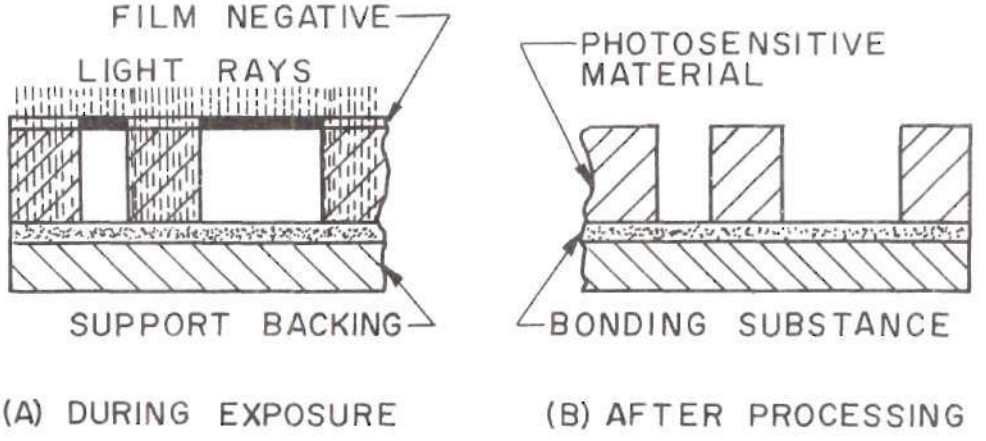

Figure 21. Pattern Material.

support backing with a bonding substance. The chosen pattern design in the form of a photographic negative is held in contact with the material during an exposure to ultraviolet light. The light rays pass through the clear sections of the negative to form the pattern design image. The unexposed areas are washed away with a dilute aqueous sodium hydroxide solution. A pattern can be made in about 20 minutes for well under $100, a price very favorable com-

pared with that for phenolic drum patterns.

The material illustrated in Figure 21 is available with steel, aluminum, or flexible plastic support backing. Relief depths from 0.008 in. to 0.042 in. may be selected. The flexible support backing (trade name is Cronar) is manufactured with a relief depth of 0.008 in. only, a value in keeping with the results of nozzle tests already described. Since the advantage of flexibility* is coupled with cost lower than for steel-backed material, it was decided to test the 0.008 in. relief, Cronar-supported pattern material as a first choice.

Response Measurements

In order to verify the analytical studies to be described in the next chapter, instrumentation was needed to measure and record the pressure transients at several strategic locations in a simulated needle control system. For this purpose a Statham strain gauge differential pressure transducer, Model No. PM295TC ± 10-350, was purchased. The wiring diagram for this transducer circuit is given in Figure 22. A calibration circuit (shown dotted in the

*Note that a choice of steel backing would necessitate special forming of a cylindrical pattern and would be more difficult to attach to a drum.

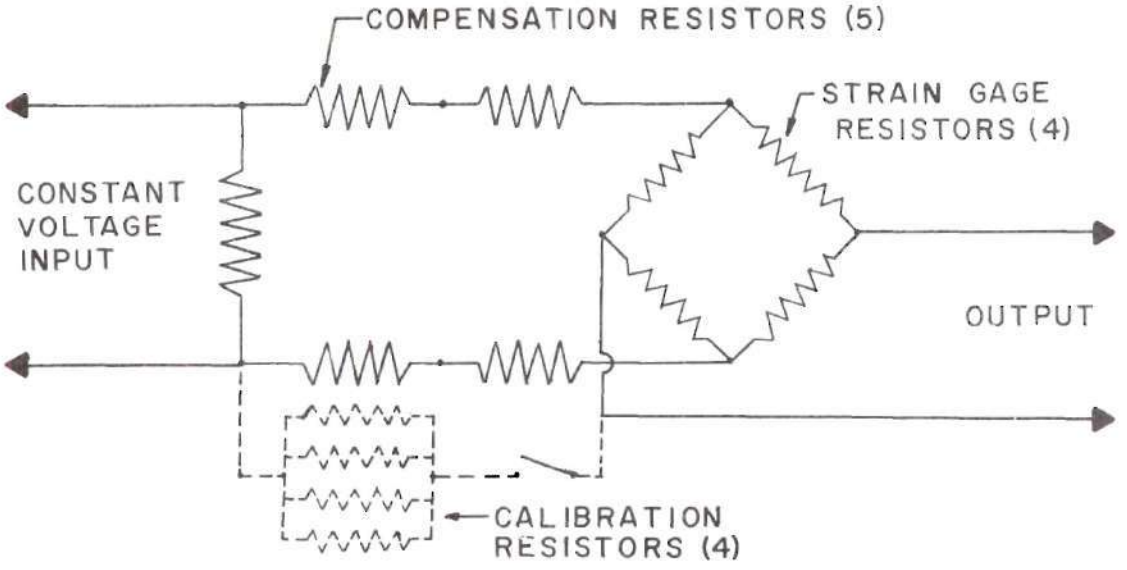

Figure 22. Wiring Diagram for Pressure Transducer.

figure) was also built as specified by the manufacturer to facilitate instrument calibration. The transducer was applied to the points of measurement and operated in conjunction with a Sanborn Carrier Preamplifier, Model 350-1100B. The measurement results were then displayed on either the corresponding Sanborn recording system or the screen of a Tektronix type 564 oscilloscope.

Some means to simulate a rotating pattern drum was needed, and for this purpose a precision gear train from a war surplus gun turret was adapted. The train was powered by a DC motor, the speed of which was adjusted using a Dodge SCR control unit. A pattern was simulated on the face of one gear of the train in a fashion to be described later. Three adjacent nozzles were machined into a

special piece which was positioned near the pattern with a micrometer screw. The center nozzle was tapped to complete the sensing phase of the control system simulation. When conducting the tests described later--even with the micrometer adjustment available--difficulty was experienced in accurately measuring the gap between the pattern and the center nozzle due to such factors as pattern separation from the gear face, slightly eccentric gear travel, and small angle between the gear face and the surface of the nozzle piece.

As a basis for comparing pressure transients with respect to time, a starting base was needed from which measurements could begin at a pattern position known with respect to the nozzle mouth. An amplified photo-reflective pickup (Power Instruments Model C-836) was purchased for this purpose. The basic circuit for the pickup unit is shown in Figure 23. Tests were conducted to determine the actual performance of the circuit under several trial conditions. The basic performance curve for the instrument is also shown in the figure as a reflective surface passes before the photocell. The major portion of voltage drop passing from a sharply defined reflective-to-non reflective edge takes place in approximately 0.04 in., a distance too great for the use intended. A feature of the oscillo-

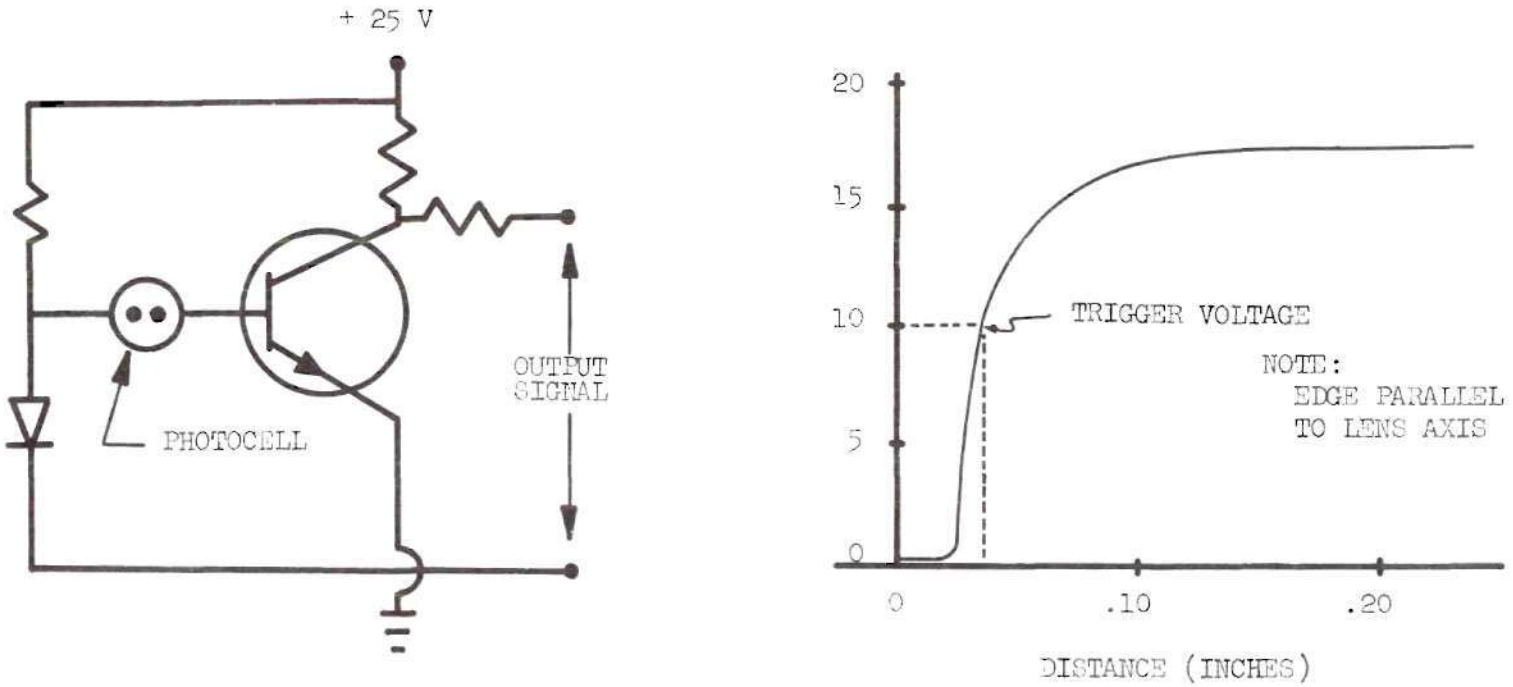

Figure 23. Photocell Circuit and Performance Curve.

scope being used, however, enabled the scope display to be triggered at a specific voltage. Here, ten volts was selected as a convenient triggering voltage on the steeply sloping section of the performance curve in Figure 23. With this technique a pressure transient curve could be captured on a memory screen with a pattern starting point which could be determined well within 0.001 in. if desired. A picture of the gear train, photo pickup, and pressure transducer in position to record the nozzle signal input is shown in Figure 24.

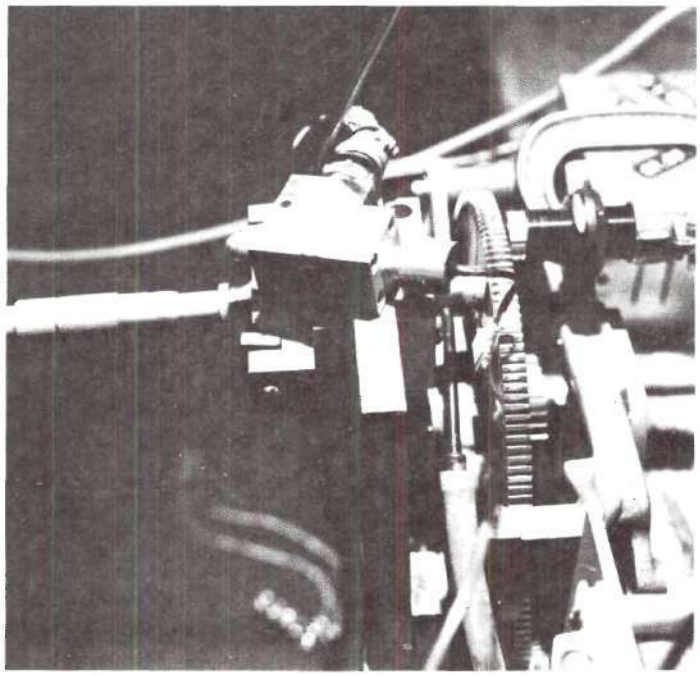

Figure 24. Response Instruments in Use.

Sensitivity Determination

In selecting a test pattern make-up using the pattern material of Figure 21, it was decided both to ascertain the basic suitability

of the material and to learn roughly the sensitivity of the sensing nozzle as well. The test pattern was made in the shape of an annular ring with a 4 in. ID and a 6 in. OD to accommodate the gear face. The pattern was glued to the test gear as pictured in Figure 25.

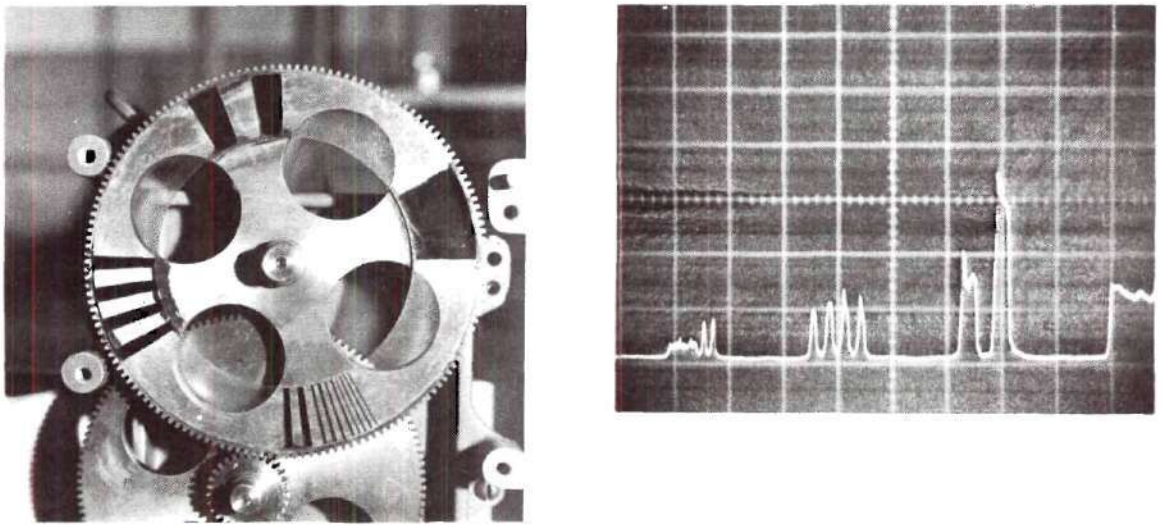

Figure 25. Test Pattern Results.

The dark radial sectors (raised surface) of the pattern ring gradually decrease in width until the smallest slivers are only about 0.02 in. wide. The qualitative response resulting from the test pattern is also pictured in Figure 25, as obtained using the measuring apparatus previously described. It can be seen that the first two pattern ring sectors in the left grouping provide distinct response signals, whereas the signals from the remainder of the group are indistinguish-

able. The two responsive sectors are slightly more than 0.1 in. wide. Also, a variation in signal strength for different surfaces is evident. The difference could be caused to some extent by an accumulation of glue between the pattern and gear face. However, it was discovered later that the gear does not run perfectly true, which probably accounts for most of the signal strength variation.

It will be recalled from the project definition in Chapter I that pattern designs to be considered would call for a minimum of three consecutive tufts. Specifically, using the proper machine and pattern scale factors, a pattern width corresponding to three tufts is 0.2 in., approximately the width of the four pattern sectors in the second grouping (from the left) in Figure 25. Thus, the sensing nozzle will detect a pattern width that is only one-half of that specified for this research project.

Nevertheless, an evaluation of the nozzle sensitivity is of interest so that the degree of extra capability of the needle control system in this respect can serve as a known basis of potential from which to examine future machine improvements. Accordingly, two points of information were sought: the smallest width of pattern surface which could readily be sensed, and the spacing between raised pattern surfaces which would permit the signal to diminish to an

acceptable level. To accomplish these objectives the gap between raised pattern surface and nozzle mouth was chosen at 0.003 in., the manifold pressure was held at 4 in. Hg, and the pressure measurements were taken close to the nozzle backpressure tap with no transmission tubing installed.* It should be recognized that a different gap, manifold pressure, or the like would produce somewhat different results quantitatively. The intent, however, was not to establish a full range of nozzle sensitivity information under multiple test configurations, but merely to provide a basic guide regarding sensitivity to aid possible developments in the future.

In order to determine the smallest width of pattern surface which could be reasonably sensed, seven small pieces of 0.007 in. shim stock were glued to the face of the test gear in widths decreasing from 0.10 in. to 0.03 in. Considering the glue thickness, a contour relief of approximately 0.008 in. was thus created to simulate the 0.008 in. relief of the Cronar-backed pattern material under consideration. The test results are given in Figure 26. For reference, the strongest signal (on the left) is 0.36 psig or 0.76 in. Hg. The fourth signal from the left, coming from a surface

---

*Pattern speed was approximately correct during the tests.

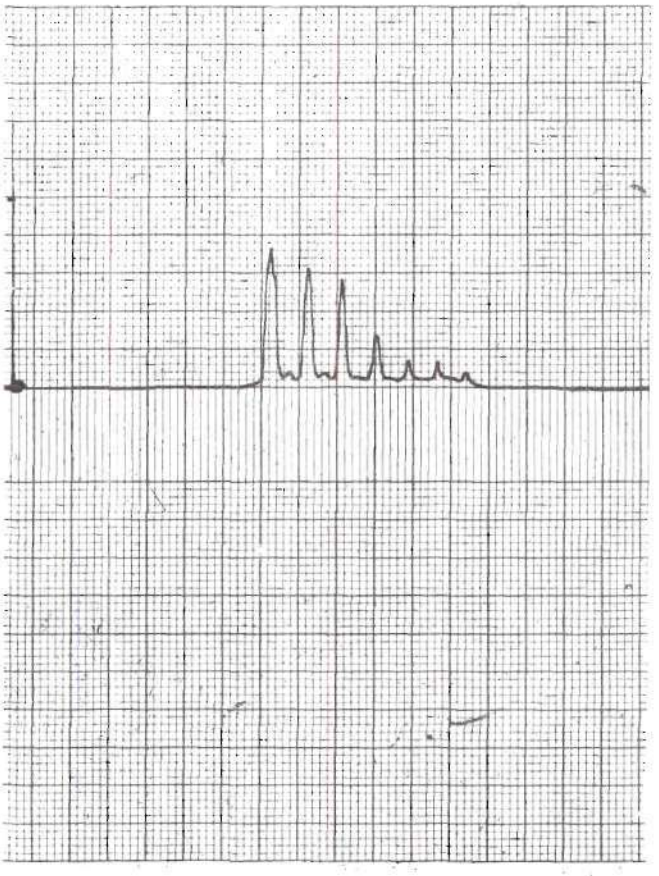

Figure 26. Minimum Surface Width Sensitivity.

0.069 in. wide is the smallest clearly distinctive signal, but its strength is only half that of the third signal, which comes from a surface width of 0.077 in. Although increased amplitude for the fourth signal was gained by increasing the manifold pressure, this course of action would ordinarily be inefficient and therefore impractical. Thus, it can be said that--under the test conditions defined--the sensing nozzle can readily detect pattern widths as small as 0.077 in., and still narrower widths can be sensed but with

sharply reduced signal strengths.

The second sensitivity criterion sought was the spacing requirement between raised pattern surfaces which permitted the signal to sufficiently diminish. The reason for this spacing study was to allay fear that air flow from the nozzle into small pattern channels might possibly behave in such a manner as to prevent the signal pressure from falling properly. The same test conditions were held for these experiments as for the minimum surface width tests. Two 0.007 in. thick, 0.2 in. wide shim pieces were glued to the test gear with an arbitrarily chosen space between of 0.05 in. Note that the 0.2 in. widths simulate the minimum pattern width specified for this project. The test results from the 0.05 in. spacing are shown in Figure 27. A pressure drop from about 0.6 in. Hg to roughly 0.2 in. Hg occurs while traversing the 0.05 in. space. (Note that the difference in signal strengths of the two shim pieces is due to a slight angle in one piece as well as a different thickness of glue.) The pressure drop across the 0.05 in. space is satisfactory for most imaginable threshold requirements. Note that the 0.05 in. space is less than the 0.077 in. corresponding to the smallest surface width that can readily be sensed. Thus, under the given test conditions, it can be conservatively said that spacing between raised pattern

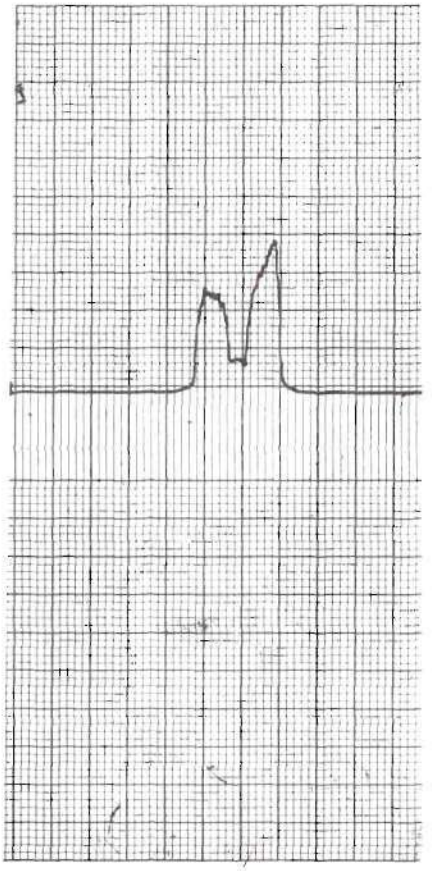

Figure 27. Minimum Pattern Spacing.

surfaces can be at least as narrow as the width of the surfaces being sensed.

Line Flexure Testing

Remembering the number of signal transmission lines (see Figure 13)--nearly 1000 separate pieces in all--necessary within the overall needle control system concept, care should be exercised in selecting the transmission line material. Since the recip-

rocating motion of the needle drive bar causes one end of more than 600 transmission tubes to oscillate, durability during repeated flexing is the one property that the line material must have. In order to test this property for several choices of tubing material, a machine was constructed as pictured in Figure 28. The machine

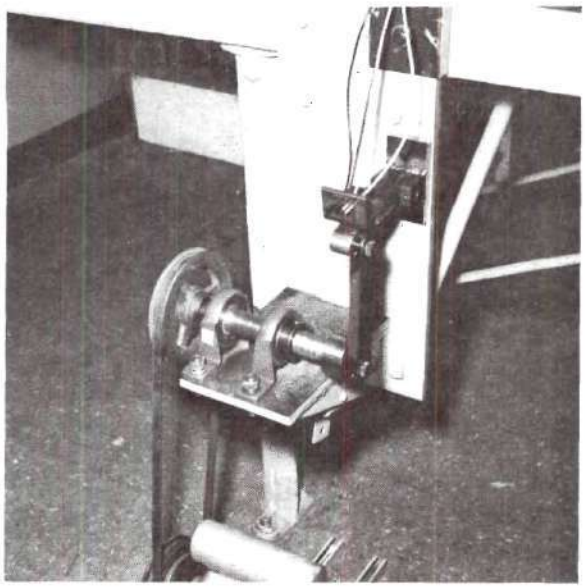

Figure 28. Tube Flexing Machine.

stroke was approximately 7/8 in., and the operating speed was 1150 strokes per minute.

Since the pressures involved are very low and the atmosphere in a textile mill would not cause abnormal deterioration in use, the choice of tubing to be tested was made chiefly with regard to economy and availability. Two inexpensive tubing materials were selected: a 1/16 in. vinyl tubing such as used for wire insulation, and a 1/8 in. heavy duty nylon tubing. Two pieces of each were tested: one

drawn relatively tight during the down stroke, and one which was very loosely connected (see Figure 28). The tubing lengths were 10 in. and 11 in. from anchor point to anchor point. After subjection to the test for over 1000 hours, or 69,000,000 flexures, neither the vinyl nor the nylon tubing evidenced any visual sign of damage. Therefore, frequent tubing replacement will probably not be a serious problem for tufting machines employing this control system.

CHAPTER IV

ANALYTICAL DEVELOPMENT

Input Signal

From the experimental discussion in Chapter III, it is evident that the key to the performance of the needle control concept lies with the parameters which govern the behavior of the sensing nozzle. By the same token, the most important link in the development of a mathematical model for the control system is the proper representation of the sensing nozzle. Specifically, the first analytical objective is the formulation of mathematical expressions which describe the input signal to the control system that results from a pattern raised surface passing in front of the mouth of a sensing nozzle.

Derivation

A sketch of a partially blocked sensing nozzle is given in Figure 29. As shown, the behavior of the pressure, P(u), constitutes the input signal. Writing the ideal gas law,

$$P(u)V = mRT \tag{4.1}$$

Because P(u) is an absolute pressure, and the maximum gage pressure involved is relatively small, it is reasonable to assume that the

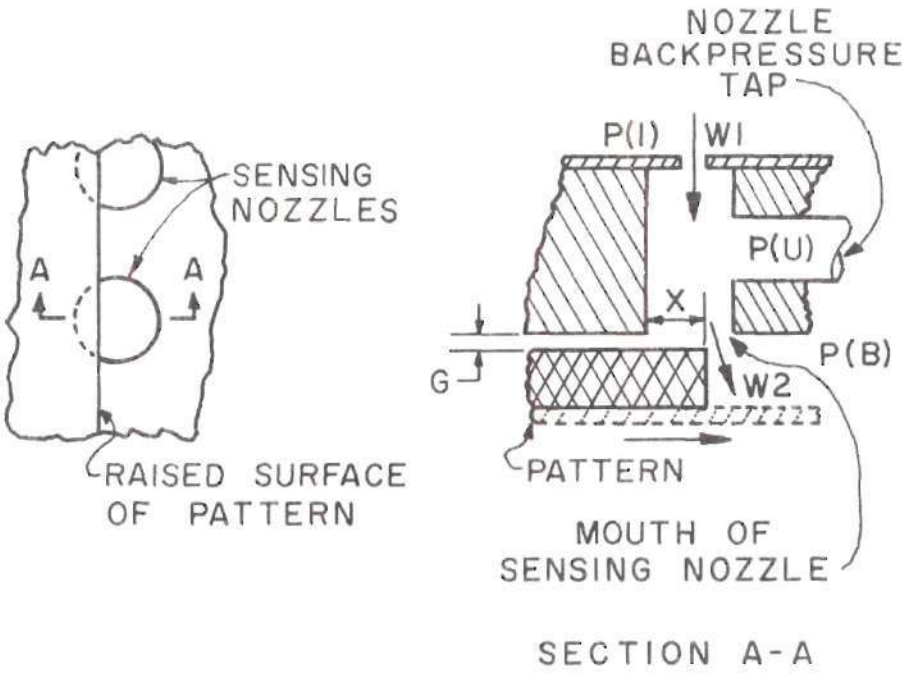

Figure 29. Partially Blocked Sensing Nozzle.

pressure varies uniformly throughout the transmission line. (The variation in the gauge pressure through the transmission line is given later.) The volume, V, includes the nozzle base from the orifice to the mouth, and the transmission line from the tap to the spool valve. Since the line is on the order of 12 feet long, the variation in total volume due to spool movement is so slight that V is considered constant. Thus, P(u) depends only upon the mass, temperature, and constants, such that the total differential of P(u) is

$$dP(u) = \left.\frac{\partial P(u)}{\partial T}\right|_m dT + \left.\frac{\partial P(u)}{\partial m}\right|_T dm \qquad (4.2)$$

Using equations (4.1) and (4.2),

$$dP(u) = \frac{Rm}{V} dT + \frac{RT}{V} dm \tag{4.3a}$$

or,

$$\frac{dP(u)}{P(u)} = \frac{dT}{T} + \frac{dm}{m} \tag{4.3b}$$

Assuming a reversible adiabatic process, the following basic equation (15) can be written

$$P(u)v^{k} = C' \tag{4.4a}$$

or,

$$P(u)^{\frac{1}{k}} \quad v^{\frac{1}{k}} = C' = C'' \tag{4.4b}$$

and, using the gas law,

$$P(u)^{\frac{1}{k}} \frac{RT}{P(u)} = C'' \tag{4.5a}$$

or,

$$TP(u)^{\frac{1-k}{k}} = \frac{C''}{R} = C''' \tag{4.5b}$$

Differentiating equation (4.5b),

$$P(u)^{\frac{1-k}{k}}\, dT + \frac{1-k}{k}\, TP(u)^{\left(\frac{1-k}{k} - 1\right)}\, dP(u) = 0 \qquad (4.6a)$$

and, dividing by $TP(u)^{\frac{1-k}{k}}$ gives

$$\frac{dT}{T} + \frac{1-k}{k}\,\frac{dP(u)}{P(u)} = 0 \qquad (4.6b)$$

Substituting equation (4.6b) into (4.3b) gives

$$\frac{dP(u)}{P(u)} = \frac{k-1}{k}\,\frac{dP(u)}{P(u)} + \frac{dm}{m} \qquad (4.7a)$$

or,

$$\frac{1}{k}\,\frac{dP(u)}{P(u)} = \frac{dm}{m} \qquad (4.7b)$$

Since variables P(u), T, and m are all dependent variables of the one independent variable, t (time), for the problem at hand, equation (4.7b) can be rewritten

$$\frac{1}{kP(u)}\,\frac{dP(u)}{dt} = \frac{1}{m}\,\frac{dm}{dt} \qquad (4.7c)$$

and, again using the gas law,

$$\frac{1}{kP(u)} \frac{dP(u)}{dt} = \frac{RT}{P(u)V} \frac{dm}{dt} \tag{4.8}$$

Substituting from equation (4.5a),

$$\frac{1}{kP(u)} \frac{dP(u)}{dt} = \frac{C'}{\frac{1}{P(u)^{\frac{1}{k}} V}} \frac{dm}{dt} \tag{4.9a}$$

and evaluating C' at initial conditions with equation (4.5a),

$$\frac{1}{kP(u)} \frac{dP(u)}{dt} = \frac{RT(i)\ P(i)^{\frac{1-k}{k}}}{\frac{1}{P(u)^{\frac{1}{k}} V}} \frac{dm}{dt} \tag{4.9b}$$

The very small temperature change that occurs during the nozzle flow process(es) is negligible in terms of numerical calculations so that T(i) is taken as room temperature. Also, P(i) = P(B) as shown in Figure 29. Equation (4.9b) can therefore be rewritten

$$\dot{P}(u) = \frac{kRT}{V} \left(\frac{P(u)}{P(B)}\right)^{\frac{k-1}{k}} \dot{m} \tag{4.9c}$$

Equation (4.9c) thus represents the behavior of the input signal P(u)

in terms of system constants and the time rate of mass change in the transmission line.

Referring again to Figure 29, it is seen that the difference in the orifice flows W1 and W2 constitutes the same time rate of mass change which appears in Equation (4.9c). Assuming the processes of flow through the entrance orifice (W1) and through the orifice at the nozzle mouth (W2) are quasi steady, the basic equation of flow of a gas through a single orifice (13) can be applied twice. Thus,

$$\frac{W1}{(CD1)(A01)} = C1 \frac{P(1)}{\sqrt{T}} \left(\frac{P(u)}{P(1)}\right)^{\frac{1}{k}} \sqrt{1 - \left(\frac{P(u)}{P(1)}\right)^{\frac{k-1}{k}}} \qquad (4.10)$$

and

$$\frac{W2}{(CD2)(A02)} = C1 \frac{P(u)}{\sqrt{T}} \left(\frac{P(B)}{P(u)}\right)^{\frac{1}{k}} \sqrt{1 - \left(\frac{P(B)}{P(u)}\right)^{\frac{k-1}{k}}} \qquad (4.11)$$

where: W1 and W2 = weight rate of flow, lb/sec

CD1 and CD2 = orifice discharge coefficients

A01 and A02 = orifice areas, sq ft

P(1) = manifold supply pressure to sensing nozzles, psfa

T = room temperature, ^{o}R

P(u) = nozzle tap backpressure (input signal), psfa

k = polytropic exponent (1.4 for air)

P(B) = discharge pressure at pattern recess, psfa

$$C1 = g\sqrt{\frac{2k}{R(k-1)}} = 2.06\ \sqrt{^{o}R}/sec$$

Also,

$$W1 - W2 = \Delta W = \frac{dm}{dt} = \dot{m} \tag{4.12}$$

Combining equations (4.9c), (4.10), (4.11), and (4.12),

$$\dot{P}(u) = \frac{kRT}{VT}\left(\frac{P(u)}{P(B)}\right)^{\frac{k-1}{k}} \frac{C1}{\sqrt{T}} \left[(CD1)(A01)P(1)\left(\frac{P(u)}{P(1)}\right)^{\frac{1}{k}}\sqrt{1-\left(\frac{P(u)}{P(1)}\right)^{\frac{k-1}{k}}}\right.$$

$$\left. - (CD2)(A02)\ P(u)\left(\frac{P(B)}{P(u)}\right)^{\frac{1}{k}}\sqrt{1-\left(\frac{P(B)}{P(u)}\right)^{\frac{k-1}{k}}}\right] \tag{4.13a}$$

Equation (4.13a) is a first order ordinary nonlinear differential equation describing the signal input, P(u), in terms of known parameters. The only other variable in the expression is A02 which of course depends upon the position of the pattern in relation to the mouth of the nozzle. Since the pattern travels at a constant rate of speed, the variable x in Figure 29 can be defined by the expression

$$\dot{x} = \text{constant} \tag{4.14a}$$

A02 varies from a maximum of $\pi(RN)^2$ at x = 0, where RN is the radius of the nozzle base hole, to a minimum of $2\pi(RN)(G)$ at x = RN. In order to complete the relationship between time and the input signal, it is necessary to express A02 as a function of x as x varies from 0 to 2(RN). Using appropriate geometrical relationships for segments of circles, etc., as developed in Appendix B--for $0 < x < RN$,

$$A02 = 2(G)(RN)\ \tan^{-1}\left(\frac{\sqrt{1-\left(\frac{RN-x}{RN}\right)^2}}{\frac{RN-x}{RN}}\right) + \pi(RN)^2$$

$$-\left[(RN)^2\ \tan^{-1}\left(\frac{\sqrt{1-\left(\frac{RN-x}{RN}\right)^2}}{\frac{RN-x}{RN}}\right) - (RN-x)\sqrt{2(RN)(x)-x^2}\right] \qquad (4.15)$$

where $A02 \leq \pi(RN)^2$

Similarly, as on the following page, for $RN \leq x \leq 2(RN)$,

$$A02 = (G)(RN)\left[2\pi - 2\tan^{-1}\left(\frac{\sqrt{1-\left(\frac{x-RN}{RN}\right)^2}}{\frac{x-RN}{RN}}\right)\right] + \frac{\pi(RN)^2}{2}$$

$$- \left[(x-RN)\sqrt{RN^2-(x-RN)^2} + (RN)^2\tan^{-1}\left(\frac{\frac{x-RN}{RN}}{\sqrt{1-\left(\frac{x-RN}{RN}\right)^2}}\right)\right] \qquad (4.16)$$

where $A02 \geq 2\pi(RN)(G)$

The mathematical model describing the overall input signal has therefore been expressed in two basic equations, (4.13a) and (4.14a) where A02 in equation (4.13a) is given by equations (4.15) and (4.16). At this point the reader may wish to refer to Appendix C wherein a sample computer program is presented in which the four equations above (together with equations describing the remainder of the control system) are written in state variable representation as first order differential equations which are solved simultaneously using a Runge-Kutta numerical integration technique. The input signal P(u) as calculated in Appendix B from the equations just derived is compared in Figure 30 with the actual input signal as measured with the response instrumentation described in Chapter III and pictured in Figure 24. Note that the close agreement between calculated and measured results as shown in Figure 30 is due largely to selection of discharge coefficients as

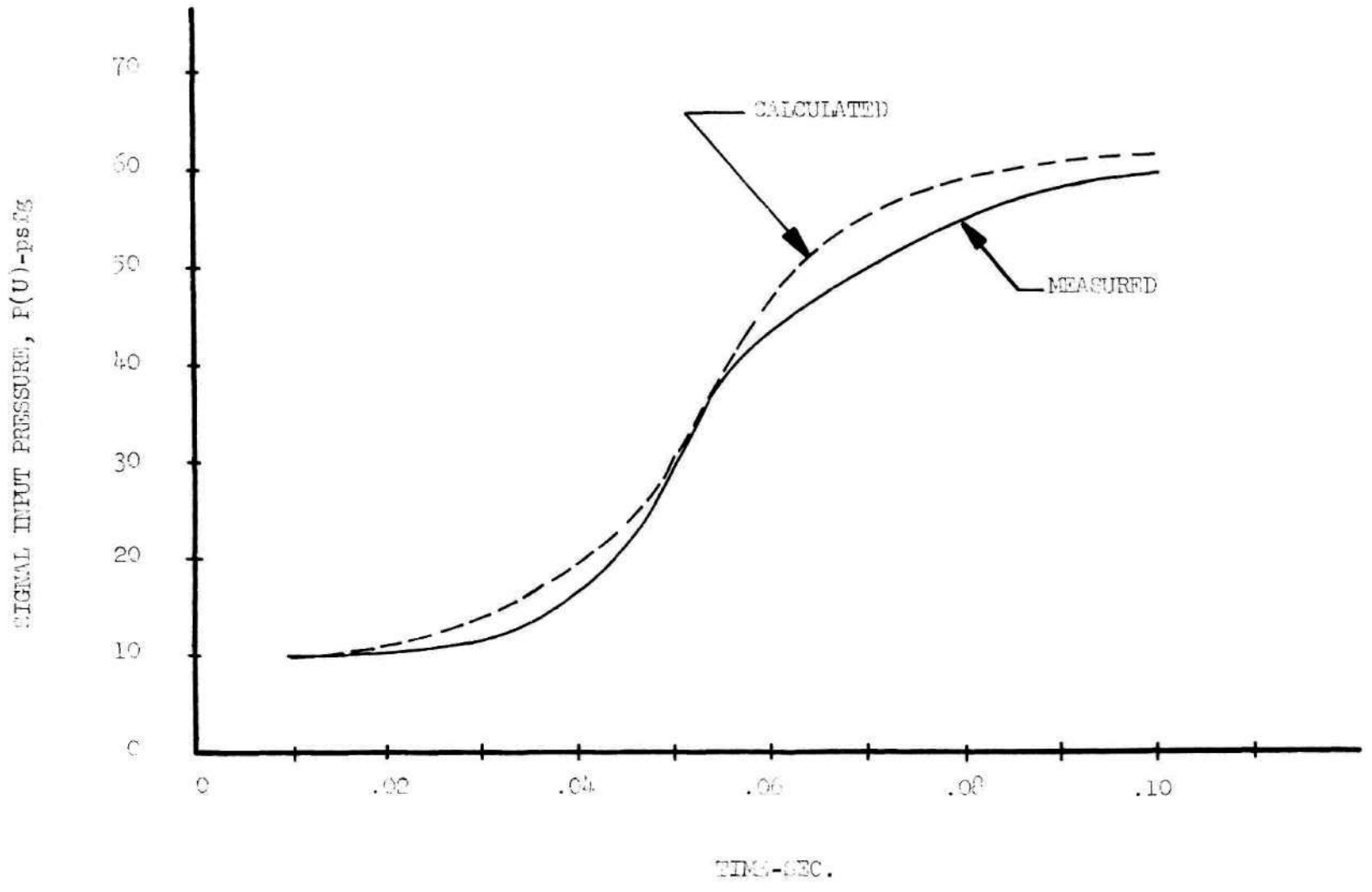

Figure 30. Signal Input--Calculated vs. Measured.

explained later.

Parameter Variation

The parameter values appearing in the mathematical model for the signal input that are most open to question are the values of the orifice discharge coefficients, CD1 and CD2--particularly the latter. The basic difficulty in selecting the appropriate discharge coefficients occurs as a result of the small sizes and pressures involved. For example, with a manifold pressure of 2 psig supplying air to an open sensing nozzle having an orifice hole of 0.020 in. and a base hole of 0.052 in., the Reynolds number is but 1400. This is well below the range of the standard curves for the VDI orifice (16). However, extrapolation of the standard curves indicates a value for CD1 somewhere between 0.60 and 0.70. The point here is that even for a physical orifice configuration which does not change, the discharge coefficient varies with Reynolds number in this low range. Thus, CD1 varies according to manifold pressure. The existence of this variation was definitely established by measuring the flow through the open sensing nozzle being discussed at several manifold pressures, and calculating coefficient values from the standard equation (16) for compressible flow through a square-edged orifice,

$$Q = CdY\, A_o \sqrt{\frac{2\Delta P}{\rho}} \qquad (4.17)$$

Values of CD1 ranging from 0.83 to 0.64 were calculated using corresponding manifold pressures of 1 psig to 5 psig. The value of CD1 used to calculate the curve presented in Figure 30 was 0.67, which was found to give a good approximation to measured results. A typical flow calculation from equation (4.17) is given in Appendix D.

The problem of selecting a value for CD2 is still more involved than for CD1, because the size of the orifice changes with pattern travel. Several approaches were taken to assign CD2 an appropriate value. First an approximate extension (17) of the standard VDI orifice curves was found in terms of the varying ratio between the area of the orifice (i.e., A02) to the area of the nozzle base hole. The curve formed from the coefficient values at the appropriate Reynolds number was then fitted using a computerized least squares technique and the fitted curve was tried in the program given in Appendix C. It was learned by comparison with measured results that the variable CD2 found in this manner was relatively poor. Thus the square-edged orifice should not be used as an approximation of the variable orifice at the mouth of the sensing nozzle.

Next it was decided to extrapolate the curves for the VDI flow nozzle (16) to the proper values of Reynolds number and repeat the above process. By limiting values of CD2 to 1.0 and below, good agreement was found between calculated and measured results; however, the

range of values used was so small, 0.80 to 1.0, that this approach seemed unnecessarily complicated. Several constant values of CD2 were tried and 0.87 was found to give very good results as shown in Figure 30.

Having now verified that the mathematical model describes the physical system in so far as the input signal is concerned, it is possible to analytically examine the effects of several parameter variations which were described in Chapter III. The most pronounced effects occur as a result of varying either the gap between the nozzle mouth and a raised pattern surface or the size of the base hole of the sensing nozzle itself.

Using the same computer program values of Appendix C which produced the curve in Figure 30, except for varying the gap, the series of curves given in Figure 31 were calculated. As expected from the experiments in Chapter III, closing the gap produces a very pronounced increase in the strength of the input signal. This effect serves to again emphasize another safety factor of operation inherent in the sensing concept, such that the simple expedient of adjusting the path of pattern travel slightly closer to the mouths of the sensing nozzles will sharply increase the ability to sense a pattern.

Again, using the same values in the computer program as before except for varying the size of the base hole of the sensing nozzle,

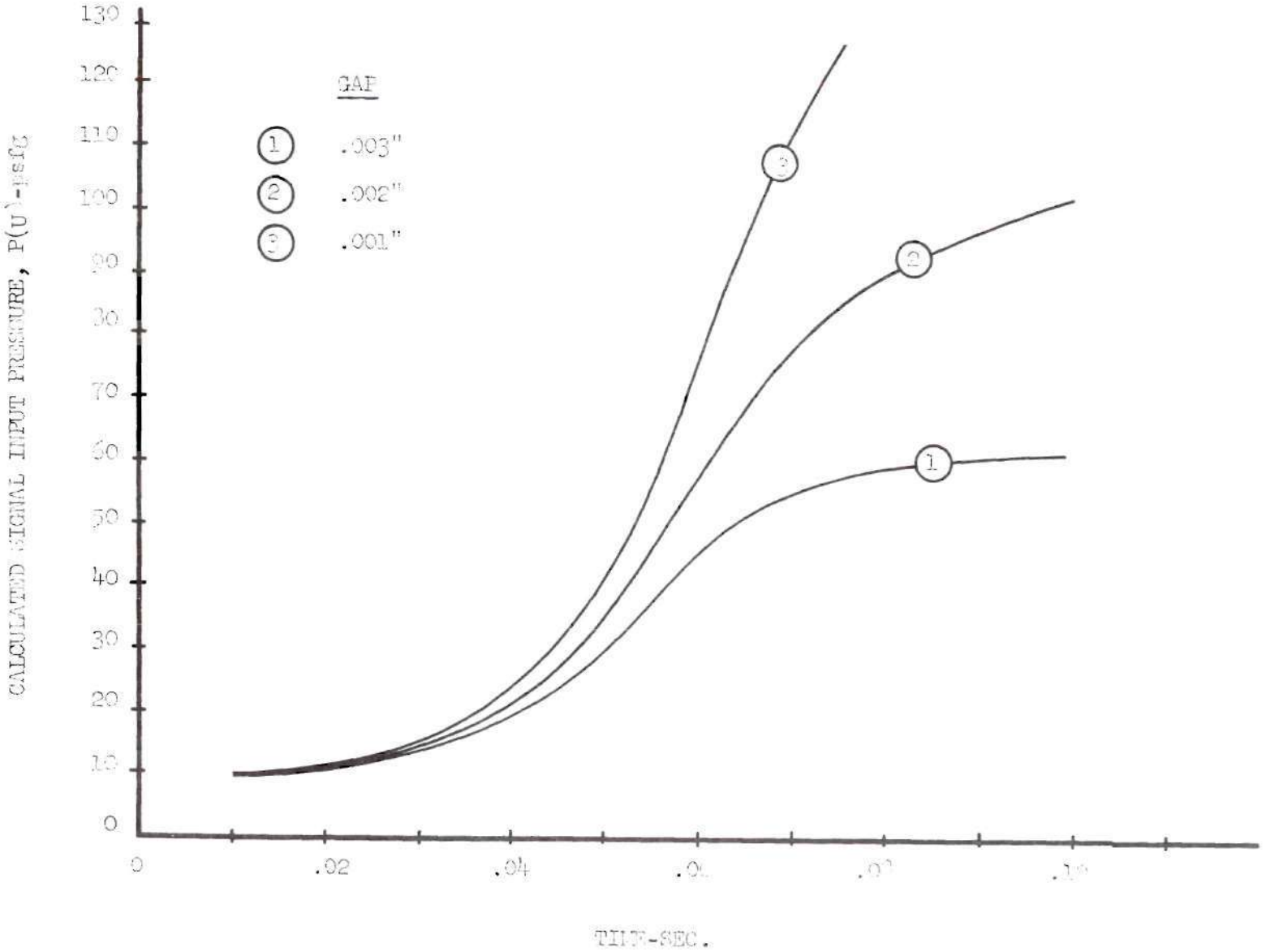

Figure 31. Results of Gap Variation.

the curves in Figure 32 were calculated. As expected, the smaller the base hole, the more quickly the signal input occurs and the stronger the signal amplitude. In the event a need existed to shorten the response time for the control system, then one logical step to consider would be that of reducing the diameter of the sensing nozzle base hole.

Pneumatic Line Transmission

The basic reference used in finding the equation for transmission of the signal input from the nozzle through a line to the spool valve is an article by Shuder and Binder (18) written in 1959. The equation derived in this work was found to accurately describe the measured transmission characteristics except that the measured pressure always lagged behind the calculated pressure. By introducing a time lag of the line length divided by the speed of sound, very good agreement was reached between the calculated and measured results of Shuder and Binder. For this reason, the same time lag was incorporated in the computer program of Appendix C with good results as seen in Figure 33. Since the time lag is a function of the length of a transmission line and a typical tufting machine is more than 10 feet wide, care should be exercised to keep the lengths of transmission lines approximately uniform. For example, a difference of less than six feet in two transmission line lengths will result in a signal being transported through the shorter line some five milliseconds sooner. The difference

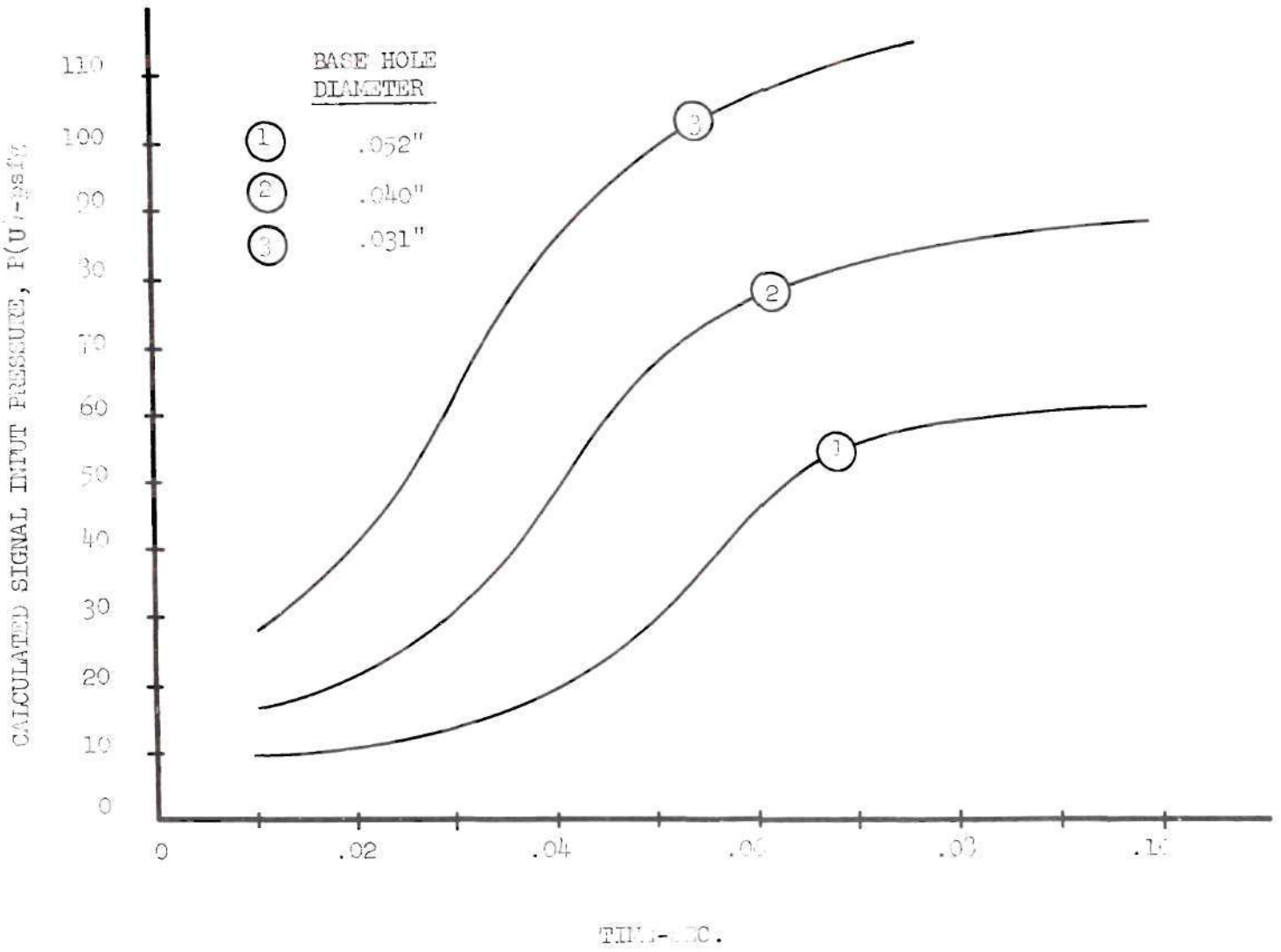

Figure 32. Results of Varying the Sensing Nozzle Base Hole.

could result in a slight distortion of the pattern being sewn for reasons which are explained later in the chapter.

The equation actually used for the signal transmission came from an article (19) based on the derivation of Shuder and Binder. This simplified relationship is applicable to pneumatic line transmission as long as the ratio of the inside diameter to the line length is quite small, as in this project. Writing the expression as a differential equation,

$$\ddot{P}(2) + 2(S1)(WN1)\,\dot{P}(2) + (WN1)^2\,P(2) = (WN1)^2\,P(u) \qquad (4.18a)$$

where:

$$S1 = \frac{(R)(L1)}{2(DE)(C)}\sqrt{\frac{1}{2} + \frac{VS}{(A1)(L1)}} \qquad (4.19)$$

$$WN1 = \frac{C}{L1\sqrt{\frac{1}{2} + \frac{VS}{(A1)(L1)}}} \qquad (4.20)$$

P(u) = pressure input signal, psfg

P(2) = pressure at end of transmission (spool entrance), psfg

S1 = damping ratio

WN1 = undamped natural frequency

$R = \frac{32U}{(D1)^2}$ = frictional resistance, lb-sec/ft^4

U = dynamic viscosity of air, slugs/ft-sec

Dl = inside diameter of line, ft

Ll = length of line, ft

DE = density of air, slugs/cu ft

C = velocity of sound, fps

VS = terminal volume at spool, cu ft

Al = cross-sectional area of line, sq ft

The terminal volume, VS, above is a variable quantity (20) which is a function of the spool displacement at a given time. A simple means to define VS is

$$VS = (A2)(z) \tag{4.21}$$

where:

A2 = area of spool face, sq ft

z = spool displacement, ft

Equations (4.18a), (4.19), (4.20), and (4.21) define the transient behavior of P(2), the pressure downstream of the transmission line, in terms of P(u), z, and known system parameters. As with the signal input equations, these relationships are also expressed in state variable representation and solved simultaneously in the same computer program given in Appendix C. The calculated values of P(2) are compared with measured values in Figure 33. As shown, the calculated values spread

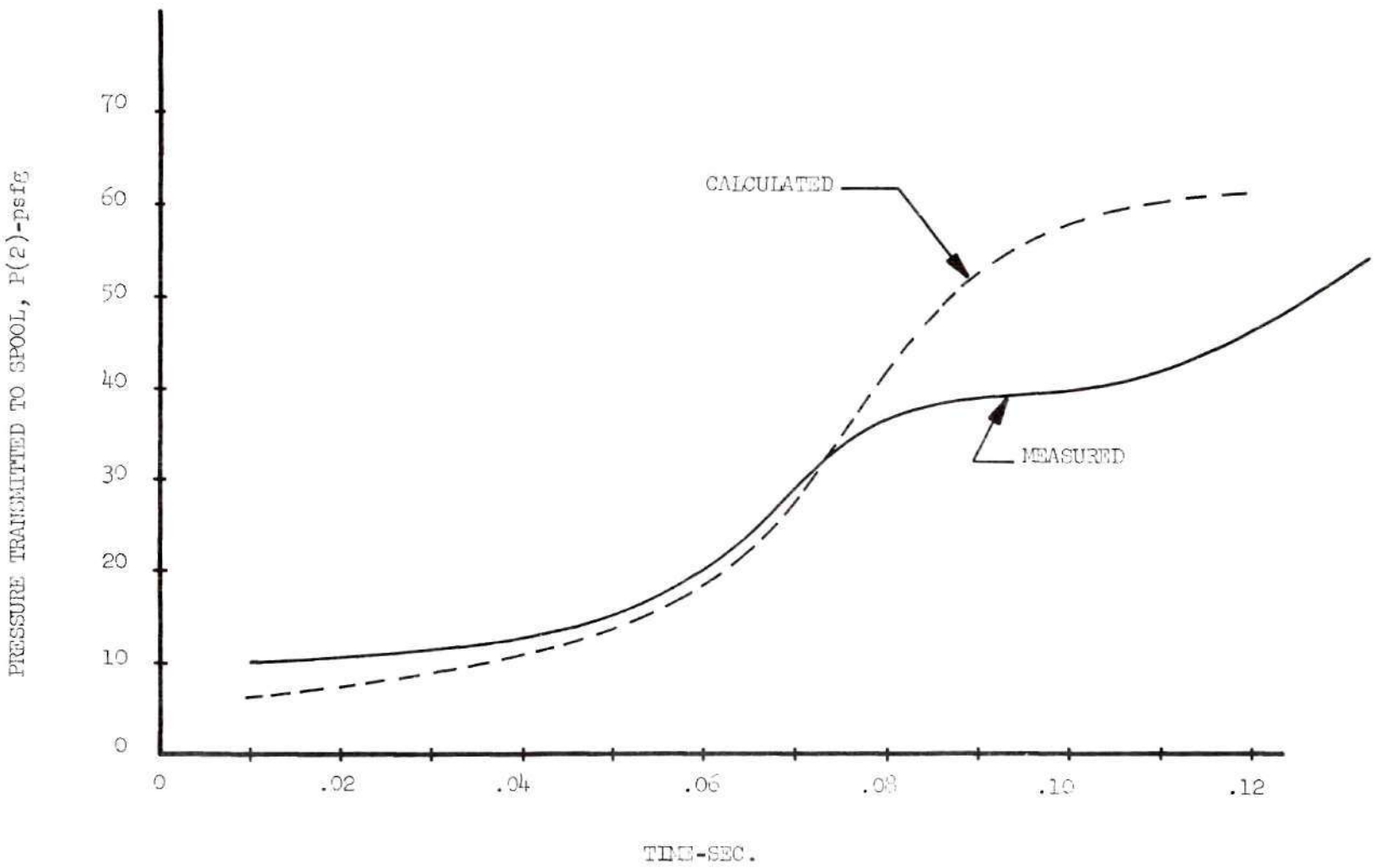

Figure 33. Transmission of Signal Through Line--Calculated vs. Measured.

somewhat above the measured values as P(2) increases. This is attributed to leakage at the spool valve itself; however, the agreement was satisfactory for the analytical purposes of this project without introducing the factor of spool leakage into the mathematical expressions.

Spool Valve Relationships

Spool Movement

The next in the series of mathematical expressions to describe the overall needle control system is that of the movement of the spring-loaded spool itself (see Figure 11). Here, the basic equation for the motion of a spring-loaded mass is applicable.

$$(M1)\ \ddot{z} + (B1)\ \dot{z} + (K1)\ z = (A2)\ P(2) \qquad (4.22a)$$

where:

M1 = mass of spool, slugs

B1 = spool damping coefficient, lb-sec/ft

K1 = spool spring constant, lb/ft

It is probable that the damping term could be omitted in equation (4.22a) without significant effect; however, realizing that very little damping is present,* the value of B1 was arbitrarily chosen as two per cent of the critical damping ratio; i.e.,

---

*Valve leakage may affect damping to some extent, however.

$$B1 = (0.02)\ \ 2\sqrt{(K1)(M1)} \tag{4.23}$$

Pressure Transient

Derivation of an expression for the pressure transient across the spool valve is somewhat similar to the input signal derivation. Beginning with the basic (13) orifice equation,

$$\frac{W}{(CD2)(A03)} = (C1)\ \frac{P(3)}{\sqrt{T}}\ \left(\frac{P(4)}{P(3)}\right)^{\frac{1}{k}} \sqrt{1 - \left(\frac{P(4)}{P(3)}\right)^{\frac{k-1}{k}}} \tag{4.24}$$

Now, using the gas law for the air passing through the valve into the volume in the transmission line, and assuming that the pressure varies uniformly through the volume,

$$P(4)V = mRT \tag{4.25}$$

In this case, the process is assumed to be isothermal,* because experimental evidence (21) indicates that an isothermal process more nearly approximates true conditions of direct line transmission than does a

*The following analysis lends credence to the assumption of an isothermal process. The maximum rise in temperature will occur if the process were reversible adiabatic. From isentropic relationships (15) for a pressure rise of 0.75 psi, the temperature rise is about 8 degrees F. The entire process occurs in less than 0.03 sec (see Appendix C). Assuming that the air temperature inside the transmission line is suddenly raised 8 degrees F, it can be shown that--at the end of 0.03 sec--the space mean temperature (22) is virtually unchanged.

reversible adiabatic process. Considering that the line volume remains essentially constant, and differentiating equation (4.25),

$$V \frac{dP(4)}{dt} = RT \frac{dm}{dt} \tag{4.26a}$$

where:

$$\frac{dm}{dt} = W$$

or, rewriting,

$$W = \frac{V}{RT} \dot{P}(4) \tag{4.26b}$$

Thus, combining equations (4.24) and (4.26b),

$$\dot{P}(4) = \left(\frac{RT}{VF}\right)(CD3)(A03)(C1) \frac{P(3)}{\sqrt{T}} \left(\frac{P(4)}{P(3)}\right)^{\frac{1}{k}} \sqrt{1 - \left(\frac{P(4)}{P(3)}\right)^{\frac{k-1}{k}}} \tag{4.27a}$$

where:

P(4) = pressure downstream of spool, psfa

VF = volume of transmission line plus entrance to piston, cu ft

CD3 = coefficient of discharge

P(3) = pressure upstream of spool, psfa

Equation (4.27a) describes the pressure P(4) across the spool in terms of known parameters and the variable orifice area, A03. Selection of the coefficient of discharge for the orifice, CD3, is governed by the

same factors which led to the choice of CD1 and CD2. Here, a value of 0.65 was taken.

Using the same geometrical relationships as those from which the relationships for the sensing nozzle orifice were found (see Appendix B), the variable spool valve orifice can be expressed with translated values of the spool displacement, z. Referring to Figure 34, section (A), for $0.00521 < z < 0.00782$,

$$A03 = (RO)^2 \tan^{-1}\left[\frac{\sqrt{1 - \left(\frac{RO - (z - 0.00521)}{RO}\right)^2}}{\frac{RO - (z - 0.00521)}{RO}}\right] - RO - (z - 0.00521)\sqrt{2(RO)(z-0.00521) - (z-0.00521)^2} \tag{4.28}$$

and, from section (B), for $0.00782 \leq x \leq 0.01042$,

$$A03 = \frac{\pi}{2}(RO)^2 + (z - 0.00782)\sqrt{(RO)^2 - (z - 0.00782)^2} + (RO)^2 \tan^{-1}\left[\frac{\left(\frac{z - 0.00782}{RO}\right)}{\sqrt{1 - \left(\frac{z - 0.00782}{RO}\right)^2}}\right] \tag{4.29}$$

Equations (4.27a), (4.28), and (4.29) complete the mathematical definition of the transient behavior of the pressure, P(4), across the spool valve. As before the equations are incorporated into the comput-

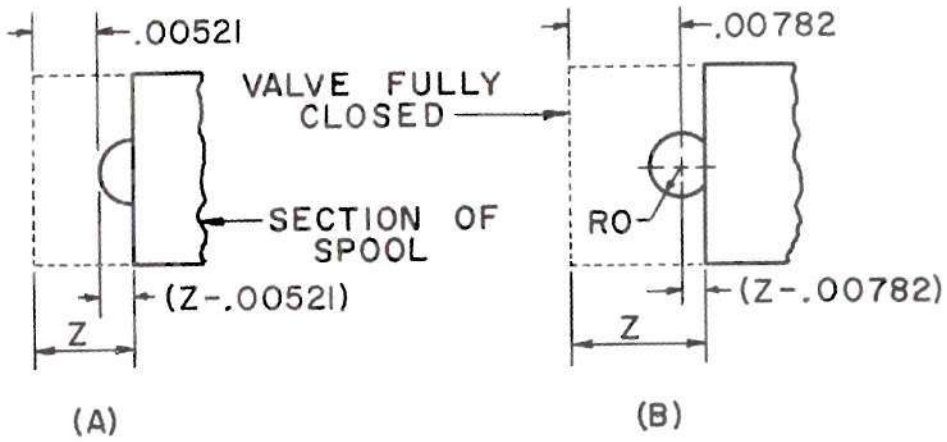

Figure 34. Partially Open Valve Port.

er program in Appendix C, and the values of P(4) calculated therefrom are compared with measured results in Figure 35. Here, the valve leakage results in a substantially lower measured pressure than that calculated, and the time delay is not as accurate as before. Apparently the supply port (see Figure 11) and exhaust port were not drilled exactly as intended. Also, the peripheral leakage effect seen in Figure 33 occurs in this case in two directions instead of one. No attempt was made to fit the calculations to the inaccurate spool valve used in the project nor to machine a more accurate valve, because the valve finally produced for an operating machine would not be accurately simulated, and because the leakage error does not prevent the mathematical model from serving its primary functions as given later in this

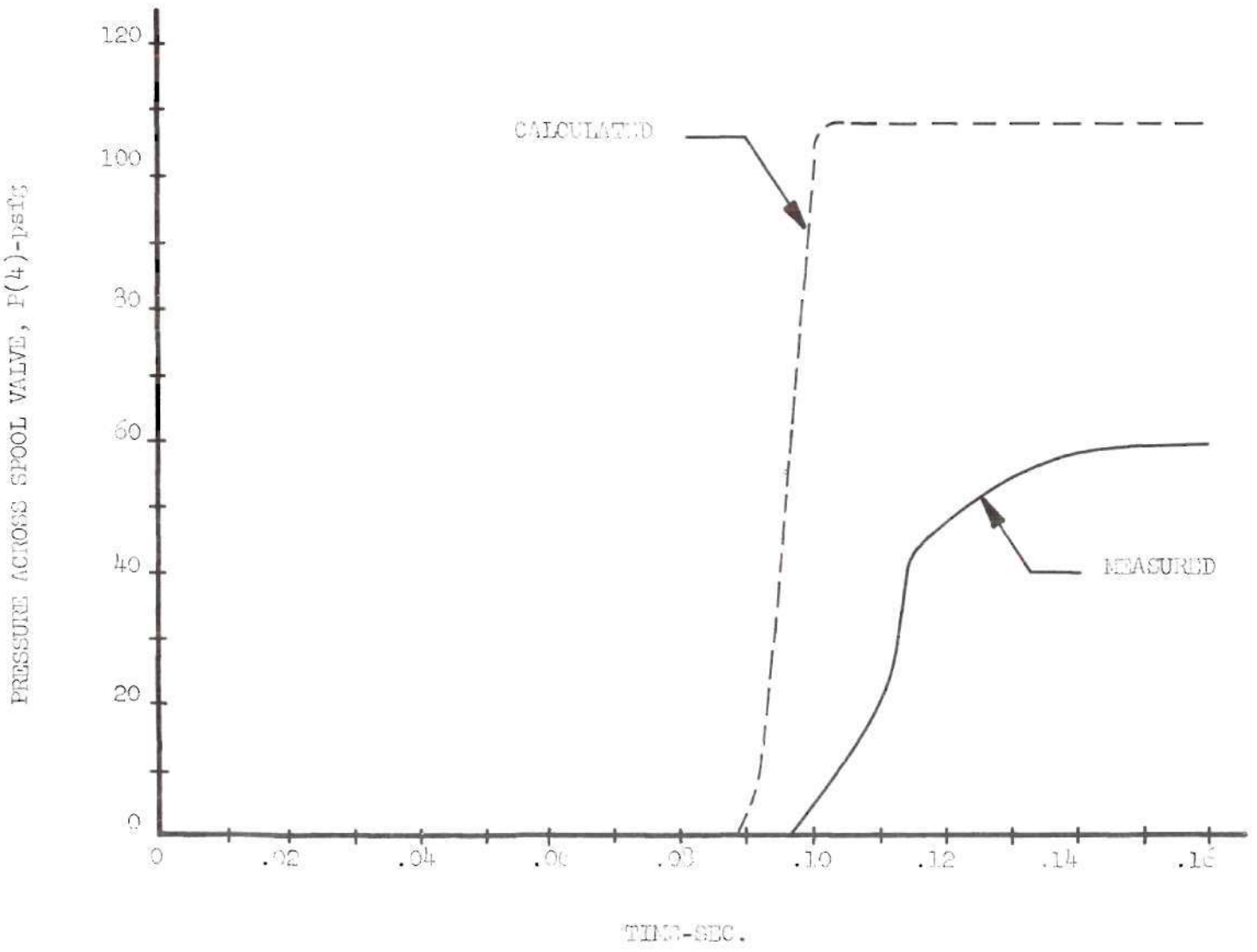

Figure 35. Transient Pressure Across Spool Valve--Calculated vs. Measured.

chapter. Since the valve used performed well enough to demonstrate the operability of the needle control system concept, it is assumed that a more accurate valve would be at least equally satisfactory.

Mathematical Model of Control System

Remaining Relationships

The final relationships necessary to complete a mathematical model of the needle control system apply to the transmission of the pressure signal, P(4), through the line to the piston, and the movement of the spring-loaded piston itself. Both expressions are arrived at in the same manner as were equations (4.18a), (4.19), (4.20), (4.21) and equations (4.22a) and (4.23).

For the transmission of pressure P(4),

$$\ddot{P}(5) + 2(S2)(WN2)\,\dot{P}(5) + (WN2)^2\,P(5) = (WN2)^2\,P(4) \qquad (4.30a)$$

where:

$$S2 = \frac{(R)(L2)}{2(DE)(C)}\sqrt{\frac{1}{2} + \frac{VP}{(A1)(L2)}} \qquad (4.31)$$

$$WN2 = \frac{C}{L2\sqrt{\frac{1}{2} + \frac{VP}{(A1)(L1)}}} \qquad (4.32)$$

$$VP = (A3)(y) \qquad (4.33)$$

P(4) = pressure downstream of spool, psfg

P(5) = pressure at piston, psfg

S2 = damping ratio

WN2 = undamped natural frequency

L2 = length of line, ft

VP = terminal volume at piston, cu ft

A3 = area of piston face, sq ft

y = piston displacement, ft

For the motion of the spring-loaded piston,

$$(M2)\ \ddot{y} + (B2)\ \dot{y} + (K2)\ y = (A3)\ P(5) \qquad (4.34a)$$

where:

$$B2 = (0.02)\ \ 2\sqrt{(K2)(M2)} \qquad (4.35)$$

M2 = mass of piston, slugs

B2 = piston damping coefficient, lb-sec/ft

K2 = piston spring constant, lb/ft

State Variable Representation

Basically, seven differential equations--(4.14a), (4.13a), (4.18a), (4.22a), (4.27a), (4.30a), and (4.34a)--have been developed to describe the transient behavior of the several respective segments of the control system--pattern movement, signal input, first line transmission, spool motion, pressure transfer across spool valve, second

line transmission, and piston motion. The composite of these seven equations make up the mathematical model sought to describe the overall needle control system complex. In order to solve the equations, the computer program of Appendix C was written making use of the Runge-Kutta numerical integration technique (23) for the simultaneous solution of first order differential equations. Of course, four of the equations are second order. Therefore, using state variable representation (24), these four were rewritten as eight first order equations, such that the final basic system equations were

$$\dot{X}(1) = \dot{x} = \text{constant} \tag{4.14b}$$

$$\dot{X}(2)=\dot{P}(u)=\frac{(k)(R)(T)}{(VT)}\left(\frac{X(2)}{P(B)}\right)^{\frac{k-1}{k}}\frac{Cl}{\sqrt{T}}\left[(CDl)(AOl)(P(1))\left(\frac{X(2)}{P(1)}\right)^{\frac{1}{k}}\sqrt{1-\left(\frac{X(2)}{P(1)}\right)^{\frac{k-1}{k}}}\right.$$

$$\left. - (CD2)(AO2)(X(2))\left(\frac{P(B)}{X(2)}\right)^{\frac{1}{k}}\sqrt{1-\left(\frac{P(B)}{X(2)}\right)^{\frac{k-1}{k}}}\right] \tag{4.13b}$$

$$\dot{X}(3) = X(4) \tag{4.18b}$$

$$\dot{X}(4) = \ddot{P}(2) = -2(Sl)(WNl)\,X(4) - (WNl)^2\,X(3) + (WNl)^2\,X(2) \tag{4.18c}$$

$$\dot{X}(5) = X(6) \tag{4.22b}$$

$$\dot{X}(6) = \ddot{z} = -\left(\frac{Bl}{Ml}\right)X(6) - \left(\frac{Kl}{Ml}\right)X(5) + \left(\frac{A2}{Ml}\right)X(3) \tag{4.22c}$$

$$\dot{X}(7)=\dot{P}(4)=\frac{(R)(T)}{(VF)}\,(CD2)(A03)(C1)\,\frac{P(3)}{\sqrt{T}}\left(\frac{X(7)}{P(3)}\right)^{\frac{1}{k}}\sqrt{1-\left(\frac{X(7)}{P(3)}\right)^{\frac{k-1}{k}}} \qquad (4.27b)$$

$$\dot{X}(8) = X(9) \qquad (4.30b)$$

$$\dot{X}(9) = \ddot{P}(5) = -2(S2)(WN2)\,X(9) - (WN2)^2\,X(8) + (WN2)^2\,X(7) \qquad (4.30c)$$

$$\dot{X}(10) = X(11) \qquad (4.34b)$$

$$\dot{X}(11) = \ddot{y} = -\left(\frac{B2}{M2}\right)X(11) - \left(\frac{X2}{M2}\right)X(10) + \left(\frac{A3}{M2}\right)X(8) \qquad (4.34c)$$

The above composite of equations together with complimentary equations (4.15), (4.16), (4.19), (4.20), (4.21), (4.23), (4.28), (4.29), (4.31), (4.32), (4.33), and (4.35) were the specific relationships used in Appendix C.

The foregoing mathematical model is intended to serve at least three needs with respect to development of an improved needle control system for tufting. First, as already illustrated in Figures 31 and 32, the effect of parameter changes in the system can be studied without physically making the changes. Secondly, troubleshooting of the system is simplified considerably with the aid of calculated results as in the computer program printout of Appendix C. For example, with these results, timing problems can be more clearly diagnosed and cor-

rective measures can be readily evaluated. Finally, the mathematical model should prove very helpful in extending the system development beyond that embodied in this thesis. Recalling from Chapter III, several alternative system components could well be found preferable to those chosen by the author. Also, cycling of air sppears to offer some advantages that have not been explored. In any event, it is hoped that the mathematical model developed here, particularly that portion describing the sensing nozzle behavior (input signal), will prove useful in future research efforts in this area.

Selection of Springs

Response Limitation

As long as components are reasonably uniform such that all 300 (plus) signals sensed from a pattern at any instant of time are transmitted to the corresponding 600 positions at the needle drive bar in approximately the same length of time, there is but one major response limitation in the control system. Enough time must elapse at the top of the tufting machine stroke to permit the piston to thrust into the notched needle holder in response to a signal to sew, or, conversely, to allow the piston to withdraw from the notch when a signal to sew no longer exists. Referring back to Figure 12, the factors which affect the piston movement are the position of the striking bar, the force exerted on the piston by the spring, and the force of the signal

pressure on the face of the piston.

The length of time at the top of the stroke during which the piston tip can move in or out of the notched recess in the needle holder is governed by the position of the cast iron striking bar. In the timing diagram of Figure 36, the total time for a complete

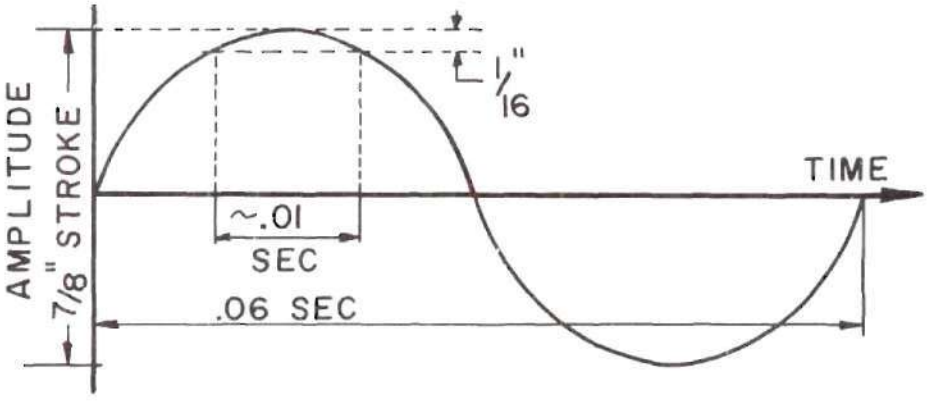

Figure 36. Timing Diagram.

cycle of the eccentric drive is shown as 0.06 sec (corresponding to 1000 strokes per minute). If the striking bar is positioned such that the needle holder is stopped 1/16 in. below the top of the stroke as shown, then approximately 0.01 sec will elapse during which the piston can move in or out of the recess.

Thus it is seen that the first step in determining the complement of springs to be used is to establish the time limitation for piston response in accordance with the position of the striking bar. For convenience, the sequential steps taken to select the proper springs are enumerated below and amplified afterward.

(1) Choose the desired piston response time (see above).

(2) Calculate the strength of the piston spring.

(3) Determine the pressure required to actuate the piston.

(4) Find the corresponding strength of the needle holder retaining spring.

(5) Select a spool valve spring.

Piston Spring

Having established a time limit in which to withdraw the piston from the needle holder notch, the minimum strength of the piston spring can be determined. Neglecting the damping term, the equation for piston withdrawal is

$$(M2)\ \ddot{y} + (K2)\ y = 0 \tag{4.36}$$

The solution to equation (4.36) is

$$y(t) = y(0)\cos\left[\sqrt{\frac{K2}{M2}}\ t\right] \tag{4.37}$$

Equation (4.37) can be rewritten

$$K2 = M2\left[\frac{\cos^{-1}\left(\frac{y(t)}{y(o)}\right)}{t}\right]^2 \tag{4.38}$$

where:

y(o) = initial spring compression, ft

t = independent variable--time, sec

From equation (4.38), the value of the spring constant can be directly calculated in keeping with the chosen time limitation.

The minimum pressure required to actuate such a spring-loaded piston is determined from

$$P(5) = \frac{(K2)\ y(o)}{A3} \tag{4.39}$$

Needle Holder Retaining Spring

Having selected a piston spring from equation (4.38) in keeping with the desired piston response behavior, the needle holder retaining spring can then be selected. First the needle holder spring must be at least strong enough to assure that the notch does not separate from the piston tip at any point during a sewing stroke; otherwise, the piston might withdraw near the bottom of a stroke and result in machine damage during the loop cutting process. Since maximum acceleration occurs at the bottom of the stroke, then the needle holder retaining spring must be strong enough to maintain an upward force at that time. Again neglecting damping, the equation of motion for the spring holder is

$$(Mh)\ \ddot{d} + (Kh)\ d = Fh \tag{4.40}$$

where:

Mh = mass of holder, slugs

d = displacement of holder from center of stroke, ft

Kh = holder spring constant, lb/ft

Fh = force on holder

The holder displacement is a function of the drive eccentric position,

$$d = A \sin (\omega t) \tag{4.41}$$

where:

A = amplitude of stroke, ft

ωt = angular position of eccentric

Combining equations (4.40) and (4.41),

$$-(Mh)(A)(\omega^2) \sin (\omega t) + (Kh)(A) \sin (\omega t) = Fh \tag{4.42}$$

Since the force, Fh, must remain positive at the bottom of the stroke, where ωt is 90 degrees, then it can be seen from equation (4.42) that the minimum spring constant is

$$Kh = (Mh)(\omega^2) \tag{4.43}$$

However, Kh must be some value above the minimum of equation (4.43)--at least enough to maintain sufficient force on the piston tip to prevent the tip from being withdrawn by the force of the piston spring. Therefore, the case must be examined in which the piston is

most likely to retract from the notched recess in the needle holder. As already explained, this likelihood is greatest at the bottom of the stroke, when the force, Fh, is least. The analysis is based upon the forces acting on the piston, as illustrated in Figure 37. P is the

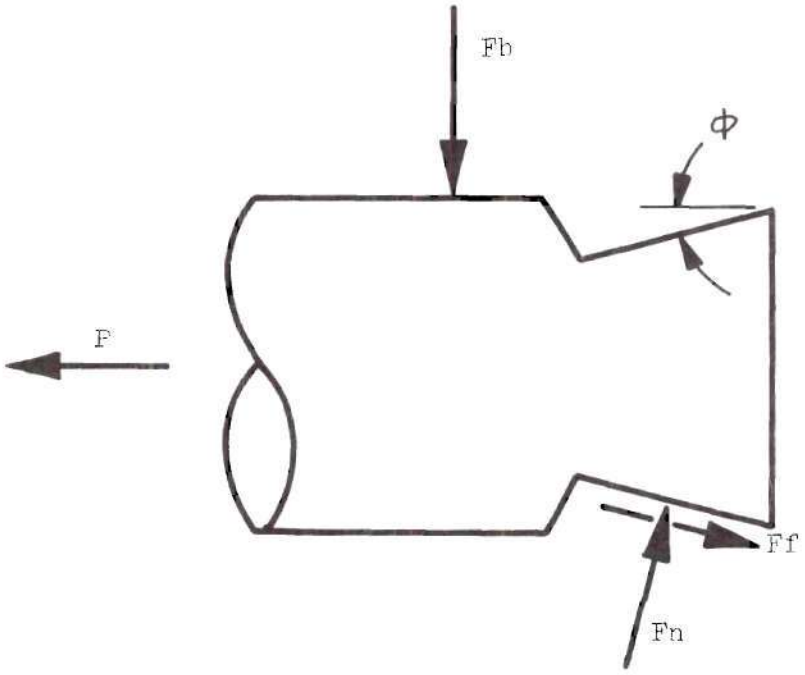

Figure 37. Forces on Piston.

force exerted by the spring on the piston, which is K2 times the spring compression distance. The slanted needle holder notch surface exerts restraining forces on the piston tip as shown. By summing forces in both the vertical and horizontal directions, an expression is derived from which the force (minimum) exerted by the needle holder retaining spring can be found to correspond to the piston spring already selected,

$$Fh = \frac{P}{\frac{\sin \varphi}{\cos \varphi - f} + \cos \varphi} \qquad (4.44)$$

where:

φ = angle of piston tip

f = coefficient of friction

From the foregoing spring calculations it is evident that the specific springs selected for use in the control system could vary in strength considerably and remain within the limitations of the system. Furthermore, the limitations can be changed if necessary. For example, increasing the angle of the notch in the needle holder recess or strengthening the needle holder retaining spring would materially increase the allowable strength of the piston spring. In the final analysis, the optimum specific complement of springs will doubtlessly be determined by actual experience with the machine in operation.

Spool Valve Spring

Just as with the piston spring, a wide range of springs for the spool valve might conceivably be chosen, depending upon the pressure level and/or response desired. There is no specific response limitation for the spool valve in the manner of that for the piston spring, except that all valves must function with essentially the same operating delay. To be certain that the behavior of individual valves does

not affect the performance of the control system, it is probably best to select a valve spring which is strong enough to insure full spool travel within 0.001 sec, thus maintaining fractional time variations relatively insignificant. Writing the fundamental relationship,

$$(M1)\ \ddot{z} + (K1)\ z = (A2)\ P(2) \tag{4.45}$$

assuming the closed valve spring is not initially compressed, equation (4.45) can be solved as

$$t = \sqrt{\frac{M1}{K1}}\ \cos^{-1}\left[\frac{(A2)\ P(2)}{K1} - z(t)\right] \tag{4.46}$$

From this expression, the time for full spool travel can be found for an assumed step pressure input.

Test Springs Selected

For this project, piston and spool springs were made with a lathe by winding 0.007 in. diameter music wire around a rod. In order to determine a working value for a particular piston spring constant, the spring was actually placed in the piston housing assembly (see Figure 12), and the extension of the piston tip was measured at a recorded pressure.

Arbitrarily assuming a time limit for piston response of 0.006 sec, a value for the piston spring constant was determined from equa-

tion (4.38) to be 2.0 lb/ft. Here, the initial spring compression was 7/32 in. From equation (4.39), the pressure required to actuate the piston is 1.6 psig. From equation (4.44), where φ is 15 degrees, the minimum Fh was found to be 0.024 lb. This value of Fh was substituted into equation (4.42)* to give a minimum needle holder spring constant, Kh, or 22.8 lb/ft. (A spring constant of 24.0 lb/ft was actually used.) For convenience, the same spring strength (2.0 lb/ft) selected for the piston was also used for the spool valve. From equation (4.46), the time required for full spool travel with this spring is 0.009 sec, where a step pressure input of 0.5 psig was assumed.

The particular piston spring strength was chosen to permit testing in the range (below 4 psig) of nozzle supply manifold pressures originally used to develop the nozzle. A machine in production would probably use higher pressures and stronger springs, an option readily available to provide a safety factor of operation. Also, a much stronger spring could be selected for the needle holder; however, an unnecessarily strong spring--when multiplied by more than 600--necessitates unwarranted use of machine power to actuate the drive bar.

---

*Where sin (ωt) = 1 at the bottom of the stroke.

CHAPTER V

DISCUSSION OF RESULTS

Performance Demonstration

The final objective of the research project was the verification of the conceived needle control system in simulated practice. To accommodate a test demonstration, a machine was constructed--using a drive eccentric and push rod from an actual tufting machine--to give the proper stroke amplitude and speed. The simulated tufting machine is pictured in Figure 38. For reference, the top of the frame stands about 21 in. above the table top. The stroke distance of the machine is 7/8 in., and the speed was measured at 1048 strokes per minute. At this speed, despite heavy frame construction and careful adjustment of a counterweight on the eccentric drive shaft, considerable vibration occurred during operation of the machine, requiring that it be securely anchored to the heavy table shown in the pictures. The slotted drive bar and associated features of the design outlined in Figure 12 were adapted to the test machine as also seen in the pictures. The horizontal rod above the drive bar anchors the top of the needle holder retaining spring. The rod level can be changed by inserting the rod through frame holes provided at different elevations. At the bottom

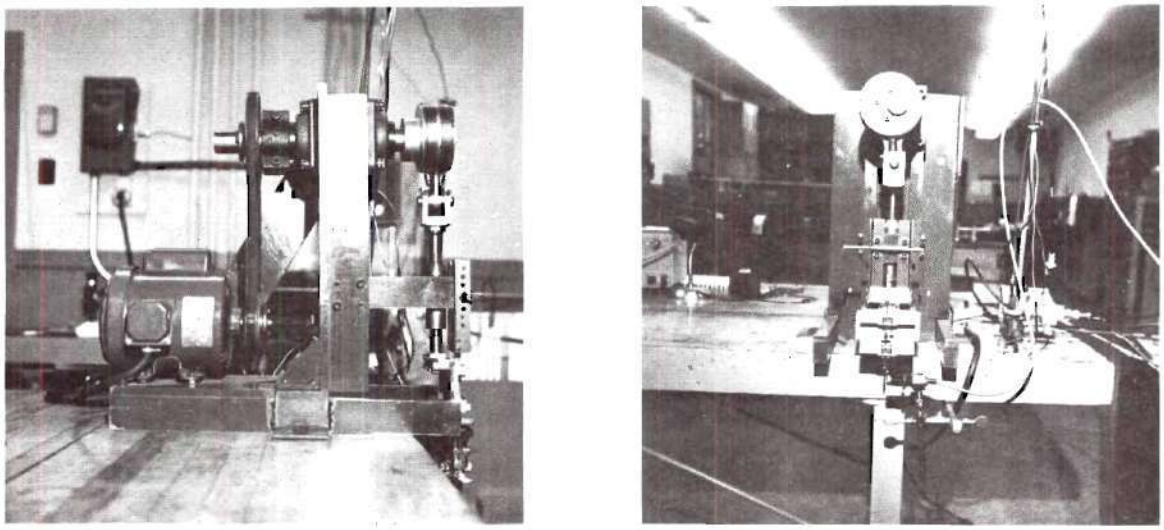

Figure 38. Simulated Tufting Machine.

of the framework holding the rod is seen the cast iron striking bar against which the retaining spring is pulling a single needle holder.

An entire needle control system was assembled in the manner diagrammed in Figure 13. The pattern and sensing nozzle arrangement of Figure 24 were connected to the spool valve of Figure 11 with a 12 ft length of 1/8 in. standard copper tubing. Six additional feet of tubing joined the spool valve to a short flexible length of 1/16 in. vinyl tubing which connected to the piston assembly in the machine drive bar.

During the tests described in Chapter IV, it was found that both the notch in the mild steel needle holder and the tip of the stainless steel piston received battering damage during operation. In order to conduct a reliability test, therefore, both the needle holder

notch and the piston tip were case-hardened with cyanide. A carbide insert in the needle holder might solve the problem of hardening the notch in a production version of the machine.

A second photocell pickup of the type shown in Figure 23 was positioned so as to sense a needle holder at the bottom of a sewing stroke only (see Figure 38). Using a simple bridge circuit the photocell signal was displayed as a blip on one channel of a Sanborn recorder. The Statham pressure transducer (Figure 22) was placed in the transmission line close to the piston at the drive bar, and the pressure signal was recorded on the other recorder channel. In this manner the pressure signals created indirectly from sensing a pattern could be compared directly with the resulting number of simulated stitches, thus demonstrating the successful performance of the needle control system concept.

For the reliability test, one piece of 0.007 in. thick shim stock approximately 0.47 in. wide was glued to the face of the test gear. It was noticed in the previous calculations (see Appendix C) that a manifold pressure of 2 psig (4 in. Hg) will barely open the spool valve, and measured pressures were found less than calculated values. For this reason the reliability test was made at a sensing nozzle supply manifold pressure of 3 psig and the gap between the pattern (shim piece) and the nozzle was narrowed to about 0.0025 in.,

thus giving added insurance of sustained operation on the first try with the specially hardened components.

The reliability test was conducted for a period of one hour, and sample recordings taken at the beginning and end of testing are given in Figure 39. It is seen that the performance was the same at

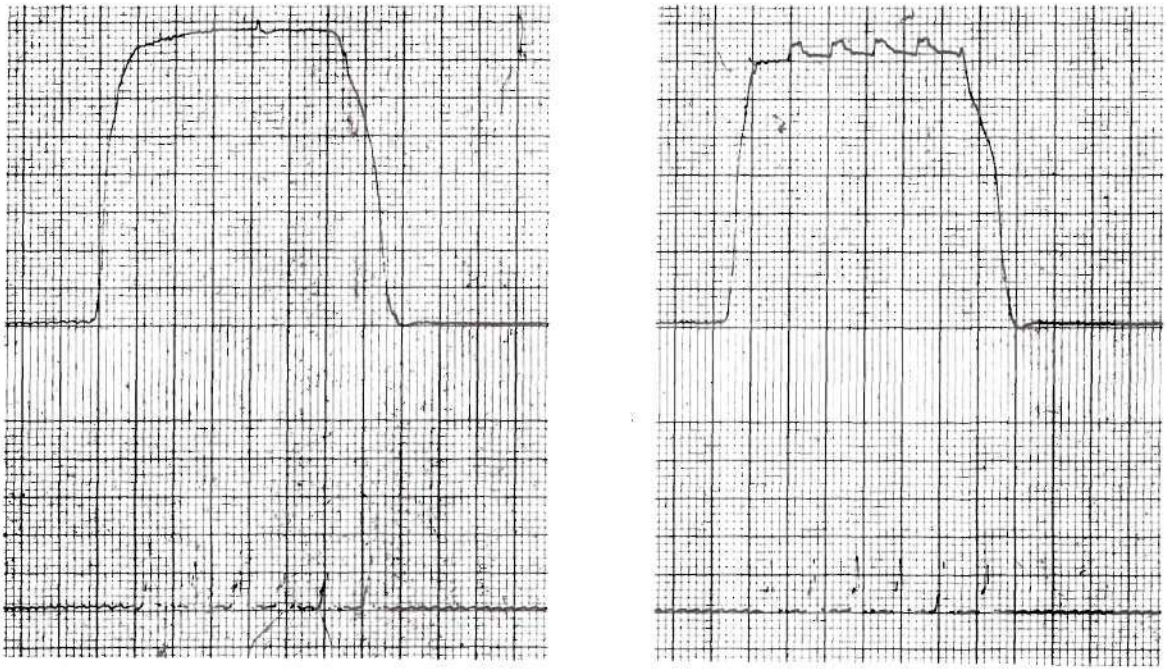

(A) At Start (B) After One Hour

Figure 39. Reliability Performance Recording.

the beginning and end of the test. A spool valve manifold supply pressure, P(3), of 1.75 psig produced a pressure signal (see Figure 39) of almost 0.8 psig at the piston for a duration of 6 stitches. (On several trials during the hour test, seven stitches were recorded.) While the repeatability of the needle control system concept was demonstrated by this test, it should be noted that the pressure signal should have

lasted long enough to produce 9 stitches instead of 6. Again, this is attributed to the excessive leakage both at the spool valve and at the piston, where cleaning a distorted piston after heat treatment introduced additional clearance and therefore leakage. A time delay of at least the transmission line lengths divided by the speed of sound always exists through the system from an input pressure signal to the corresponding pressure buildup at the piston. On the other hand, leakage will allow the pressure to dissipate without the same time delay when the input signal is removed. It is believed that this explains the shortage of stitches in the test. Several potential remedies to correct this problem are:

1. Eliminate significant leakage at the spool and piston with O-ring seals or the like.
2. Shorten the transmission lines as necessary to remove the problem.
3. Gear down the pattern drive in a manner to produce the correct number of stitches to correspond to a given pattern area.
4. Use a shrink rule to construct the lengthwise pattern dimensions at the proper proportion to produce the desired number of stitches.

By locating the spool valve near the sensing nozzle, thus essentially eliminating the first transmission line delay, 7 and 8 stitches

were produced as compared with the 6 of Figure 39.

Results Compared with Objectives

Single needle control on 3/16 in. centers has been accomplished by converting to a needle holder with rectangular cross section. It is believed that the individual needle holders will actually maintain orientation better than the dual holders now in service, and that replacement of the holders due to wear will occur less often.

The design criterion for machine speed was 1000 strokes per minute, a rate less than that demonstrated with the simulated machine. This speed is by no means the maximum which can be achieved using the concepts generated in this research project. Vibration problems in the existing machine may be found to limit machine speed before the upper reaches of response using the described control system are explored.

The sensitivity requirements were more than met as discussed in Chapter III, and the desired pattern scale factors were adhered to except as noted above. The control system is not at all difficult to understand and should prove relatively easy to maintain by semiskilled personnel. From the pattern to pistons, very little wear should occur, which should make for a long-lived system.

It is difficult to assess the cost of all elements of the control system without having fabricated an entire machine. It is expec-

ted that the cost (in production) will be less than half that specified in the project definition, including the air compressor equipment required. As already mentioned, pattern costs will be less than a third of the phenolic drums now in use.

An important feature of the needle control system described herein is the safety factor of operation. As discussed before, a number of courses of action are available with which to adjust the performance of a machine in use. Also, several dimensional changes can easily be made to materially alter the control system response and sensitivity. Much of the research conducted during this project was relatively conservative in premise, and performance considerably superior to that indicated could reasonably be achieved by close control of machine tolerances.

Present Status

Of course, a great deal of difference exists between successfully conceiving a control concept and fabricating an actual machine which operates reliably for long periods at a competitively favorable cost. Undoubtedly, problems that have not been foreseen will be encountered in the endeavor to convert the concepts of this project into an operating tufting machine. Also, additional precautions may be found necessary to permit a pneumatic concept of this nature to function for long periods in the heavily lint-laden atmosphere commonly found in tufting

mills. A method for accurately attaching a pattern to a drum is an exacting design project as envisioned for piece goods such as bedspreads. A means to mount a pattern on the drum for tufting continuous goods must yet be worked out.

In conclusion, this was an unusual research and development project in which virtually all of the objectives originally envisioned were met or bettered. Using the needle control system concept developed, it appears that a tufting machine can be manufactured which gives improved performance at greater speed, is less expensive to build and operate, and is subjected to less wear and maintenance requirements when compared to existing machines in comparable service. It is the wish of the author that some variation of the needle control system spawned through this project will prove to be a significant contribution to tufting and allied industries.

APPENDIX

APPENDIX A

FLUID AMPLIFIERS

A great many variations exist in fluidic devices, but these studies were confined to three basic kinds for purposes of evaluation only.

Bistable Amplifier

A typical bistable (25, 26, 27, 28, 29) fluid amplifier is illustrated in Figure 40. This device employs the Coanda effect of jet attachment to a nearby wall. As an air jet approaches a wall, the pressure near the wall is lowered due to reduced counterflow area such that the jet will attach to the wall in a stable manner. As shown in the figure, a small control jet properly positioned will separate a power jet from the wall and deflect it to the opposite wall, where it clings until a signal is applied through the corresponding control jet. Pressure gains of five to seven are obtained per stage in cascades of these amplifiers, with response speeds above 1000 cycles per second.

Using a controlled bleed variation of the bistable amplifier to harness the dynamic pressure, it is entirely conceivable that a satisfactory pneumatic control system could be devised for tufting machinery.

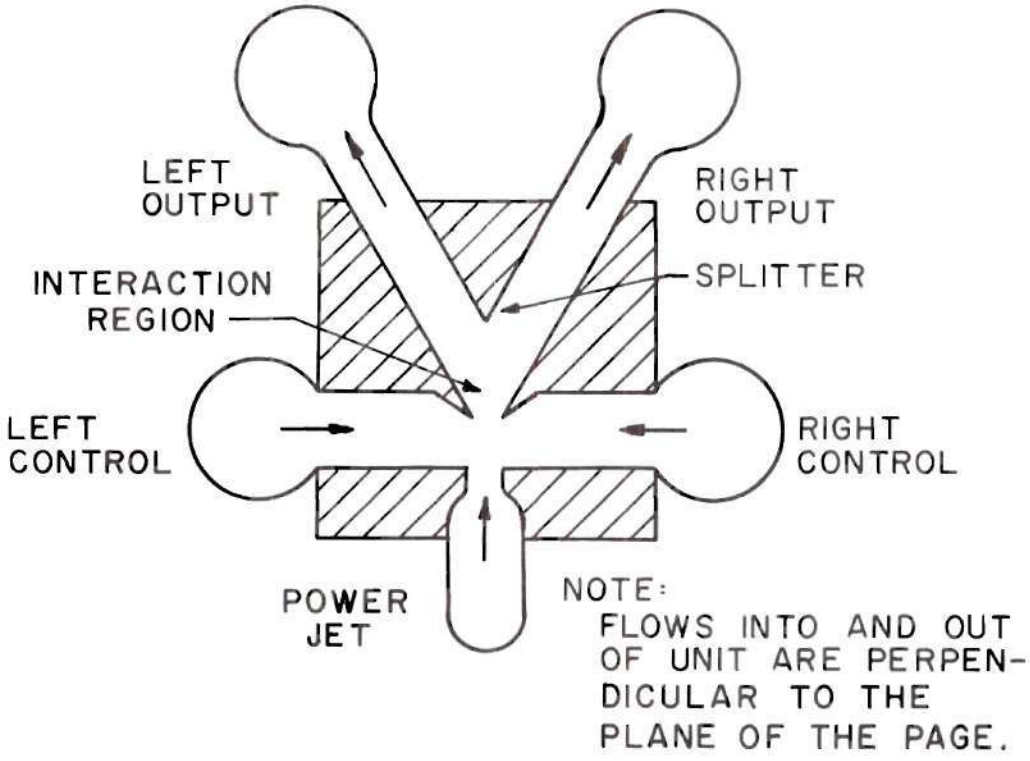

Figure 40. Bistable Amplifier.

Inexpensive manufacturing costs and absence of wear would be principal attractive features, whereas problems might be encountered with air consumption rates, staging transients, and the low signal-to-noise ratio.

Turbulence Amplifier

A second basic kind of fluid amplifier is the turbulence amplifier (30, 3) as represented in Figure 41. A laminar stream of air can be projected across a gap as great as 100 times the diameter of a

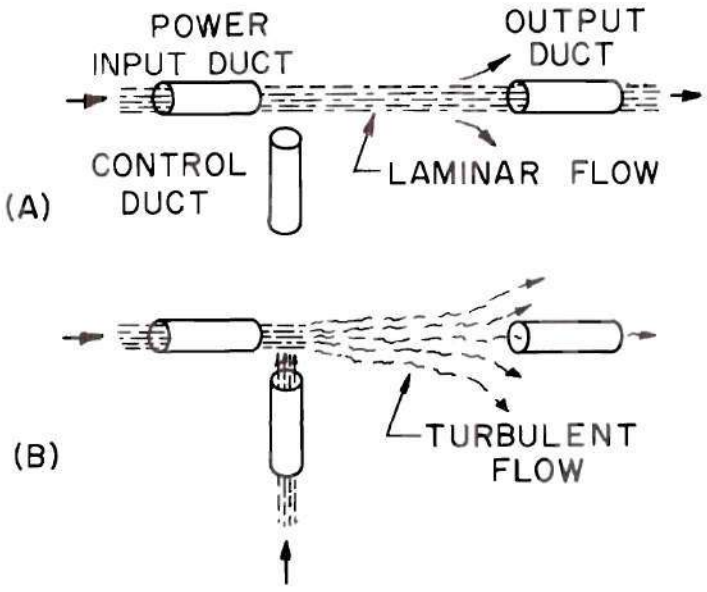

Figure 41. Turbulence Amplifier.

smooth-walled tube. Thus, in (A) of the figure most of the pressure from the power input duct is captured in the output duct. A small disturbance through the control duct, however, will cause the projected stream to become turbulent, resulting in a sharp drop in output duct pressure.

A slower response speed of less than 100 cycles per second may be adequate in the proposed service but would nevertheless be somewhat of a liability for the turbulence amplifier. As compared with the bistable device, air consumption is less and transient difficulties are far less. Again, inexpensive manufacturing costs and lack of moving parts are assets. But perhaps the most severe restriction in use of

turbulence amplifiers concerns the low power which can be developed. The maximum supply pressure is approximately 3/4 psig, a low borderline value for the defined application.

Vortex Amplifier

The last fluid amplifier considered was the vortex amplifier (32, 33) as pictured in Figure 42. With no control flow, the power

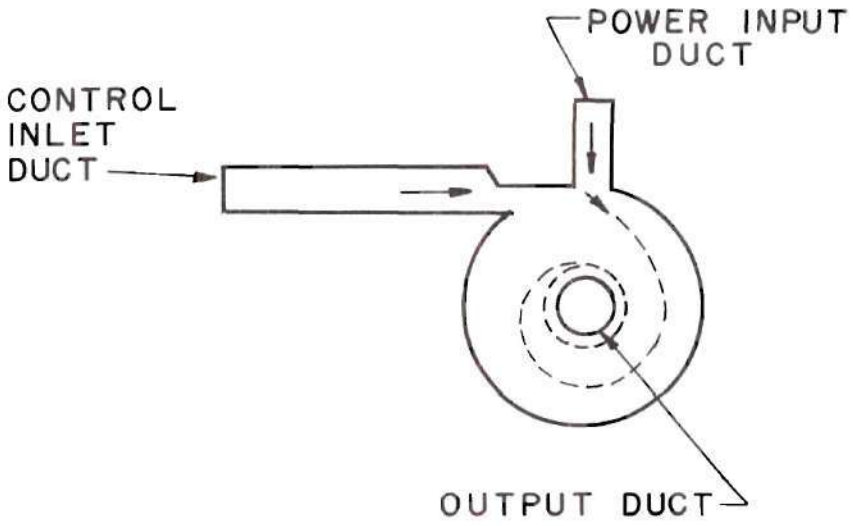

Figure 42. Vortex Amplifier.

stream flows radially across the cylinder to the output duct, encountering very little impedence to flow. When a control input flow is admitted tangential to the outer wall of the cylinder, a spiraling flow results causing increased impedence and greatly diminishing the flow output. A frequency response in the order of 150 cycles per second is obtained with this instrument.

As with the bistable and turbulence devices, vortex amplifiers are relatively low in cost and have no wear problems. A detrimental feature is the three dimensional space required for each unit.

APPENDIX B

GEOMETRICAL VARIATION OF SENSING NOZZLE ORIFICE

A sensing nozzle having a base hole radius of RN and a gap between the nozzle mouth and a pattern raised surface of G can create a maximum orifice size of $\pi(RN)^2$ and a minimum of $2\pi(RN)(G)$. In between the orifice size is a combination of areas A1, a segment of a circle, and A2, a portion of a cylinder wall, as pictured in Figure 43.

In section (A) of the figure, the area of the segment A3 for $0 < X < RN$ is given by

$$A3 = (RN)^2 \cos^{-1}\left(\frac{RN-x}{RN}\right) - (RN-x)\sqrt{2(RN)(x) - x^2} \qquad (B.1)$$

In order that the equation can be computerized, $\cos^{-1}$ is converted into $\tan^{-1}$ using the relationship

$$\cos^{-1}\left(\frac{RN-x}{RN}\right) = \tan^{-1}\left(\frac{\sqrt{1-\left(\frac{RN-x}{RN}\right)^2}}{\frac{RN-x}{RN}}\right) \qquad (B.2)$$

By inspection,

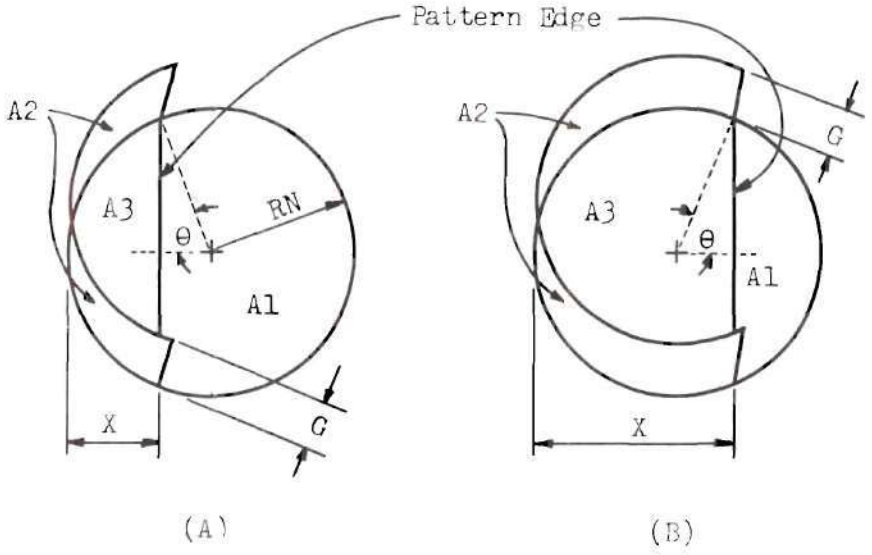

Figure 43. Sensing Nozzle Orifice Diagrams.

$$\cos \theta = \frac{RN-x}{RN} \tag{B.3}$$

and

$$A2 = (RN)(2\theta)(G) \tag{B.4}$$

and

$$AO2 = A2 + A1 = A2 + (\pi)(RN)^2 - A3 \tag{B.5}$$

Combining the equations above on the following page, for $0 < x < RN$,

$$AO2 = 2(G)(RN)\ \tan^{-1}\left(\frac{\sqrt{1-\left(\frac{RN-x}{RN}\right)^2}}{\frac{RN-x}{RN}}\right) + \pi(RN)^2$$

$$- \left[(RN)^2\ \tan^{-1}\left(\frac{\sqrt{1-\left(\frac{RN-x}{RN}\right)^2}}{\frac{RN-x}{RN}}\right) - (RN-x)\sqrt{2(RN)(x)-x^2}\right] \qquad (B.6)$$

where:

$$AO2 \leq \pi(RN)^2$$

Similarly, referring to section (B) of Figure 43, for $RN \leq x \leq 2(RN)$,

$$A1 = \frac{\pi}{2}(RN)^2 - \left[(x-RN)\sqrt{(RN)^2-(x-RN)^2} + (RN)^2\ \sin^{-1}\left(\frac{x-RN}{RN}\right)\right] \qquad (B.7)$$

$$\sin^{-1}\left(\frac{x-RN}{RN}\right) = \tan^{-1}\left(\frac{\frac{x-RN}{RN}}{\sqrt{1-\left(\frac{x-RN}{RN}\right)^2}}\right) \qquad (B.8)$$

$$\theta = \cos^{-1}\left(\frac{x-RN}{RN}\right) = \tan^{-1}\left(\frac{\sqrt{1-\left(\frac{x-RN}{RN}\right)^2}}{\frac{x-RN}{RN}}\right) \qquad (B.9)$$

$$A2 = (G)(RN)(2\pi - 2\theta) \qquad (B.10)$$

Thus,

$$AO2 = (G)(RN)\left[2\pi - 2\tan^{-1}\left(\frac{\sqrt{1-\left(\frac{x-RN}{RN}\right)^2}}{\frac{x-RN}{RN}}\right)\right] + \frac{\pi(RN)^2}{2}$$

$$-\left[(x-RN)\sqrt{RN^2-(x-RN)^2} + (RN)^2\tan^{-1}\left(\frac{\frac{x-RN}{RN}}{\sqrt{1-\left(\frac{x-RN}{RN}\right)^2}}\right)\right] \quad \text{(B 11)}$$

where:

$$AO2 \geq 2\pi(RN)(G)$$

APPENDIX C

REPRESENTATIVE COMPUTER PROGRAM

```
BEGIN                                                                    0
COMMENT  MATHEMATICAL MODEL OF NEEDLE CONTROL SYSTEM                    10
                FOR TUFTING MACHINERY                S F PETRY      ;   20
INTEGER  H1,H2,I,J,L,M,N,ND1,ND2,S                                  ;   30
REAL     A1,A2,A3,ADJK,AD1,AD2,B1,B2,C,C1,CD1,CD2,CD3,D1,D2,D3,DE,DT,    40
         FC1,FC2,FC3,FC4,FC5,FIN,G,K1,K2,KA,KF1,KF2,L1,L2,M1,M2,PA,PB,   50
         PI,POS,P1,P2,P3,P4,P5,R,RA,RN,RO,S1,S2,T,TA,TB,TF,TI,U,V1,V2,   60
         VF,VP,VS,VT,WN1,WN2                                        ;   70
LABEL    CALL,SKIP,BAT,EQ1,EQ2,EQ3,RUN,FINIS                        ;   80
ARRAY    AX[0:13],X[0:11,0:599],K[0:12,0:4],DX[0:13]                ;   90
FILE     LINES 6(2,15)                                              ;  100
LIST     IN1(TB,DT,M),                                                 110
         IN2(FOR J ← 1 STEP 1 UNTIL M DO X[J,0])                    ;  120
FORMAT   FL1(X35,"TB =",F7.3,X5,"DT =",F7.4,X5,"M =",I3//),            130
         FL2(X45,"INITIAL CONDITIONS",/)                            ,  140
         FL3(X48,F10.4),                                               150
         FL4(//,X3,"N",X5,"TIME",X7,"X[1,N]",X8,"X[2,N]",X8,"X[3,N]",X8,  160
         "X[5,N]",X8 ,"X[7,N]",X8 ,"X[8,N]",X8 ,"X[10,N]",/),          170
         FL5(X22,"X",X13,"PU",X12,"P2",X12,"Z",X13,"P4",X12,"P5",       180
         X13,"Y",//),                                                  190
         FL6(I4,F10.4,7E14.4)                                       ;  200
COMMENT  A1 = INSIDE AREA OF TRANSMISSION LINE, SQ FT                   210
         A2 = AREA OF SPOOL FACE, SQ FT                                 220
         A3 = AREA OF PISTON FACE, SQ FT                                230
         ADJK = ADJUSTMENT FACTOR FOR ALL VARIABLES                     240
         AD1 = AREA OF ORIFICE FROM MANIFOLD INTO SENSING NOZZLE        250
               (0.00000218 SQ FT)                                       260
         AD2 = VARIABLE AREA OF ORIFICE AT MOUTH OF SENSING NOZZLE,SQ FT 270
         AD3 = VARIABLE AREA OF ORIFICE AT MANIFOLD ENTRANCE TO SPOOL   280
               VALVE, SQ FT                                             290
         B1 = SPOOL DAMPING COEFFICIENT, LB-SEC/FT                      300
         B2 = PISTON DAMPING COEFFICIENT, LB-SEC/FT                     310
         C = SPEED OF SOUND (1130 FPS)                                  320
         C1 = 2.06 DEG R/SEC                                            330
         CD1 = COEFFICIENT OF DISCHARGE, ORIFICE AT MANIFOLD ENTRANCE   340
               TO SENSING NOZZLE                                        350
         CD2 = COEFFICIENT OF DISCHARGE, ORIFICE AT MOUTH OF SENSING    360
               NOZZLE                                                   370
         CD3 = COEFFICIENT OF DISCHARGE, ORIFICE AT MANIFOLD ENTRANCE   380
               TO SPOOL VALVE                                           390
         D1 = INSIDE DIAMETER OF TRANSMISSION LINE (0.00521 FT)         400
         D2 = DIAMETER OF SPOOL FACE (0.0156 FT)                        410
         D3 = DIAMETER OF PISTON FACE (0.0146 FT)                       420
         DE = DENSITY OF AIR (0.0023 SLUGS/FT-SEC)                      430
         DT = STEP INCREMENT OF TIME, SEC                               440
         FC1 = FACTOR USED TO CALCULATE FC2                             450
         FC2 = FACTOR USED TO CALCULATE AD2                             460
         FC3 = FACTOR USED TO CALCULATE FC4 AND FC5                     470
         FC4 = FACTOR USED TO CALCULATE AD2                             480
         FC5 = FACTOR USED TO CALCULATE AD2                             490
         FIN = REAL NUMBER APPROXIMATING UNITY (1.000000001)            500
         G = GAP BETWEEN RAISED PATTERN SURFACE AND MOUTH OF SENSING    510
             NOZZLE (0.00025 FT)                                        520
         H1 = TIME DELAY INDEX THROUGH FIRST TRANSMISSION LINE          530
         H2 = TIME DELAY INDEX THROUGH SECOND TRANSMISSION LINE         540
         K1 = SPOOL SPRING CONSTANT (2.0 LB/FT)                         550
         K2 = PISTON SPRING CONSTANT (2.0 LB/FT)                        560
         KA = POLYTROPIC EXPONENT FOR AIR (1.4)                         570
         L1 = LENGTH OF FIRST TRANSMISSION LINE, FROM SENSING NOZZLE    580
              TO SPOOL VALVE (12.0 FT)                                  590
         L2 = LENGTH OF SECOND TRANSMISSION LINE, FROM SPOOL VALVE      600
              TO PISTON (6.0 FT)                                        610
```

```
M = NUMBER OF STATE VARIABLES                                              620
M1 = MASS OF SPOOL (0.0001485 SLUGS)                                       630
M2 = MASS OF PISTON (0.000118 SLUGS)                                       640
N = INTEGRAL NUMBER OF TIME INCREMENTS                                     650
ND1 = TIME DELAY FACTOR THROUGH FIRST TRANSMISSION LINE                    660
ND2 = TIME DELAY FACTOR THROUGH SECOND TRANSMISSION LINE                   670
PA = ATMOSPHERIC PRESSURE (2116.8 PSFA)                                    680
PB = PRESSURE OUTSIDE OF SENSING NOZZLE MOUTH, PSFG                        690
PI = 3.1416                                                                700
PUS = FACTOR USED AS LIMIT GAUGE IN PROGRAM                                710
P1 = PRESSURE IN NOZZLE SUPPLY MANIFOLD (288.0 PSFG)                       720
P2 = X[3,N] = VARIABLE PRESSURE SIGNAL AT SPOOL FACE, PSFG                 730
P3 = MANIFOLD SUPPLY PRESSURE TO SPOOL VALVE (108.0 PSFG)                  740
P4 = X[7,N] = VARIABLE PRESSURE DOWNSTREAM OF SPOOL VALVE, PSFG            750
P5 = X[8,N] = VARIABLE PRESSURE AT PISTON FACE , PSFG                      760
R = FRICTIONAL RESISTANCE OF TRANSMISSION LINE, LB-SEC/(FT)*4              770
RA = GAS CONSTANT (53.3 FT/DEG R)                                          780
RN = RADIUS OF SENSING NOZZLE BASE HOLE (0.002167 FT)                      790
RO = RADIUS OF HOLE AT SPOOL VALVE MANIFOLD SUPPLY (0.0026 FT)             800
S1 = DAMPING RATIO OF FIRST TRANSMISSION LINE                              810
S2 = DAMPING RATIO OF SECOND TRANSMISSION LINE                             820
T = TIME,SEC                                                               830
TA = TEMPERATURE OF AIR (530.0 DEG R)                                      840
TB = STARTING TIME (0.0 SEC)                                               850
TF = SQUARE ROOT OF TA                                                     860
TI = TIME ACCUMULATED, SEC                                                 870
U = DYNAMIC VISCOSITY OF AIR (0.0000004 SLUGS/FT-SEC)                      880
V1 = VOLUME OF FIRST TRANSMISSION LINE (0.000278 CU FT)                    890
V2 = VOLUME OF SECOND TRANSMISSION LINE (0.0001277 CU FT)                  900
VF = TOTAL VOLUME BETWEEN SPOOL AND PISTON (V2 + VP)                       910
VP = VARIABLE TERMINAL VOLUME AT PISTON, CU FT                             920
VS = VARIABLE TERMINAL VOLUME AT SPOOL, CU FT                              930
VT = TOTAL VOLUME BETWEEN NOZZLE AND SPOOL (V1 + VS)                       940
WN1 = UNDAMPED NATURAL FREQUENCY, FIRST TRANSMISSION LINE                  950
WN2 = UNDAMPED NATURAL FREQUENCY, SECOND TRANSMISSION LINE      ;          960
TB ← 0.00                                                       ;          970
DT ← 0.0002                                                     ;          980
M ← 11                                                          ;          990
WRITE (LINES,FL1,IN1)                                           ;         1000
FOR J ← 1 STEP 1 UNTIL M DO                                               1010
X[J,0] ← 0.0                                                    ;         1020
X[2,0] ← 6.00                                                   ;         1030
X[3,0] ← 6.00                                                   ;         1040
WRITE (LINES,FL2)                                               ;         1050
FOR J ← 1 STEP 1 UNTIL M DO                                               1060
WRITE(LINES,FL3,X[J,0])                                         ;         1070
T ← TB                                                          ;         1080
WRITE (LINES,FL4)                                               ;         1090
WRITE (LINES,FL5)                                               ;         1100
P1 ← 288.0                                                      ;         1110
PI ← 3.1416                                                     ;         1120
U ← 4.0@-07                                                     ;         1130
DE ← 2.3@-03                                                    ;         1140
D1 ← 5.21@-03                                                   ;         1150
R ← (32)×(U/(D1*2))                                             ;         1160
C ← 1130.0                                                      ;         1170
A1 ← (3.1416/4.0)×(D1*2)                                        ;         1180
L1 ← 12.0                                                       ;         1190
M1 ← 1.485@-04                                                  ;         1200
K1 ← 2.0                                                        ;         1210
B1 ← (0.02)×(2.0×((K1×M1)*0.5))                                 ;         1220
D2 ← 0.0156                                                     ;         1230
A2 ← (3.1416/4.0)×(D2*2)                                        ;         1240
```

```
          CD1 ← 0.67                                                          ;    1250
          CD2 ← 0.87                                                          ;    1260
          CD3 ← 0.65                                                          ;    1270
          C1 ← 2.06                                                           ;    1280
          P3 ← 108.0                                                          ;    1290
          PA ← 2116.8                                                         ;    1300
          PB ← PA + X[2,0]                                                    ;    1310
          TA ← 530.0                                                          ;    1320
          TF ← (TA*0.5)                                                       ;    1330
          KA ← 1.4                                                            ;    1340
          KF1 ← (KA - 1.0)/KA                                                 ;    1350
          KF2 ← (1.0/KA)                                                      ;    1360
          RA ← 53.3                                                           ;    1370
          RU ← 0.0026                                                         ;    1380
          V1 ← 2.78@-04                                                       ;    1390
          V2 ← 1.277@-04                                                      ;    1400
          AU1 ← 2.18@-06                                                      ;    1410
          G ← .00025                                                          ;    1420
          RN ← .002167                                                        ;    1430
          L2 ← 6.0                                                            ;    1440
          M2 ← 1.18@-04                                                       ;    1450
          K2 ← 2.0                                                            ;    1460
          B2 ← (0.02)×(2.0×((K2×M2)*0.5))                                     ;    1470
          D3 ← 0.0146                                                         ;    1480
          A3 ← (3.1416/4.0)×(D3*2)                                            ;    1490
          FIN ← 1.000000001                                                   ;    1500
          ND1 ← ENTIER (L1/(C×DT))                                            ;    1510
          ND2 ← ENTIER (L2/(C×DT))                                            ;    1520
          S ← 0                                                               ;    1530
          H1 ← 0                                                              ;    1540
          H2 ← 0                                                              ;    1550
          N ← 0                                                               ;    1560
CALL:     IF H1 = 0 THEN DX[12] ← 0.0 ELSE                                         1570
          DX[12]← ((KA×KA×TA)/VT)×(((X[2,H1]+PA )/PA)*KF1)×(C1/TF)×                1580
          ((((CD1×AU1×(P1 + PA))×(((X[2,H1]+PA)/(P1 + PA))*KF2)×                   1590
          ((1.0 - (((X[2,H1]+PA)/(P1 + PA))*KF1))*0.5)) -                          1600
          (((CD2×AU2×(X[2,H1]+PA))×((PA/(X[2,H1]+PA))*KF2) ×                       1610
          ((1.0 - ((PA/(X[2,H1]+PA))*KF1))*0.5)))                             ;    1620
          IF X[5,H2] ≤ 0.00521 THEN DX[13] ← 0.0                              ;    1630
          IF S ≠ 0 THEN GO TO SKIP                                            ;    1640
          IF X[7,N] > 0.0 THEN S ← (N-1+ND2)                                  ;    1650
SKIP:     IF N ≤ S OR S = 0 THEN                                                   1660
BEGIN                                                                              1670
          DX[13] ← 0.0                                                        ;    1680
          GO TO BAT                                                           ;    1690
END                                                                           ;    1700
          IF (X[5,H2] > 0.00521) AND (X[5,H2] ≤ 0.00782) THEN                      1710
          DX[13]← (RA×TA/VF)×(CD3)×((RO*2)×(ARCTAN((RO×((1.0-(((RO-               1720
          (X[5,H2]-0.00521))/RO)*2))*0.5))/(RO-(X[5,H2]-0.00521))))                1730
          -((RO-(X[5,H2]-0.00521))×((((2.0×RO)×(X[5,H2]-0.00521))-                 1740
          ((X[5,H2]-0.00521)*2))*0.5)))×(((C1×(P3 + PA))/(TA*0.5)) ×               1750
          (((X[7,H2]+PA)/(P3 +PA))*(1.0/KA))×((1.0-(((X[7,H2]+PA)                  1760
          /(P3+  PA ))*((KA-1.0)/KA)))*0.5))                                  ;    1770
          IF X[5,H2] > 0.00782 THEN                                                1780
          DX[13] ← (RA×TA/VF)×(CD3)×((PI×(RO*2)/2.0)+(X[5,H2]-0.00782)             1790
          ×(((RO*2)-((X[5,H2]-.00782)*2))*0.5)+(RO*2)×(ARCTAN((X[5,H2]-            1800
          0.00782)/(RO×((1.0-(((X[5,H2]-.00782)/RO)*2))*0.5)))))×                  1810
          ((((C1×(P3 + PA ))/(TA*0.5)) ×  (((X[7,H2]+ PA )/(P3 + PA)) *            1820
          (1.0/KA))×((1.0-(((AX[7]   +PA)/(P3+PA)))*((KA-1.0)/KA)))*0.5)) ;    1830
BAT:      FOR L ← 1 STEP 1 UNTIL 4 DO                                              1840
BEGIN                                                                              1850
COMMENT   SELECT APPROPRIATE ADJUSTMENT FACTOR FOR K                          ;    1860
          ADJK ← IF L = 1 THEN 0 ELSE IF L = 4 THEN 1 ELSE 0.5                ;    1870
          T ← T + ADJK×DT                                                     ;    1880
          FOR I ← 1 STEP 1 UNTIL M DO                                              1890
```

```
BEGIN                                                                    1900
COMMENT  NOW ADJUST X WITH ADJUSTED K                                ;   1910
         AX[I] ← X[I,N] + ADJK × K[I,L-1]                            ;   1920
         AX[12]← X[2,H1]+ ADJK × DT × DX[12]                         ;   1930
         IF N ≤ ND1 THEN                                                 1940
BEGIN                                                                    1950
         AX[12] ← 0.0                                                ;   1960
         AX[3] ← 0.0                                                 ;   1970
END                                                                  ;   1980
         AX[13]← X[7,H2]+ ADJK × DT × DX[13]                         ;   1990
END                                                                  ;   2000
COMMENT  INSERT DIFFERENTIAL EQUATIONS ,LINEAR OR NON-LINEAR, IN         2010
         SELECTED STATE VARIABLE REPRESENTATION (USE ADJUSTED X)     ;   2020
         IF (N-ND1) < 0 THEN H1 ← 0 ELSE H1 ← (N - ND1)              ;   2030
         IF (N-ND2) < 0 THEN H2 ← 0 ELSE H2 ← (N - ND2)              ;   2040
         DX[1] ← 0.06944                                             ;   2050
         FC1 ← ((RN - AX[1])/RN)                                     ;   2060
         IF FC1 < 0.0 THEN FC1 ← 0.00000001                          ;   2070
         FC2 ← ARCTAN(((1.0 -(FC1*2))*0.5)/FC1)                      ;   2080
         FC3 ←  ((AX[1] - RN)/RN)                                    ;   2090
         IF FC3> 1.0 THEN FC3 ← 1.0                                  ;   2100
         FC4 ← ARCTAN(((1.0 - (FC3*2))*0.5)/FC3)                     ;   2110
         FC5 ← ARCTAN(FC3/((FIN - (FC3*2))*0.5))                     ;   2120
         IF X[1,N] < RN THEN                                             2130
         AU2 ← ((2.0×G×RN×FC2) + (3.1416×(RN*2)) -(((RN*2)×FC2) -        2140
         ((RN - AX[1])×(((2.0×RN×AX[1]) - (AX[1]*2))*0.5))))         ;   2150
         POS ← (AX[1] - RN)                                          ;   2160
         IF POS > RN THEN POS ← RN                                   ;   2170
         IF (X[1,N] ≥RN) AND (X[1,N] < (RN×2.0)) THEN                    2180
         AU2 ← (G×RN×((2.0×PI)-(2.0×FC4)))+(PI×(RN*2)/2.0)-(((AX[1]-RN)  2190
         ×(((RN*2) - ((    POS    )*2))*0.5)) + ((RN*2)×FC5))       ;   2200
         IF X[1,N] ≥(RN×2.0) THEN AU2 ← (2.0×3.1416×RN×G)            ;   2210
         IF X[5,N] = 0.0 THEN VS ← 0.0 ELSE                              2220
         VS ← X[5,N] × A2                                            ;   2230
         VT ← V1 + VS                                                ;   2240
         DX[2] ← ((KA×RA×TA)/VT)×(((AX[2] + PA )/PB)*KF1)×(C1/TF)×       2250
         ((((CD1×AU1×(P1 + PA))×(((AX[2] + PA)/(P1 + PA))*KF2)×          2260
         ((1.0 - (((AX[2] + PA)/(P1 + PA))*KF1))*0.5)) -                 2270
         (((CD2×AU2×(AX[2] + PA))×((PB/(AX[2] + PA))*KF2) ×              2280
         ((1.0 - ((PB/(AX[2] + PA))*KF1))*0.5)))                     ;   2290
         DX[3] ← AX[4]                                               ;   2300
         S1 ← ((R×L1)/(2.0×DE×C))×((0.5 + (VS/(A1×L1)))*0.5)         ;   2310
         WN1 ← C/((L1)×((0.5+(VS/(A1×L1)))*0.5))                     ;   2320
         DX[4] ← -(2.0×S1×WN1×AX[4])-((WN1*2)×(AX[3]))+((WN1*2)×AX[12]);  2330
         DX[5] ← AX[6]                                               ;   2340
         IF AX[7] ≥108.0  THEN AX[7] ←107.995                        ;   2350
         DX[6] ← -(B1/M1)×(AX[6])-(K1/M1)×(AX[5])+(A2/M1)×(AX[3])    ;   2360
         IF AX[5] ≥ 0.01042 THEN AX[5] ← 0.01041                     ;   2370
         IF X[5,N] ≤ 0.00521 THEN GO TO EQ1                          ;   2380
         VP ← X[10,N] × A3                                           ;   2390
         VF ← V2 + VP                                                ;   2400
         S2 ← ((R×L2)/(2.0×DE×C))×((0.5 + (VP/(A1×L2)))*0.5)         ;   2410
         WN2 ← C/((L2)×((0.5+(VP/(A1×L2)))*0.5))                     ;   2420
         IF (X[5,N]>0.00521) AND (X[5,N]≤0.00782)THEN GO TO EQ2      ;   2430
         IF X[5,N] > 0.00782 THEN GO TO EQ3                          ;   2440
EQ1:     X[7,N] ← 0.0                                                ;   2450
         X[8,N] ← 0.0                                                ;   2460
         X[10,N] ← 0.0                                               ;   2470
         GO TO RUN                                                   ;   2480
```

```
EQ2:    DX[7] ← (RA×IA/VF)×(CD3)×((RO*2)×(ARCTAN((RO×((1.0-(((RO-          2490
        (AX[5]-0.00521))/RO)*2))*0.5))/(RO-(AX[5]-0.00521))))              2500
        - ((RO-(AX[5] -0.00521))×((((2.0×RO)×(AX[5] -0.00521)) -           2510
        ((AX[5] -0.00521)*2))*0.5)))×(((C1×(P3+  PA ))/(TA*0.5))×          2520
        (((AX[7] + PA)/(P3 +PA))*(1.0/KA))×((1.0-(((AX[7] + PA)            2530
        /(P3+  PA ))*((KA-1.0)/KA)))*0.5))                                 ;  2540
        DX[8] ← AX[9]                                                      ;  2550
        DX[9] ← -(2.0×S2×WN2×AX[9])-((WN2*2)×(AX[8]))+((WN2*2)×AX[13]);    2560
        DX[10] ← AX[11]                                                    ;  2570
        DX[11] ← -(B2/M2) × (AX[11])-(K2/M2)×(AX[10])+(A3/M2)×(AX[8]) ;    2580
        GO TO RUN                                                          ;  2590
EQ3:    DX[7] ← (RA×IA/VF)×(CD3)×((PI×(RO*2)/2.0)+(AX[5]-0.00782)          2600
        ×(((RO*2)-((AX[5] -0.00782)*2))*0.5)+(RO*2)×(ARCTAN((AX[5] -       2610
        0.00782)/(RO×((1.0-(((AX[5] -0.00782)/RO)*2))*0.5)))))×            2620
        ((((C1×(P3 + PA ))/(TA*0.5)) ×  (((X[7,H2]+ PA )/(P3 + PA)) *      2630
        (1.0/KA))×((1.0-(((X[7,H2]+PA)/(P3+PA))*((KA-1.0)/KA)))*0.5)) ;    2640
        DX[8] ← AX[9]                                                      ;  2650
        DX[9] ← -(2.0×S2×WN2×AX[9])-((WN2*2)×(AX[8]))+((WN2*2)×AX[13]);    2660
        DX[10] ← AX[11]                                                    ;  2670
        DX[11] ← -(B2/M2) × (AX[11])-(K2/M2)×(AX[10])+(A3/M2)×(AX[8]) ;    2680
RUN:    FOR I ← 1 STEP 1 UNTIL M DO                                        2690
        K[I,L] ← DT×DX[I]                                                  ;  2700
END                                                                        ;  2710
        FOR I ← 1 STEP 1 UNTIL M DO                                        2720
        X[I,N+1] ← X[I,N]+(K[I,1]+2×(K[I,2]+K[I,3])+K[I,4])/6              ;  2730
        N ← N + 1                                                          ;  2740
        TI ← N × DT                                                        ;  2750
        IF X[5,N] > 0.01041 THEN X[5,N] ← 0.0104175                        ;  2760
        IF X[7,N] ≥ 108.0  THEN X[7,N] ← 107.995                           ;  2770
        WRITE (LINES,FL6,N,TI,X[1,N],X[2,N],X[3,N],X[5,N],X[7,N],          2780
        X[8,N],X[10,N])                                                    ;  2790
        IF N > 598 THEN GO TO FINIS                                        ;  2800
        IF X[10,N] > 0.0078 THEN GO TO FINIS                               ;  2810
        GO TO CALL                                                         ;  2820
FINIS:  END.                                                               2830
```

TB = 0.000 DT = 0.0002 M = 11

INITIAL CONDITIONS

0.0000
6.0000
6.0000
0.0000
0.0000
0.0000
0.0000
0.0000
0.0000
0.0000
0.0000

N	TIME	X(1,N) X	X(2,N) PJ	X(3,N) P2	X(5,N) Z	X(7,N) P4	X(8,N) P5	X(10,N) Y
1	0.0002	1.3888E-05	9.9863E+00	6.0000E+00	0.0000E+00	0.0000E+00	0.0000E+00	0.0000E+00
2	0.0004	2.7776E-05	9.9866E+00	6.0000E+00	0.0000E+00	0.0000E+00	0.0000E+00	0.0000E+00
3	0.0006	4.1664E-05	9.9872E+00	6.0000E+00	0.0000E+00	0.0000E+00	0.0000E+00	0.0000E+00
4	0.0008	5.5552E-05	9.9879E+00	6.0000E+00	0.0000E+00	0.0000E+00	0.0000E+00	0.0000E+00
5	0.0010	6.9440E-05	9.9886E+00	6.0000E+00	0.0000E+00	0.0000E+00	0.0000E+00	0.0000E+00
6	0.0012	8.3328E-05	9.9894E+00	6.0000E+00	0.0000E+00	0.0000E+00	0.0000E+00	0.0000E+00
7	0.0014	9.7216E-05	9.9902E+00	6.0000E+00	0.0000E+00	0.0000E+00	0.0000E+00	0.0000E+00
8	0.0016	1.1110E-04	9.9911E+00	6.0000E+00	0.0000E+00	0.0000E+00	0.0000E+00	0.0000E+00
9	0.0018	1.2499E-04	9.9920E+00	6.0000E+00	0.0000E+00	0.0000E+00	0.0000E+00	0.0000E+00
10	0.0020	1.3888E-04	9.9929E+00	6.0000E+00	0.0000E+00	0.0000E+00	0.0000E+00	0.0000E+00
11	0.0022	1.5277E-04	9.9939E+00	6.0000E+00	0.0000E+00	0.0000E+00	0.0000E+00	0.0000E+00
12	0.0024	1.6666E-04	9.9949E+00	6.0000E+00	0.0000E+00	0.0000E+00	0.0000E+00	0.0000E+00
13	0.0026	1.8054E-04	9.9959E+00	6.0000E+00	0.0000E+00	0.0000E+00	0.0000E+00	0.0000E+00
14	0.0028	1.9443E-04	9.9969E+00	6.0000E+00	0.0000E+00	0.0000E+00	0.0000E+00	0.0000E+00
15	0.0030	2.0832E-04	9.9979E+00	6.0000E+00	0.0000E+00	0.0000E+00	0.0000E+00	0.0000E+00
16	0.0032	2.2221E-04	9.9991E+00	6.0000E+00	0.0000E+00	0.0000E+00	0.0000E+00	0.0000E+00
17	0.0034	2.3610E-04	9.9999E+00	6.0000E+00	0.0000E+00	0.0000E+00	0.0000E+00	0.0000E+00
18	0.0036	2.4998E-04	9.0009E+00	6.0000E+00	0.0000E+00	0.0000E+00	0.0000E+00	0.0000E+00
19	0.0038	2.6387E-04	9.0021E+00	6.0000E+00	0.0000E+00	0.0000E+00	0.0000E+00	0.0000E+00
20	0.0040	2.7776E-04	9.0033E+00	6.0000E+00	0.0000E+00	0.0000E+00	0.0000E+00	0.0000E+00
21	0.0042	2.9165E-04	9.0045E+00	6.0000E+00	0.0000E+00	0.0000E+00	0.0000E+00	0.0000E+00
22	0.0044	3.0554E-04	9.0058E+00	6.0000E+00	0.0000E+00	0.0000E+00	0.0000E+00	0.0000E+00
23	0.0046	3.1942E-04	9.0069E+00	6.0000E+00	0.0000E+00	0.0000E+00	0.0000E+00	0.0000E+00
24	0.0048	3.3331E-04	9.0083E+00	6.0000E+00	0.0000E+00	0.0000E+00	0.0000E+00	0.0000E+00
25	0.0050	3.4720E-04	9.0097E+00	6.0000E+00	0.0000E+00	0.0000E+00	0.0000E+00	0.0000E+00
26	0.0052	3.6109E-04	9.0107E+00	6.0000E+00	0.0000E+00	0.0000E+00	0.0000E+00	0.0000E+00
27	0.0054	3.7498E-04	9.0121E+00	6.0000E+00	0.0000E+00	0.0000E+00	0.0000E+00	0.0000E+00
28	0.0056	3.8886E-04	9.0137E+00	6.0000E+00	0.0000E+00	0.0000E+00	0.0000E+00	0.0000E+00
29	0.0058	4.0275E-04	9.0149E+00	6.0000E+00	0.0000E+00	0.0000E+00	0.0000E+00	0.0000E+00
30	0.0060	4.1664E-04	9.0161E+00	6.0000E+00	0.0000E+00	0.0000E+00	0.0000E+00	0.0000E+00
31	0.0062	4.3053E-04	9.0176E+00	6.0000E+00	0.0000E+00	0.0000E+00	0.0000E+00	0.0000E+00
32	0.0064	4.4442E-04	9.0192E+00	6.0000E+00	0.0000E+00	0.0000E+00	0.0000E+00	0.0000E+00
33	0.0066	4.5830E-04	9.0208E+00	6.0000E+00	0.0000E+00	0.0000E+00	0.0000E+00	0.0000E+00
34	0.0068	4.7219E-04	9.0221E+00	6.0000E+00	0.0000E+00	0.0000E+00	0.0000E+00	0.0000E+00
35	0.0070	4.8608E-04	9.0235E+00	6.0000E+00	0.0000E+00	0.0000E+00	0.0000E+00	0.0000E+00
36	0.0072	4.9997E-04	9.0174E+00	6.0000E+00	0.0000E+00	0.0000E+00	0.0000E+00	0.0000E+00
37	0.0074	5.1386E-04	9.6295E+00	6.0000E+00	0.0000E+00	0.0000E+00	0.0000E+00	0.0000E+00
38	0.0076	5.2774E-04	9.6420E+00	6.0000E+00	0.0000E+00	0.0000E+00	0.0000E+00	0.0000E+00
39	0.0078	5.4163E-04	9.6548E+00	6.0000E+00	0.0000E+00	0.0000E+00	0.0000E+00	0.0000E+00
40	0.0080	5.5552E-04	9.6680E+00	6.0000E+00	0.0000E+00	0.0000E+00	0.0000E+00	0.0000E+00
41	0.0082	5.6941E-04	9.6815E+00	6.0000E+00	0.0000E+00	0.0000E+00	0.0000E+00	0.0000E+00
42	0.0084	5.8330E-04	9.6954E+00	6.0000E+00	0.0000E+00	0.0000E+00	0.0000E+00	0.0000E+00
43	0.0086	5.9718E-04	9.7096E+00	6.0000E+00	0.0000E+00	0.0000E+00	0.0000E+00	0.0000E+00
44	0.0088	6.1107E-04	9.7241E+00	6.0000E+00	0.0000E+00	0.0000E+00	0.0000E+00	0.0000E+00
45	0.0090	6.2496E-04	9.7390E+00	6.0000E+00	0.0000E+00	0.0000E+00	0.0000E+00	0.0000E+00
46	0.0092	6.3885E-04	9.7542E+00	6.0000E+00	0.0000E+00	0.0000E+00	0.0000E+00	0.0000E+00
47	0.0094	6.5274E-04	9.7698E+00	6.0000E+00	0.0000E+00	0.0000E+00	0.0000E+00	0.0000E+00
48	0.0096	6.6662E-04	9.7858E+00	6.0000E+00	0.0000E+00	0.0000E+00	0.0000E+00	0.0000E+00
49	0.0098	6.8051E-04	9.8020E+00	6.0000E+00	0.0000E+00	0.0000E+00	0.0000E+00	0.0000E+00
50	0.0100	6.9440E-04	9.8187E+00	6.0000E+00	0.0000E+00	0.0000E+00	0.0000E+00	0.0000E+00
51	0.0102	7.0829E-04	9.8357E+00	6.0000E+00	0.0000E+00	0.0000E+00	0.0000E+00	0.0000E+00
52	0.0104	7.2218E-04	9.8530E+00	6.0000E+00	0.0000E+00	0.0000E+00	0.0000E+00	0.0000E+00
53	0.0106	7.3606E-04	9.8707E+00	6.0000E+00	0.0000E+00	0.0000E+00	0.0000E+00	0.0000E+00
54	0.0108	7.4995E-04	9.8887E+00	6.0000E+00	0.0000E+00	0.0000E+00	0.0000E+00	0.0000E+00
55	0.0110	7.6384E-04	9.9071E+00	6.0002E+00	1.5448E-07	0.0000E+00	0.0000E+00	0.0000E+00
56	0.0112	7.7773E-04	9.9258E+00	6.0012E+00	6.1731E-07	0.0000E+00	0.0000E+00	0.0000E+00
57	0.0114	7.9162E-04	9.9449E+00	6.0032E+00	1.3883E-06	0.0000E+00	0.0000E+00	0.0000E+00
58	0.0116	8.0550E-04	9.9643E+00	6.0064E+00	2.4668E-06	0.0000E+00	0.0000E+00	0.0000E+00
59	0.0118	8.1939E-04	9.9841E+00	6.0108E+00	3.8529E-06	0.0000E+00	0.0000E+00	0.0000E+00
60	0.0120	8.3328E-04	1.0009E+01	6.0165E+00	5.5431E-06	0.0000E+00	0.0000E+00	0.0000E+00
61	0.0122	8.4717E-04	1.0025E+01	6.0242E+00	7.5393E-06	0.0000E+00	0.0000E+00	0.0000E+00
62	0.0124	8.6106E-04	1.0046E+01	6.0331E+00	9.8396E-06	0.0000E+00	0.0000E+00	0.0000E+00
63	0.0126	8.7496E-04	1.0067E+01	6.0435E+00	1.2443E-05	0.0000E+00	0.0000E+00	0.0000E+00
64	0.0128	8.8883E-04	1.0088E+01	6.0553E+00	1.5348E-05	0.0000E+00	0.0000E+00	0.0000E+00
65	0.0130	9.0272E-04	1.0110E+01	6.0687E+00	1.8554E-05	0.0000E+00	0.0000E+00	0.0000E+00
66	0.0132	9.1661E-04	1.0133E+01	6.0836E+00	2.2059E-05	0.0000E+00	0.0000E+00	0.0000E+00
67	0.0134	9.3050E-04	1.0159E+01	6.0999E+00	2.5862E-05	0.0000E+00	0.0000E+00	0.0000E+00
68	0.0136	9.4438E-04	1.0179E+01	6.1171E+00	2.9962E-05	0.0000E+00	0.0000E+00	0.0000E+00
69	0.0138	9.5827E-04	1.0202E+01	6.1350E+00	3.4358E-05	0.0000E+00	0.0000E+00	0.0000E+00
70	0.0140	9.7216E-04	1.0226E+01	6.1536E+00	3.9048E-05	0.0000E+00	0.0000E+00	0.0000E+00
71	0.0142	9.8605E-04	1.0250E+01	6.1732E+00	4.4032E-05	0.0000E+00	0.0000E+00	0.0000E+00
72	0.0144	9.9994E-04	1.0275E+01	6.1936E+00	4.9291E-05	0.0000E+00	0.0000E+00	0.0000E+00
73	0.0146	1.0138E-03	1.0300E+01	6.2232E+00	5.4847E-05	0.0000E+00	0.0000E+00	0.0000E+00
74	0.0148	1.0277E-03	1.0325E+01	6.2477E+00	6.0659E-05	0.0000E+00	0.0000E+00	0.0000E+00
75	0.0150	1.0416E-03	1.0351E+01	6.2731E+00	6.6814E-05	0.0000E+00	0.0000E+00	0.0000E+00
76	0.0152	1.0555E-03	1.0377E+01	6.2998E+00	7.3220E-05	0.0000E+00	0.0000E+00	0.0000E+00
77	0.0154	1.0694E-03	1.0404E+01	6.3273E+00	7.9905E-05	0.0000E+00	0.0000E+00	0.0000E+00
78	0.0156	1.0833E-03	1.0431E+01	6.3554E+00	8.6868E-05	0.0000E+00	0.0000E+00	0.0000E+00
79	0.0158	1.0972E-03	1.0458E+01	6.3842E+00	9.4101E-05	0.0000E+00	0.0000E+00	0.0000E+00
80	0.0160	1.1110E-03	1.0486E+01	6.4136E+00	1.0161E-04	0.0000E+00	0.0000E+00	0.0000E+00
81	0.0162	1.1249E-03	1.0514E+01	6.4452E+00	1.0938E-04	0.0000E+00	0.0000E+00	0.0000E+00
82	0.0164	1.1388E-03	1.0543E+01	6.4765E+00	1.1742E-04	0.0000E+00	0.0000E+00	0.0000E+00
83	0.0166	1.1527E-03	1.0572E+01	6.5088E+00	1.2573E-04	0.0000E+00	0.0000E+00	0.0000E+00
84	0.0168	1.1666E-03	1.0602E+01	6.5410E+00	1.3429E-04	0.0000E+00	0.0000E+00	0.0000E+00
85	0.0170	1.1805E-03	1.0632E+01	6.5741E+00	1.4311E-04	0.0000E+00	0.0000E+00	0.0000E+00
86	0.0172	1.1944E-03	1.0662E+01	6.6078E+00	1.5218E-04	0.0000E+00	0.0000E+00	0.0000E+00
87	0.0174	1.2083E-03	1.0693E+01	6.6419E+00	1.6150E-04	0.0000E+00	0.0000E+00	0.0000E+00
88	0.0176	1.2221E-03	1.0724E+01	6.6765E+00	1.7107E-04	0.0000E+00	0.0000E+00	0.0000E+00
89	0.0178	1.2360E-03	1.0755E+01	6.7119E+00	1.8088E-04	0.0000E+00	0.0000E+00	0.0000E+00
90	0.0180	1.2499E-03	1.0786E+01	6.7478E+00	1.9093E-04	0.0000E+00	0.0000E+00	0.0000E+00
91	0.0182	1.2638E-03	1.0818E+01	6.7844E+00	2.0121E-04	0.0000E+00	0.0000E+00	0.0000E+00
92	0.0184	1.2777E-03	1.0850E+01	6.8216E+00	2.1173E-04	0.0000E+00	0.0000E+00	0.0000E+00
93	0.0186	1.2916E-03	1.0883E+01	6.8594E+00	2.2247E-04	0.0000E+00	0.0000E+00	0.0000E+00
94	0.0188	1.3055E-03	1.0916E+01	6.8977E+00	2.3343E-04	0.0000E+00	0.0000E+00	0.0000E+00
95	0.0190	1.3194E-03	1.0949E+01	6.9367E+00	2.4462E-04	0.0000E+00	0.0000E+00	0.0000E+00
96	0.0192	1.3332E-03	1.0982E+01	6.9765E+00	2.5602E-04	0.0000E+00	0.0000E+00	0.0000E+00
97	0.0194	1.3471E-03	1.1016E+01	7.0169E+00	2.6763E-04	0.0000E+00	0.0000E+00	0.0000E+00
98	0.0196	1.3610E-03	1.1050E+01	7.0581E+00	2.7944E-04	0.0000E+00	0.0000E+00	0.0000E+00
99	0.0198	1.3749E-03	1.1101E+01	7.0709E+00	2.9145E-04	0.0000E+00	0.0000E+00	0.0000E+00
100	0.0200	1.3888E-03	1.1138E+01	7.1174E+00	3.0367E-04	0.0000E+00	0.0000E+00	0.0000E+00
101	0.0202	1.4027E-03	1.1176E+01	7.1555E+00	3.1607E-04	0.0000E+00	0.0000E+00	0.0000E+00
102	0.0204	1.4166E-03	1.1214E+01	7.1937E+00	3.2868E-04	0.0000E+00	0.0000E+00	0.0000E+00
103	0.0206	1.4305E-03	1.1253E+01	7.2320E+00	3.4149E-04	0.0000E+00	0.0000E+00	0.0000E+00
104	0.0208	1.4444E-03	1.1293E+01	7.2703E+00	3.5448E-04	0.0000E+00	0.0000E+00	0.0000E+00
105	0.0210	1.4582E-03	1.1333E+01	7.3088E+00	3.6749E-04	0.0000E+00	0.0000E+00	0.0000E+00

106	0.0212	1.4721E-03	1.1373E+01	7.3473E+00	3.4078E-04	0.0000E+00	0.0000E+00	0.0000E+00
107	0.0214	1.4860E-03	1.1414E+01	7.3858E+00	3.9422E-04	0.0000E+00	0.0000E+00	0.0000E+00
108	0.0216	1.4999E-03	1.1456E+01	7.4263E+00	4.0783E-04	0.0000E+00	0.0000E+00	0.0000E+00
109	0.0218	1.5138E-03	1.1498E+01	7.4629E+00	4.2158E-04	0.0000E+00	0.0000E+00	0.0000E+00
110	0.0220	1.5277E-03	1.1541E+01	7.5016E+00	4.3547E-04	0.0000E+00	0.0000E+00	0.0000E+00
111	0.0222	1.5416E-03	1.1585E+01	7.5389E+00	4.4950E-04	0.0000E+00	0.0000E+00	0.0000E+00
112	0.0224	1.5555E-03	1.1629E+01	7.5786E+00	4.6367E-04	0.0000E+00	0.0000E+00	0.0000E+00
113	0.0226	1.5693E-03	1.1673E+01	7.6169E+00	4.7796E-04	0.0000E+00	0.0000E+00	0.0000E+00
114	0.0228	1.5832E-03	1.1719E+01	7.6553E+00	4.9238E-04	0.0000E+00	0.0000E+00	0.0000E+00
115	0.0230	1.5971E-03	1.1765E+01	7.6936E+00	5.0691E-04	0.0000E+00	0.0000E+00	0.0000E+00
116	0.0232	1.6110E-03	1.1811E+01	7.7319E+00	5.2155E-04	0.0000E+00	0.0000E+00	0.0000E+00
117	0.0234	1.6249E-03	1.1859E+01	7.7701E+00	5.3629E-04	0.0000E+00	0.0000E+00	0.0000E+00
118	0.0236	1.6388E-03	1.1907E+01	7.8083E+00	5.5113E-04	0.0000E+00	0.0000E+00	0.0000E+00
119	0.0238	1.6527E-03	1.1955E+01	7.8463E+00	5.6606E-04	0.0000E+00	0.0000E+00	0.0000E+00
120	0.0240	1.6666E-03	1.2005E+01	7.8843E+00	5.8108E-04	0.0000E+00	0.0000E+00	0.0000E+00
121	0.0242	1.6804E-03	1.2055E+01	7.9222E+00	5.9618E-04	0.0000E+00	0.0000E+00	0.0000E+00
122	0.0244	1.6943E-03	1.2105E+01	7.9599E+00	6.1134E-04	0.0000E+00	0.0000E+00	0.0000E+00
123	0.0246	1.7082E-03	1.2157E+01	7.9976E+00	6.2658E-04	0.0000E+00	0.0000E+00	0.0000E+00
124	0.0248	1.7221E-03	1.2209E+01	8.0352E+00	6.4187E-04	0.0000E+00	0.0000E+00	0.0000E+00
125	0.0250	1.7360E-03	1.2262E+01	8.0726E+00	6.5722E-04	0.0000E+00	0.0000E+00	0.0000E+00
126	0.0252	1.7499E-03	1.2315E+01	8.1100E+00	6.7262E-04	0.0000E+00	0.0000E+00	0.0000E+00
127	0.0254	1.7638E-03	1.2370E+01	8.1472E+00	6.8806E-04	0.0000E+00	0.0000E+00	0.0000E+00
128	0.0256	1.7777E-03	1.2425E+01	8.1844E+00	7.0353E-04	0.0000E+00	0.0000E+00	0.0000E+00
129	0.0258	1.7916E-03	1.2481E+01	8.2214E+00	7.1903E-04	0.0000E+00	0.0000E+00	0.0000E+00
130	0.0260	1.8054E-03	1.2537E+01	8.2583E+00	7.3455E-04	0.0000E+00	0.0000E+00	0.0000E+00
131	0.0262	1.8193E-03	1.2595E+01	8.2951E+00	7.5008E-04	0.0000E+00	0.0000E+00	0.0000E+00
132	0.0264	1.8332E-03	1.2653E+01	8.3317E+00	7.6563E-04	0.0000E+00	0.0000E+00	0.0000E+00
133	0.0266	1.8471E-03	1.2712E+01	8.3683E+00	7.8117E-04	0.0000E+00	0.0000E+00	0.0000E+00
134	0.0268	1.8610E-03	1.2772E+01	8.4047E+00	7.9671E-04	0.0000E+00	0.0000E+00	0.0000E+00
135	0.0270	1.8749E-03	1.2833E+01	8.4410E+00	8.1224E-04	0.0000E+00	0.0000E+00	0.0000E+00
136	0.0272	1.8888E-03	1.2895E+01	8.4773E+00	8.2776E-04	0.0000E+00	0.0000E+00	0.0000E+00
137	0.0274	1.9027E-03	1.2957E+01	8.5134E+00	8.4325E-04	0.0000E+00	0.0000E+00	0.0000E+00
138	0.0276	1.9165E-03	1.3020E+01	8.5493E+00	8.5871E-04	0.0000E+00	0.0000E+00	0.0000E+00
139	0.0278	1.9304E-03	1.3085E+01	8.5852E+00	8.7413E-04	0.0000E+00	0.0000E+00	0.0000E+00
140	0.0280	1.9443E-03	1.3150E+01	8.6210E+00	8.8951E-04	0.0000E+00	0.0000E+00	0.0000E+00
141	0.0282	1.9582E-03	1.3216E+01	8.6567E+00	9.0484E-04	0.0000E+00	0.0000E+00	0.0000E+00
142	0.0284	1.9721E-03	1.3283E+01	8.6923E+00	9.2011E-04	0.0000E+00	0.0000E+00	0.0000E+00
143	0.0286	1.9860E-03	1.3351E+01	8.7278E+00	9.3532E-04	0.0000E+00	0.0000E+00	0.0000E+00
144	0.0288	1.9999E-03	1.3420E+01	8.7632E+00	9.5047E-04	0.0000E+00	0.0000E+00	0.0000E+00
145	0.0290	2.0138E-03	1.3491E+01	8.7985E+00	9.6553E-04	0.0000E+00	0.0000E+00	0.0000E+00
146	0.0292	2.0276E-03	1.3560E+01	8.8337E+00	9.8052E-04	0.0000E+00	0.0000E+00	0.0000E+00
147	0.0294	2.0415E-03	1.3632E+01	8.8689E+00	9.9542E-04	0.0000E+00	0.0000E+00	0.0000E+00
148	0.0296	2.0554E-03	1.3705E+01	8.9039E+00	1.0102E-03	0.0000E+00	0.0000E+00	0.0000E+00
149	0.0298	2.0693E-03	1.3779E+01	8.9390E+00	1.0249E-03	0.0000E+00	0.0000E+00	0.0000E+00
150	0.0300	2.0832E-03	1.3854E+01	8.9739E+00	1.0395E-03	0.0000E+00	0.0000E+00	0.0000E+00
151	0.0302	2.0971E-03	1.3930E+01	9.0088E+00	1.0540E-03	0.0000E+00	0.0000E+00	0.0000E+00
152	0.0304	2.1110E-03	1.4007E+01	9.0436E+00	1.0684E-03	0.0000E+00	0.0000E+00	0.0000E+00
153	0.0306	2.1249E-03	1.4085E+01	9.0784E+00	1.0826E-03	0.0000E+00	0.0000E+00	0.0000E+00
154	0.0308	2.1388E-03	1.4164E+01	9.1132E+00	1.0968E-03	0.0000E+00	0.0000E+00	0.0000E+00
155	0.0310	2.1526E-03	1.4245E+01	9.1479E+00	1.1107E-03	0.0000E+00	0.0000E+00	0.0000E+00
156	0.0312	2.1665E-03	1.4326E+01	9.1825E+00	1.1246E-03	0.0000E+00	0.0000E+00	0.0000E+00
157	0.0314	2.1804E-03	1.4407E+01	9.2172E+00	1.1383E-03	0.0000E+00	0.0000E+00	0.0000E+00
158	0.0316	2.1943E-03	1.4491E+01	9.2518E+00	1.1518E-03	0.0000E+00	0.0000E+00	0.0000E+00
159	0.0318	2.2082E-03	1.4576E+01	9.2865E+00	1.1652E-03	0.0000E+00	0.0000E+00	0.0000E+00
160	0.0320	2.2221E-03	1.4662E+01	9.3211E+00	1.1785E-03	0.0000E+00	0.0000E+00	0.0000E+00
161	0.0322	2.2360E-03	1.4750E+01	9.3557E+00	1.1915E-03	0.0000E+00	0.0000E+00	0.0000E+00
162	0.0324	2.2498E-03	1.4839E+01	9.3903E+00	1.2044E-03	0.0000E+00	0.0000E+00	0.0000E+00
163	0.0326	2.2637E-03	1.4928E+01	9.4250E+00	1.2171E-03	0.0000E+00	0.0000E+00	0.0000E+00
164	0.0328	2.2776E-03	1.5020E+01	9.4597E+00	1.2297E-03	0.0000E+00	0.0000E+00	0.0000E+00
165	0.0330	2.2915E-03	1.5112E+01	9.4944E+00	1.2420E-03	0.0000E+00	0.0000E+00	0.0000E+00
166	0.0332	2.3054E-03	1.5206E+01	9.5291E+00	1.2541E-03	0.0000E+00	0.0000E+00	0.0000E+00
167	0.0334	2.3193E-03	1.5301E+01	9.5639E+00	1.2661E-03	0.0000E+00	0.0000E+00	0.0000E+00
168	0.0336	2.3332E-03	1.5397E+01	9.5987E+00	1.2779E-03	0.0000E+00	0.0000E+00	0.0000E+00
169	0.0338	2.3471E-03	1.5495E+01	9.6336E+00	1.2896E-03	0.0000E+00	0.0000E+00	0.0000E+00
170	0.0340	2.3610E-03	1.5594E+01	9.6686E+00	1.3007E-03	0.0000E+00	0.0000E+00	0.0000E+00
171	0.0342	2.3748E-03	1.5695E+01	9.7036E+00	1.3119E-03	0.0000E+00	0.0000E+00	0.0000E+00
172	0.0344	2.3887E-03	1.5797E+01	9.7388E+00	1.3228E-03	0.0000E+00	0.0000E+00	0.0000E+00
173	0.0346	2.4026E-03	1.5900E+01	9.7740E+00	1.3335E-03	0.0000E+00	0.0000E+00	0.0000E+00
174	0.0348	2.4165E-03	1.6005E+01	9.8093E+00	1.3439E-03	0.0000E+00	0.0000E+00	0.0000E+00
175	0.0350	2.4304E-03	1.6111E+01	9.8447E+00	1.3542E-03	0.0000E+00	0.0000E+00	0.0000E+00
176	0.0352	2.4443E-03	1.6219E+01	9.8801E+00	1.3642E-03	0.0000E+00	0.0000E+00	0.0000E+00
177	0.0354	2.4582E-03	1.6328E+01	9.9156E+00	1.3739E-03	0.0000E+00	0.0000E+00	0.0000E+00
178	0.0356	2.4721E-03	1.6439E+01	9.9512E+00	1.3835E-03	0.0000E+00	0.0000E+00	0.0000E+00
179	0.0358	2.4860E-03	1.6551E+01	9.9877E+00	1.3928E-03	0.0000E+00	0.0000E+00	0.0000E+00
180	0.0360	2.4998E-03	1.6665E+01	1.0024E+01	1.4018E-03	0.0000E+00	0.0000E+00	0.0000E+00
181	0.0362	2.5137E-03	1.6781E+01	1.0060E+01	1.4106E-03	0.0000E+00	0.0000E+00	0.0000E+00
182	0.0364	2.5276E-03	1.6898E+01	1.0096E+01	1.4191E-03	0.0000E+00	0.0000E+00	0.0000E+00
183	0.0366	2.5415E-03	1.7016E+01	1.0133E+01	1.4274E-03	0.0000E+00	0.0000E+00	0.0000E+00
184	0.0368	2.5554E-03	1.7137E+01	1.0170E+01	1.4355E-03	0.0000E+00	0.0000E+00	0.0000E+00
185	0.0370	2.5693E-03	1.7259E+01	1.0207E+01	1.4432E-03	0.0000E+00	0.0000E+00	0.0000E+00
186	0.0372	2.5832E-03	1.7383E+01	1.0244E+01	1.4508E-03	0.0000E+00	0.0000E+00	0.0000E+00
187	0.0374	2.5971E-03	1.7508E+01	1.0281E+01	1.4580E-03	0.0000E+00	0.0000E+00	0.0000E+00
188	0.0376	2.6109E-03	1.7636E+01	1.0319E+01	1.4650E-03	0.0000E+00	0.0000E+00	0.0000E+00
189	0.0378	2.6248E-03	1.7765E+01	1.0357E+01	1.4718E-03	0.0000E+00	0.0000E+00	0.0000E+00
190	0.0380	2.6387E-03	1.7895E+01	1.0395E+01	1.4782E-03	0.0000E+00	0.0000E+00	0.0000E+00
191	0.0382	2.6526E-03	1.8028E+01	1.0433E+01	1.4844E-03	0.0000E+00	0.0000E+00	0.0000E+00
192	0.0384	2.6665E-03	1.8163E+01	1.0472E+01	1.4904E-03	0.0000E+00	0.0000E+00	0.0000E+00
193	0.0386	2.6804E-03	1.8299E+01	1.0511E+01	1.4960E-03	0.0000E+00	0.0000E+00	0.0000E+00
194	0.0388	2.6943E-03	1.8437E+01	1.0550E+01	1.5014E-03	0.0000E+00	0.0000E+00	0.0000E+00
195	0.0390	2.7082E-03	1.8577E+01	1.0589E+01	1.5065E-03	0.0000E+00	0.0000E+00	0.0000E+00
196	0.0392	2.7220E-03	1.8719E+01	1.0629E+01	1.5114E-03	0.0000E+00	0.0000E+00	0.0000E+00
197	0.0394	2.7359E-03	1.8863E+01	1.0669E+01	1.5160E-03	0.0000E+00	0.0000E+00	0.0000E+00
198	0.0396	2.7498E-03	1.9009E+01	1.0709E+01	1.5203E-03	0.0000E+00	0.0000E+00	0.0000E+00
199	0.0398	2.7637E-03	1.9157E+01	1.0750E+01	1.5243E-03	0.0000E+00	0.0000E+00	0.0000E+00
200	0.0400	2.7776E-03	1.9307E+01	1.0791E+01	1.5281E-03	0.0000E+00	0.0000E+00	0.0000E+00
201	0.0402	2.7915E-03	1.9459E+01	1.0832E+01	1.5316E-03	0.0000E+00	0.0000E+00	0.0000E+00
202	0.0404	2.8054E-03	1.9613E+01	1.0874E+01	1.5348E-03	0.0000E+00	0.0000E+00	0.0000E+00
203	0.0406	2.8193E-03	1.9769E+01	1.0916E+01	1.5378E-03	0.0000E+00	0.0000E+00	0.0000E+00
204	0.0408	2.8332E-03	1.9928E+01	1.0958E+01	1.5404E-03	0.0000E+00	0.0000E+00	0.0000E+00
205	0.0410	2.8470E-03	2.0088E+01	1.1001E+01	1.5429E-03	0.0000E+00	0.0000E+00	0.0000E+00
206	0.0412	2.8609E-03	2.0251E+01	1.1044E+01	1.5450E-03	0.0000E+00	0.0000E+00	0.0000E+00
207	0.0414	2.8748E-03	2.0415E+01	1.1088E+01	1.5469E-03	0.0000E+00	0.0000E+00	0.0000E+00
208	0.0416	2.8887E-03	2.0582E+01	1.1132E+01	1.5485E-03	0.0000E+00	0.0000E+00	0.0000E+00
209	0.0418	2.9026E-03	2.0752E+01	1.1176E+01	1.5499E-03	0.0000E+00	0.0000E+00	0.0000E+00
210	0.0420	2.9165E-03	2.0923E+01	1.1221E+01	1.5510E-03	0.0000E+00	0.0000E+00	0.0000E+00
211	0.0422	2.9304E-03	2.1097E+01	1.1266E+01	1.5518E-03	0.0000E+00	0.0000E+00	0.0000E+00
212	0.0424	2.9443E-03	2.1273E+01	1.1312E+01	1.5524E-03	0.0000E+00	0.0000E+00	0.0000E+00
213	0.0426	2.9581E-03	2.1451E+01	1.1358E+01	1.5527E-03	0.0000E+00	0.0000E+00	0.0000E+00
214	0.0428	2.9720E-03	2.1632E+01	1.1405E+01	1.5528E-03	0.0000E+00	0.0000E+00	0.0000E+00
215	0.0430	2.9859E-03	2.1815E+01	1.1452E+01	1.5526E-03	0.0000E+00	0.0000E+00	0.0000E+00
216	0.0432	2.9998E-03	2.2001E+01	1.1500E+01	1.5522E-03	0.0000E+00	0.0000E+00	0.0000E+00
217	0.0434	3.0137E-03	2.2189E+01	1.1548E+01	1.5515E-03	0.0000E+00	0.0000E+00	0.0000E+00
218	0.0436	3.0276E-03	2.2379E+01	1.1597E+01	1.5506E-03	0.0000E+00	0.0000E+00	0.0000E+00
219	0.0438	3.0415E-03	2.2572E+01	1.1646E+01	1.5495E-03	0.0000E+00	0.0000E+00	0.0000E+00
220	0.0440	3.0554E-03	2.2767E+01	1.1696E+01	1.5481E-03	0.0000E+00	0.0000E+00	0.0000E+00
221	0.0442	3.0692E-03	2.2965E+01	1.1746E+01	1.5465E-03	0.0000E+00	0.0000E+00	0.0000E+00
222	0.0444	3.0831E-03	2.3165E+01	1.1797E+01	1.5447E-03	0.0000E+00	0.0000E+00	0.0000E+00
223	0.0446	3.0970E-03	2.3368E+01	1.1848E+01	1.5426E-03	0.0000E+00	0.0000E+00	0.0000E+00
224	0.0448	3.1109E-03	2.3574E+01	1.1900E+01	1.5404E-03	0.0000E+00	0.0000E+00	0.0000E+00
225	0.0450	3.1248E-03	2.3782E+01	1.1953E+01	1.5379E-03	0.0000E+00	0.0000E+00	0.0000E+00
226	0.0452	3.1387E-03	2.3992E+01	1.2006E+01	1.5352E-03	0.0000E+00	0.0000E+00	0.0000E+00
227	0.0454	3.1526E-03	2.4206E+01	1.2060E+01	1.5323E-03	0.0000E+00	0.0000E+00	0.0000E+00
228	0.0456	3.1665E-03	2.4422E+01	1.2115E+01	1.5292E-03	0.0000E+00	0.0000E+00	0.0000E+00
229	0.0458	3.1804E-03	2.4640E+01	1.2170E+01	1.5258E-03	0.0000E+00	0.0000E+00	0.0000E+00
230	0.0460	3.1942E-03	2.4862E+01	1.2226E+01	1.5223E-03	0.0000E+00	0.0000E+00	0.0000E+00
231	0.0462	3.2081E-03	2.5085E+01	1.2282E+01	1.5187E-03	0.0000E+00	0.0000E+00	0.0000E+00
232	0.0464	3.2220E-03	2.5312E+01	1.2339E+01	1.5148E-03	0.0000E+00	0.0000E+00	0.0000E+00
233	0.0466	3.2359E-03	2.5542E+01	1.2397E+01	1.5108E-03	0.0000E+00	0.0000E+00	0.0000E+00

234	0.0466	3.2498E-03	2.5774E+01	1.2456E+01	1.5065E-03	0.0000E+00	0.0000E+00	0.0000E+00
235	0.0470	3.2637E-03	2.6009E+01	1.2515E+01	1.5022E-03	0.0000E+00	0.0000E+00	0.0000E+00
236	0.0472	3.2776E-03	2.6247E+01	1.2575E+01	1.4978E-03	0.0000E+00	0.0000E+00	0.0000E+00
237	0.0474	3.2915E-03	2.6487E+01	1.2636E+01	1.4934E-03	0.0000E+00	0.0000E+00	0.0000E+00
238	0.0476	3.3053E-03	2.6730E+01	1.2697E+01	1.4891E-03	0.0000E+00	0.0000E+00	0.0000E+00
239	0.0478	3.3192E-03	2.6976E+01	1.2759E+01	1.4847E-03	0.0000E+00	0.0000E+00	0.0000E+00
240	0.0480	3.3331E-03	2.7225E+01	1.2822E+01	1.4804E-03	0.0000E+00	0.0000E+00	0.0000E+00
241	0.0482	3.3470E-03	2.7477E+01	1.2886E+01	1.4727E-03	0.0000E+00	0.0000E+00	0.0000E+00
242	0.0484	3.3609E-03	2.7732E+01	1.2951E+01	1.4673E-03	0.0000E+00	0.0000E+00	0.0000E+00
243	0.0486	3.3748E-03	2.7989E+01	1.3016E+01	1.4618E-03	0.0000E+00	0.0000E+00	0.0000E+00
244	0.0488	3.3887E-03	2.8249E+01	1.3083E+01	1.4562E-03	0.0000E+00	0.0000E+00	0.0000E+00
245	0.0490	3.4026E-03	2.8512E+01	1.3150E+01	1.4505E-03	0.0000E+00	0.0000E+00	0.0000E+00
246	0.0492	3.4164E-03	2.8778E+01	1.3218E+01	1.4446E-03	0.0000E+00	0.0000E+00	0.0000E+00
247	0.0494	3.4303E-03	2.9047E+01	1.3287E+01	1.4387E-03	0.0000E+00	0.0000E+00	0.0000E+00
248	0.0496	3.4442E-03	2.9319E+01	1.3356E+01	1.4327E-03	0.0000E+00	0.0000E+00	0.0000E+00
249	0.0498	3.4581E-03	2.9593E+01	1.3427E+01	1.4267E-03	0.0000E+00	0.0000E+00	0.0000E+00
250	0.0500	3.4720E-03	2.9871E+01	1.3499E+01	1.4205E-03	0.0000E+00	0.0000E+00	0.0000E+00
251	0.0502	3.4859E-03	3.0151E+01	1.3571E+01	1.4143E-03	0.0000E+00	0.0000E+00	0.0000E+00
252	0.0504	3.4998E-03	3.0434E+01	1.3645E+01	1.4080E-03	0.0000E+00	0.0000E+00	0.0000E+00
253	0.0506	3.5137E-03	3.0720E+01	1.3719E+01	1.4017E-03	0.0000E+00	0.0000E+00	0.0000E+00
254	0.0508	3.5276E-03	3.1008E+01	1.3795E+01	1.3953E-03	0.0000E+00	0.0000E+00	0.0000E+00
255	0.0510	3.5414E-03	3.1300E+01	1.3871E+01	1.3889E-03	0.0000E+00	0.0000E+00	0.0000E+00
256	0.0512	3.5553E-03	3.1594E+01	1.3948E+01	1.3825E-03	0.0000E+00	0.0000E+00	0.0000E+00
257	0.0514	3.5692E-03	3.1891E+01	1.4027E+01	1.3761E-03	0.0000E+00	0.0000E+00	0.0000E+00
258	0.0516	3.5831E-03	3.2191E+01	1.4106E+01	1.3696E-03	0.0000E+00	0.0000E+00	0.0000E+00
259	0.0518	3.5970E-03	3.2493E+01	1.4187E+01	1.3631E-03	0.0000E+00	0.0000E+00	0.0000E+00
260	0.0520	3.6109E-03	3.2798E+01	1.4268E+01	1.3567E-03	0.0000E+00	0.0000E+00	0.0000E+00
261	0.0522	3.6248E-03	3.3106E+01	1.4351E+01	1.3502E-03	0.0000E+00	0.0000E+00	0.0000E+00
262	0.0524	3.6387E-03	3.3416E+01	1.4435E+01	1.3438E-03	0.0000E+00	0.0000E+00	0.0000E+00
263	0.0526	3.6525E-03	3.3729E+01	1.4519E+01	1.3374E-03	0.0000E+00	0.0000E+00	0.0000E+00
264	0.0528	3.6664E-03	3.4045E+01	1.4605E+01	1.3310E-03	0.0000E+00	0.0000E+00	0.0000E+00
265	0.0530	3.6803E-03	3.4363E+01	1.4691E+01	1.3247E-03	0.0000E+00	0.0000E+00	0.0000E+00
266	0.0532	3.6942E-03	3.4684E+01	1.4778E+01	1.3184E-03	0.0000E+00	0.0000E+00	0.0000E+00
267	0.0534	3.7081E-03	3.5007E+01	1.4870E+01	1.3121E-03	0.0000E+00	0.0000E+00	0.0000E+00
268	0.0536	3.7220E-03	3.5332E+01	1.4961E+01	1.3060E-03	0.0000E+00	0.0000E+00	0.0000E+00
269	0.0538	3.7359E-03	3.5660E+01	1.5053E+01	1.2999E-03	0.0000E+00	0.0000E+00	0.0000E+00
270	0.0540	3.7498E-03	3.5990E+01	1.5146E+01	1.2939E-03	0.0000E+00	0.0000E+00	0.0000E+00
271	0.0542	3.7636E-03	3.6322E+01	1.5240E+01	1.2879E-03	0.0000E+00	0.0000E+00	0.0000E+00
272	0.0544	3.7775E-03	3.6658E+01	1.5334E+01	1.2821E-03	0.0000E+00	0.0000E+00	0.0000E+00
273	0.0546	3.7914E-03	3.6995E+01	1.5431E+01	1.2764E-03	0.0000E+00	0.0000E+00	0.0000E+00
274	0.0548	3.8053E-03	3.7335E+01	1.5531E+01	1.2708E-03	0.0000E+00	0.0000E+00	0.0000E+00
275	0.0550	3.8192E-03	3.7677E+01	1.5630E+01	1.2653E-03	0.0000E+00	0.0000E+00	0.0000E+00
276	0.0552	3.8331E-03	3.8024E+01	1.5731E+01	1.2599E-03	0.0000E+00	0.0000E+00	0.0000E+00
277	0.0554	3.8470E-03	3.8373E+01	1.5833E+01	1.2547E-03	0.0000E+00	0.0000E+00	0.0000E+00
278	0.0556	3.8609E-03	3.8725E+01	1.5937E+01	1.2496E-03	0.0000E+00	0.0000E+00	0.0000E+00
279	0.0558	3.8748E-03	3.9080E+01	1.6041E+01	1.2447E-03	0.0000E+00	0.0000E+00	0.0000E+00
280	0.0560	3.8886E-03	3.9438E+01	1.6148E+01	1.2399E-03	0.0000E+00	0.0000E+00	0.0000E+00
281	0.0562	3.9025E-03	3.9798E+01	1.6255E+01	1.2353E-03	0.0000E+00	0.0000E+00	0.0000E+00
282	0.0564	3.9164E-03	4.0161E+01	1.6363E+01	1.2308E-03	0.0000E+00	0.0000E+00	0.0000E+00
283	0.0566	3.9303E-03	4.0528E+01	1.6475E+01	1.2266E-03	0.0000E+00	0.0000E+00	0.0000E+00
284	0.0568	3.9442E-03	4.0898E+01	1.6587E+01	1.2225E-03	0.0000E+00	0.0000E+00	0.0000E+00
285	0.0570	3.9581E-03	4.1272E+01	1.6701E+01	1.2187E-03	0.0000E+00	0.0000E+00	0.0000E+00
286	0.0572	3.9720E-03	4.1651E+01	1.6816E+01	1.2150E-03	0.0000E+00	0.0000E+00	0.0000E+00
287	0.0574	3.9859E-03	4.2033E+01	1.6932E+01	1.2115E-03	0.0000E+00	0.0000E+00	0.0000E+00
288	0.0576	3.9997E-03	4.2421E+01	1.7050E+01	1.2084E-03	0.0000E+00	0.0000E+00	0.0000E+00
289	0.0578	4.0136E-03	4.2812E+01	1.7170E+01	1.2054E-03	0.0000E+00	0.0000E+00	0.0000E+00
290	0.0580	4.0275E-03	4.3208E+01	1.7291E+01	1.2027E-03	0.0000E+00	0.0000E+00	0.0000E+00
291	0.0582	4.0414E-03	4.3608E+01	1.7414E+01	1.2001E-03	0.0000E+00	0.0000E+00	0.0000E+00
292	0.0584	4.0553E-03	4.4013E+01	1.7538E+01	1.1979E-03	0.0000E+00	0.0000E+00	0.0000E+00
293	0.0586	4.0692E-03	4.4423E+01	1.7665E+01	1.1959E-03	0.0000E+00	0.0000E+00	0.0000E+00
294	0.0588	4.0831E-03	4.4838E+01	1.7792E+01	1.1942E-03	0.0000E+00	0.0000E+00	0.0000E+00
295	0.0590	4.0970E-03	4.5258E+01	1.7922E+01	1.1927E-03	0.0000E+00	0.0000E+00	0.0000E+00
296	0.0592	4.1108E-03	4.5682E+01	1.8053E+01	1.1916E-03	0.0000E+00	0.0000E+00	0.0000E+00
297	0.0594	4.1247E-03	4.6113E+01	1.8186E+01	1.1907E-03	0.0000E+00	0.0000E+00	0.0000E+00
298	0.0596	4.1386E-03	4.6549E+01	1.8320E+01	1.1901E-03	0.0000E+00	0.0000E+00	0.0000E+00
299	0.0598	4.1525E-03	4.6991E+01	1.8456E+01	1.1898E-03	0.0000E+00	0.0000E+00	0.0000E+00
300	0.0600	4.1664E-03	4.7438E+01	1.8594E+01	1.1899E-03	0.0000E+00	0.0000E+00	0.0000E+00
301	0.0602	4.1803E-03	4.7892E+01	1.8734E+01	1.1902E-03	0.0000E+00	0.0000E+00	0.0000E+00
302	0.0604	4.1942E-03	4.8352E+01	1.8876E+01	1.1909E-03	0.0000E+00	0.0000E+00	0.0000E+00
303	0.0606	4.2081E-03	4.8818E+01	1.9019E+01	1.1919E-03	0.0000E+00	0.0000E+00	0.0000E+00
304	0.0608	4.2220E-03	4.9290E+01	1.9164E+01	1.1932E-03	0.0000E+00	0.0000E+00	0.0000E+00
305	0.0610	4.2358E-03	4.9768E+01	1.9311E+01	1.1949E-03	0.0000E+00	0.0000E+00	0.0000E+00
306	0.0612	4.2497E-03	5.0252E+01	1.9460E+01	1.1969E-03	0.0000E+00	0.0000E+00	0.0000E+00
307	0.0614	4.2636E-03	5.0743E+01	1.9611E+01	1.1993E-03	0.0000E+00	0.0000E+00	0.0000E+00
308	0.0616	4.2775E-03	5.1240E+01	1.9764E+01	1.2020E-03	0.0000E+00	0.0000E+00	0.0000E+00
309	0.0618	4.2914E-03	5.1744E+01	1.9919E+01	1.2051E-03	0.0000E+00	0.0000E+00	0.0000E+00
310	0.0620	4.3053E-03	5.2255E+01	2.0075E+01	1.2086E-03	0.0000E+00	0.0000E+00	0.0000E+00
311	0.0622	4.3192E-03	5.2773E+01	2.0233E+01	1.2125E-03	0.0000E+00	0.0000E+00	0.0000E+00
312	0.0624	4.3331E-03	5.3299E+01	2.0394E+01	1.2167E-03	0.0000E+00	0.0000E+00	0.0000E+00
313	0.0626	4.3469E-03	5.3832E+01	2.0556E+01	1.2213E-03	0.0000E+00	0.0000E+00	0.0000E+00
314	0.0628	4.3608E-03	5.4374E+01	2.0721E+01	1.2264E-03	0.0000E+00	0.0000E+00	0.0000E+00
315	0.0630	4.3747E-03	5.4925E+01	2.0887E+01	1.2318E-03	0.0000E+00	0.0000E+00	0.0000E+00
316	0.0632	4.3886E-03	5.5485E+01	2.1055E+01	1.2376E-03	0.0000E+00	0.0000E+00	0.0000E+00
317	0.0634	4.4025E-03	5.6055E+01	2.1225E+01	1.2439E-03	0.0000E+00	0.0000E+00	0.0000E+00
318	0.0636	4.4164E-03	5.6634E+01	2.1397E+01	1.2506E-03	0.0000E+00	0.0000E+00	0.0000E+00
319	0.0638	4.4303E-03	5.7224E+01	2.1571E+01	1.2576E-03	0.0000E+00	0.0000E+00	0.0000E+00
320	0.0640	4.4442E-03	5.7824E+01	2.1748E+01	1.2652E-03	0.0000E+00	0.0000E+00	0.0000E+00
321	0.0642	4.4580E-03	5.8435E+01	2.1926E+01	1.2731E-03	0.0000E+00	0.0000E+00	0.0000E+00
322	0.0644	4.4719E-03	5.9057E+01	2.2108E+01	1.2815E-03	0.0000E+00	0.0000E+00	0.0000E+00
323	0.0646	4.4858E-03	5.9690E+01	2.2291E+01	1.2903E-03	0.0000E+00	0.0000E+00	0.0000E+00
324	0.0648	4.4997E-03	6.0337E+01	2.2476E+01	1.2996E-03	0.0000E+00	0.0000E+00	0.0000E+00
325	0.0650	4.5136E-03	6.0996E+01	2.2664E+01	1.3093E-03	0.0000E+00	0.0000E+00	0.0000E+00
326	0.0652	4.5275E-03	6.1668E+01	2.2853E+01	1.3194E-03	0.0000E+00	0.0000E+00	0.0000E+00
327	0.0654	4.5414E-03	6.2352E+01	2.3044E+01	1.3301E-03	0.0000E+00	0.0000E+00	0.0000E+00
328	0.0656	4.5553E-03	6.3049E+01	2.3237E+01	1.3411E-03	0.0000E+00	0.0000E+00	0.0000E+00
329	0.0658	4.5692E-03	6.3761E+01	2.3431E+01	1.3527E-03	0.0000E+00	0.0000E+00	0.0000E+00
330	0.0660	4.5830E-03	6.4486E+01	2.3627E+01	1.3647E-03	0.0000E+00	0.0000E+00	0.0000E+00
331	0.0662	4.5969E-03	6.5226E+01	2.3825E+01	1.3772E-03	0.0000E+00	0.0000E+00	0.0000E+00
332	0.0664	4.6108E-03	6.5981E+01	2.4026E+01	1.3901E-03	0.0000E+00	0.0000E+00	0.0000E+00
333	0.0666	4.6247E-03	6.6752E+01	2.4229E+01	1.4036E-03	0.0000E+00	0.0000E+00	0.0000E+00
334	0.0668	4.6386E-03	6.7539E+01	2.4434E+01	1.4175E-03	0.0000E+00	0.0000E+00	0.0000E+00
335	0.0670	4.6525E-03	6.8343E+01	2.4641E+01	1.4319E-03	0.0000E+00	0.0000E+00	0.0000E+00
336	0.0672	4.6664E-03	6.9164E+01	2.4850E+01	1.4467E-03	0.0000E+00	0.0000E+00	0.0000E+00
337	0.0674	4.6803E-03	7.0003E+01	2.5062E+01	1.4621E-03	0.0000E+00	0.0000E+00	0.0000E+00
338	0.0676	4.6941E-03	7.0860E+01	2.5276E+01	1.4780E-03	0.0000E+00	0.0000E+00	0.0000E+00
339	0.0678	4.7080E-03	7.1736E+01	2.5491E+01	1.4943E-03	0.0000E+00	0.0000E+00	0.0000E+00
340	0.0680	4.7219E-03	7.2631E+01	2.5710E+01	1.5111E-03	0.0000E+00	0.0000E+00	0.0000E+00
341	0.0682	4.7358E-03	7.3545E+01	2.5931E+01	1.5285E-03	0.0000E+00	0.0000E+00	0.0000E+00
342	0.0684	4.7497E-03	7.4479E+01	2.6154E+01	1.5463E-03	0.0000E+00	0.0000E+00	0.0000E+00
343	0.0686	4.7636E-03	7.5434E+01	2.6379E+01	1.5646E-03	0.0000E+00	0.0000E+00	0.0000E+00
344	0.0688	4.7775E-03	7.6410E+01	2.6606E+01	1.5834E-03	0.0000E+00	0.0000E+00	0.0000E+00
345	0.0690	4.7914E-03	7.7408E+01	2.6835E+01	1.6028E-03	0.0000E+00	0.0000E+00	0.0000E+00
346	0.0692	4.8052E-03	7.8429E+01	2.7066E+01	1.6226E-03	0.0000E+00	0.0000E+00	0.0000E+00
347	0.0694	4.8191E-03	7.9473E+01	2.7300E+01	1.6429E-03	0.0000E+00	0.0000E+00	0.0000E+00
348	0.0696	4.8330E-03	8.0541E+01	2.7537E+01	1.6638E-03	0.0000E+00	0.0000E+00	0.0000E+00
349	0.0698	4.8469E-03	8.1634E+01	2.7776E+01	1.6851E-03	0.0000E+00	0.0000E+00	0.0000E+00
350	0.0700	4.8608E-03	8.2752E+01	2.8017E+01	1.7069E-03	0.0000E+00	0.0000E+00	0.0000E+00
351	0.0702	4.8747E-03	8.3896E+01	2.8260E+01	1.7293E-03	0.0000E+00	0.0000E+00	0.0000E+00
352	0.0704	4.8886E-03	8.5066E+01	2.8506E+01	1.7521E-03	0.0000E+00	0.0000E+00	0.0000E+00
353	0.0706	4.9025E-03	8.6263E+01	2.8754E+01	1.7755E-03	0.0000E+00	0.0000E+00	0.0000E+00
354	0.0708	4.9164E-03	8.7487E+01	2.9004E+01	1.7994E-03	0.0000E+00	0.0000E+00	0.0000E+00
355	0.0710	4.9302E-03	8.8740E+01	2.9256E+01	1.8239E-03	0.0000E+00	0.0000E+00	0.0000E+00
356	0.0712	4.9441E-03	9.0021E+01	2.9511E+01	1.8488E-03	0.0000E+00	0.0000E+00	0.0000E+00
357	0.0714	4.9580E-03	9.1332E+01	2.9768E+01	1.8743E-03	0.0000E+00	0.0000E+00	0.0000E+00
358	0.0716	4.9719E-03	9.2673E+01	3.0028E+01	1.9003E-03	0.0000E+00	0.0000E+00	0.0000E+00
359	0.0718	4.9858E-03	9.4045E+01	3.0291E+01	1.9268E-03	0.0000E+00	0.0000E+00	0.0000E+00
360	0.0720	4.9997E-03	9.5447E+01	3.0556E+01	1.9537E-03	0.0000E+00	0.0000E+00	0.0000E+00
361	0.0722	5.0136E-03	9.6880E+01	3.0824E+01	1.9812E-03	0.0000E+00	0.0000E+00	0.0000E+00

362	0.0724	5.0275E+03	5.6545E+01	3.1116E+01	2.0083E+03	0.0000E+00	0.0000E+00	0.0000E+00
363	0.0726	5.0413E+03	5.6630E+01	3.1405E+01	2.0367E+03	0.0000E+00	0.0000E+00	0.0000E+00
364	0.0728	5.0552E+03	5.6714E+01	3.1675E+01	2.0656E+03	0.0000E+00	0.0000E+00	0.0000E+00
365	0.0730	5.0691E+03	5.6797E+01	3.1947E+01	2.0949E+03	0.0000E+00	0.0000E+00	0.0000E+00
366	0.0732	5.0830E+03	5.6878E+01	3.2220E+01	2.1247E+03	0.0000E+00	0.0000E+00	0.0000E+00
367	0.0734	5.0969E+03	5.6958E+01	3.2495E+01	2.1551E+03	0.0000E+00	0.0000E+00	0.0000E+00
368	0.0736	5.1108E+03	5.7037E+01	3.2771E+01	2.1859E+03	0.0000E+00	0.0000E+00	0.0000E+00
369	0.0738	5.1247E+03	5.7114E+01	3.3048E+01	2.2171E+03	0.0000E+00	0.0000E+00	0.0000E+00
370	0.0740	5.1386E+03	5.7190E+01	3.3326E+01	2.2489E+03	0.0000E+00	0.0000E+00	0.0000E+00
371	0.0742	5.1524E+03	5.7265E+01	3.3605E+01	2.2812E+03	0.0000E+00	0.0000E+00	0.0000E+00
372	0.0744	5.1663E+03	5.7339E+01	3.3885E+01	2.3139E+03	0.0000E+00	0.0000E+00	0.0000E+00
373	0.0746	5.1802E+03	5.7412E+01	3.4166E+01	2.3470E+03	0.0000E+00	0.0000E+00	0.0000E+00
374	0.0748	5.1941E+03	5.7484E+01	3.4447E+01	2.3807E+03	0.0000E+00	0.0000E+00	0.0000E+00
375	0.0750	5.2080E+03	5.7554E+01	3.4729E+01	2.4148E+03	0.0000E+00	0.0000E+00	0.0000E+00
376	0.0752	5.2219E+03	5.7624E+01	3.5011E+01	2.4493E+03	0.0000E+00	0.0000E+00	0.0000E+00
377	0.0754	5.2358E+03	5.7692E+01	3.5293E+01	2.4843E+03	0.0000E+00	0.0000E+00	0.0000E+00
378	0.0756	5.2497E+03	5.7759E+01	3.5576E+01	2.5198E+03	0.0000E+00	0.0000E+00	0.0000E+00
379	0.0758	5.2636E+03	5.7826E+01	3.5859E+01	2.5557E+03	0.0000E+00	0.0000E+00	0.0000E+00
380	0.0760	5.2774E+03	5.7891E+01	3.6142E+01	2.5920E+03	0.0000E+00	0.0000E+00	0.0000E+00
381	0.0762	5.2913E+03	5.7955E+01	3.6425E+01	2.6288E+03	0.0000E+00	0.0000E+00	0.0000E+00
382	0.0764	5.3052E+03	5.8018E+01	3.6707E+01	2.6660E+03	0.0000E+00	0.0000E+00	0.0000E+00
383	0.0766	5.3191E+03	5.8081E+01	3.6990E+01	2.7036E+03	0.0000E+00	0.0000E+00	0.0000E+00
384	0.0768	5.3330E+03	5.8142E+01	3.7272E+01	2.7416E+03	0.0000E+00	0.0000E+00	0.0000E+00
385	0.0770	5.3469E+03	5.8202E+01	3.7554E+01	2.7800E+03	0.0000E+00	0.0000E+00	0.0000E+00
386	0.0772	5.3608E+03	5.8262E+01	3.7835E+01	2.8188E+03	0.0000E+00	0.0000E+00	0.0000E+00
387	0.0774	5.3747E+03	5.8320E+01	3.8115E+01	2.8580E+03	0.0000E+00	0.0000E+00	0.0000E+00
388	0.0776	5.3885E+03	5.8378E+01	3.8395E+01	2.8976E+03	0.0000E+00	0.0000E+00	0.0000E+00
389	0.0778	5.4024E+03	5.8434E+01	3.8674E+01	2.9376E+03	0.0000E+00	0.0000E+00	0.0000E+00
390	0.0780	5.4163E+03	5.8490E+01	3.8953E+01	2.9780E+03	0.0000E+00	0.0000E+00	0.0000E+00
391	0.0782	5.4302E+03	5.8545E+01	3.9230E+01	3.0187E+03	0.0000E+00	0.0000E+00	0.0000E+00
392	0.0784	5.4441E+03	5.8599E+01	3.9507E+01	3.0598E+03	0.0000E+00	0.0000E+00	0.0000E+00
393	0.0786	5.4580E+03	5.8652E+01	3.9782E+01	3.1012E+03	0.0000E+00	0.0000E+00	0.0000E+00
394	0.0788	5.4719E+03	5.8705E+01	4.0057E+01	3.1429E+03	0.0000E+00	0.0000E+00	0.0000E+00
395	0.0790	5.4858E+03	5.8756E+01	4.0330E+01	3.1850E+03	0.0000E+00	0.0000E+00	0.0000E+00
396	0.0792	5.4996E+03	5.8807E+01	4.0602E+01	3.2274E+03	0.0000E+00	0.0000E+00	0.0000E+00
397	0.0794	5.5135E+03	5.8857E+01	4.0873E+01	3.2702E+03	0.0000E+00	0.0000E+00	0.0000E+00
398	0.0796	5.5274E+03	5.8906E+01	4.1143E+01	3.3132E+03	0.0000E+00	0.0000E+00	0.0000E+00
399	0.0798	5.5413E+03	5.8955E+01	4.1411E+01	3.3565E+03	0.0000E+00	0.0000E+00	0.0000E+00
400	0.0800	5.5552E+03	5.9003E+01	4.1678E+01	3.4001E+03	0.0000E+00	0.0000E+00	0.0000E+00
401	0.0802	5.5691E+03	5.9050E+01	4.1943E+01	3.4440E+03	0.0000E+00	0.0000E+00	0.0000E+00
402	0.0804	5.5830E+03	5.9096E+01	4.2207E+01	3.4881E+03	0.0000E+00	0.0000E+00	0.0000E+00
403	0.0806	5.5969E+03	5.9142E+01	4.2469E+01	3.5325E+03	0.0000E+00	0.0000E+00	0.0000E+00
404	0.0808	5.6108E+03	5.9186E+01	4.2729E+01	3.5771E+03	0.0000E+00	0.0000E+00	0.0000E+00
405	0.0810	5.6246E+03	5.9231E+01	4.2988E+01	3.6220E+03	0.0000E+00	0.0000E+00	0.0000E+00
406	0.0812	5.6385E+03	5.9274E+01	4.3246E+01	3.6671E+03	0.0000E+00	0.0000E+00	0.0000E+00
407	0.0814	5.6524E+03	5.9317E+01	4.3501E+01	3.7124E+03	0.0000E+00	0.0000E+00	0.0000E+00
408	0.0816	5.6663E+03	5.9359E+01	4.3755E+01	3.7578E+03	0.0000E+00	0.0000E+00	0.0000E+00
409	0.0818	5.6802E+03	5.9401E+01	4.4006E+01	3.8035E+03	0.0000E+00	0.0000E+00	0.0000E+00
410	0.0820	5.6941E+03	5.9442E+01	4.4254E+01	3.8494E+03	0.0000E+00	0.0000E+00	0.0000E+00
411	0.0822	5.7080E+03	5.9482E+01	4.4500E+01	3.8954E+03	0.0000E+00	0.0000E+00	0.0000E+00
412	0.0824	5.7219E+03	5.9522E+01	4.4743E+01	3.9415E+03	0.0000E+00	0.0000E+00	0.0000E+00
413	0.0826	5.7357E+03	5.9561E+01	4.4985E+01	3.9878E+03	0.0000E+00	0.0000E+00	0.0000E+00
414	0.0828	5.7496E+03	5.9599E+01	4.5227E+01	4.0343E+03	0.0000E+00	0.0000E+00	0.0000E+00
415	0.0830	5.7635E+03	5.9637E+01	4.5467E+01	4.0808E+03	0.0000E+00	0.0000E+00	0.0000E+00
416	0.0832	5.7774E+03	5.9674E+01	4.5705E+01	4.1274E+03	0.0000E+00	0.0000E+00	0.0000E+00
417	0.0834	5.7913E+03	5.9711E+01	4.5941E+01	4.1742E+03	0.0000E+00	0.0000E+00	0.0000E+00
418	0.0836	5.8052E+03	5.9747E+01	4.6175E+01	4.2210E+03	0.0000E+00	0.0000E+00	0.0000E+00
419	0.0838	5.8191E+03	5.9783E+01	4.6407E+01	4.2678E+03	0.0000E+00	0.0000E+00	0.0000E+00
420	0.0840	5.8330E+03	5.9818E+01	4.6637E+01	4.3147E+03	0.0000E+00	0.0000E+00	0.0000E+00
421	0.0842	5.8468E+03	5.9852E+01	4.6867E+01	4.3617E+03	0.0000E+00	0.0000E+00	0.0000E+00
422	0.0844	5.8607E+03	5.9886E+01	4.7095E+01	4.4088E+03	0.0000E+00	0.0000E+00	0.0000E+00
423	0.0846	5.8746E+03	5.9920E+01	4.7323E+01	4.4558E+03	0.0000E+00	0.0000E+00	0.0000E+00
424	0.0848	5.8885E+03	5.9953E+01	4.7549E+01	4.5029E+03	0.0000E+00	0.0000E+00	0.0000E+00
425	0.0850	5.9024E+03	5.9985E+01	4.7774E+01	4.5499E+03	0.0000E+00	0.0000E+00	0.0000E+00
426	0.0852	5.9163E+03	6.0017E+01	4.7998E+01	4.5968E+03	0.0000E+00	0.0000E+00	0.0000E+00
427	0.0854	5.9302E+03	6.0048E+01	4.8220E+01	4.6432E+03	0.0000E+00	0.0000E+00	0.0000E+00
428	0.0856	5.9441E+03	6.0079E+01	4.8440E+01	4.6900E+03	0.0000E+00	0.0000E+00	0.0000E+00
429	0.0858	5.9580E+03	6.0110E+01	4.8659E+01	4.7367E+03	0.0000E+00	0.0000E+00	0.0000E+00
430	0.0860	5.9718E+03	6.0140E+01	4.8876E+01	4.7833E+03	0.0000E+00	0.0000E+00	0.0000E+00
431	0.0862	5.9857E+03	6.0169E+01	4.9092E+01	4.8298E+03	0.0000E+00	0.0000E+00	0.0000E+00
432	0.0864	5.9996E+03	6.0199E+01	4.9307E+01	4.8762E+03	0.0000E+00	0.0000E+00	0.0000E+00
433	0.0866	6.0135E+03	6.0227E+01	4.9520E+01	4.9225E+03	0.0000E+00	0.0000E+00	0.0000E+00
434	0.0868	6.0274E+03	6.0256E+01	4.9732E+01	4.9686E+03	0.0000E+00	0.0000E+00	0.0000E+00
435	0.0870	6.0413E+03	6.0283E+01	4.9942E+01	5.0145E+03	0.0000E+00	0.0000E+00	0.0000E+00
436	0.0872	6.0552E+03	6.0311E+01	5.0151E+01	5.0603E+03	0.0000E+00	0.0000E+00	0.0000E+00
437	0.0874	6.0691E+03	6.0338E+01	5.0359E+01	5.1059E+03	0.0000E+00	0.0000E+00	0.0000E+00
438	0.0876	6.0829E+03	6.0364E+01	5.0565E+01	5.1512E+03	0.0000E+00	0.0000E+00	0.0000E+00
439	0.0878	6.0968E+03	6.0390E+01	5.0770E+01	5.1964E+03	0.0000E+00	0.0000E+00	0.0000E+00
440	0.0880	6.1107E+03	6.0416E+01	5.0974E+01	5.2413E+03	0.0000E+00	0.0000E+00	0.0000E+00
441	0.0882	6.1246E+03	6.0442E+01	5.1176E+01	5.2859E+03	9.5211E-12	0.0000E+00	0.0000E+00
442	0.0884	6.1385E+03	6.0467E+01	5.1378E+01	5.3303E+03	8.8681E-12	0.0000E+00	0.0000E+00
443	0.0886	6.1524E+03	6.0491E+01	5.1578E+01	5.3744E+03	1.9319E-01	0.0000E+00	0.0000E+00
444	0.0888	6.1663E+03	6.0515E+01	5.1778E+01	5.4182E+03	3.5277E-01	0.0000E+00	0.0000E+00
445	0.0890	6.1802E+03	6.0539E+01	5.1976E+01	5.4617E+03	5.4977E-01	0.0000E+00	0.0000E+00
446	0.0892	6.1940E+03	6.0563E+01	5.2173E+01	5.5049E+03	8.4918E-01	0.0000E+00	0.0000E+00
447	0.0894	6.2079E+03	6.0586E+01	5.2369E+01	5.5477E+03	1.1943E+00	0.0000E+00	0.0000E+00
448	0.0896	6.2218E+03	6.0609E+01	5.2563E+01	5.5902E+03	1.5932E+00	0.0000E+00	0.0000E+00
449	0.0898	6.2357E+03	6.0631E+01	5.2756E+01	5.6324E+03	2.1759E+00	0.0000E+00	0.0000E+00
450	0.0900	6.2496E+03	6.0653E+01	5.2947E+01	5.6741E+03	2.6738E+00	0.0000E+00	0.0000E+00
451	0.0902	6.2635E+03	6.0675E+01	5.3137E+01	5.7155E+03	3.3129E+00	0.0000E+00	0.0000E+00
452	0.0904	6.2774E+03	6.0696E+01	5.3326E+01	5.7566E+03	4.0458E+00	0.0000E+00	0.0000E+00
453	0.0906	6.2913E+03	6.0717E+01	5.3513E+01	5.7970E+03	4.8539E+00	0.0000E+00	0.0000E+00
454	0.0908	6.3052E+03	6.0738E+01	5.3699E+01	5.8371E+03	5.7418E+00	0.0000E+00	0.0000E+00
455	0.0910	6.3190E+03	6.0759E+01	5.3884E+01	5.8767E+03	6.7131E+00	0.0000E+00	0.0000E+00
456	0.0912	6.3329E+03	6.0779E+01	5.4068E+01	5.9159E+03	7.7669E+00	0.0000E+00	0.0000E+00
457	0.0914	6.3468E+03	6.0799E+01	5.4251E+01	5.9546E+03	8.9039E+00	0.0000E+00	0.0000E+00
458	0.0916	6.3607E+03	6.0818E+01	5.4432E+01	5.9929E+03	1.0131E+01	0.0000E+00	0.0000E+00
459	0.0918	6.3746E+03	6.0838E+01	5.4612E+01	6.0306E+03	1.1441E+01	0.0000E+00	0.0000E+00
460	0.0920	6.3885E+03	6.0857E+01	5.4791E+01	6.0678E+03	1.2797E+01	0.0000E+00	0.0000E+00
461	0.0922	6.4024E+03	6.0875E+01	5.4969E+01	6.1046E+03	1.4256E+01	0.0000E+00	0.0000E+00
462	0.0924	6.4163E+03	6.0894E+01	5.5145E+01	6.1407E+03	1.5746E+01	0.0000E+00	0.0000E+00
463	0.0926	6.4301E+03	6.0912E+01	5.5320E+01	6.1764E+03	1.7303E+01	0.0000E+00	0.0000E+00
464	0.0928	6.4440E+03	6.0930E+01	5.5495E+01	6.2114E+03	1.9013E+01	0.0000E+00	0.0000E+00
465	0.0930	6.4579E+03	6.0947E+01	5.5668E+01	6.2459E+03	2.0822E+01	0.0000E+00	0.0000E+00
466	0.0932	6.4718E+03	6.0964E+01	5.5841E+01	6.2798E+03	2.2617E+01	0.0000E+00	0.0000E+00
467	0.0934	6.4857E+03	6.0981E+01	5.6013E+01	6.3132E+03	2.4517E+01	0.0000E+00	0.0000E+00
468	0.0936	6.4996E+03	6.0998E+01	5.6184E+01	6.3459E+03	2.6417E+01	2.4775E-05	0.0000E+00
469	0.0938	6.5135E+03	6.1015E+01	5.6353E+01	6.3780E+03	2.8452E+01	2.1150E-04	2.2959E-12
470	0.0940	6.5274E+03	6.1031E+01	5.6521E+01	6.4095E+03	3.0505E+01	6.0770E-04	1.7810E-11
471	0.0942	6.5412E+03	6.1047E+01	5.6687E+01	6.4403E+03	3.2605E+01	2.1993E-03	8.2531E-11
472	0.0944	6.5551E+03	6.1063E+01	5.6853E+01	6.4705E+03	3.4752E+01	4.9195E-03	2.7746E-10
473	0.0946	6.5690E+03	6.1078E+01	5.7018E+01	6.5001E+03	3.6948E+01	9.6498E-03	7.5949E-10
474	0.0948	6.5829E+03	6.1094E+01	5.7181E+01	6.5290E+03	3.9165E+01	1.7222E-02	1.8017E-09
475	0.0950	6.5968E+03	6.1109E+01	5.7343E+01	6.5572E+03	4.1434E+01	2.8626E-02	3.8311E-09
476	0.0952	6.6107E+03	6.1123E+01	5.7505E+01	6.5847E+03	4.3711E+01	4.5004E-02	7.5047E-09
477	0.0954	6.6246E+03	6.1138E+01	5.7664E+01	6.6116E+03	4.6022E+01	6.7450E-02	1.3762E-08
478	0.0956	6.6385E+03	6.1153E+01	5.7823E+01	6.6377E+03	4.8353E+01	9.6005E-02	2.3944E-08
479	0.0958	6.6524E+03	6.1167E+01	5.7980E+01	6.6632E+03	5.0698E+01	1.3266E-01	3.9510E-08
480	0.0960	6.6662E+03	6.1181E+01	5.8136E+01	6.6879E+03	5.3054E+01	1.8833E-01	6.3051E-08
481	0.0962	6.6801E+03	6.1195E+01	5.8291E+01	6.7119E+03	5.5418E+01	2.5186E-01	9.7145E-08
482	0.0964	6.6940E+03	6.1208E+01	5.8445E+01	6.7352E+03	5.7774E+01	3.3723E-01	1.4540E-07
483	0.0966	6.7079E+03	6.1221E+01	5.8598E+01	6.7578E+03	6.0119E+01	4.2552E-01	2.1248E-07
484	0.0968	6.7218E+03	6.1235E+01	5.8749E+01	6.7796E+03	6.2476E+01	5.3087E-01	3.0376E-07
485	0.0970	6.7357E+03	6.1248E+01	5.8899E+01	6.8007E+03	6.4807E+01	6.7558E-01	4.2556E-07
486	0.0972	6.7496E+03	6.1260E+01	5.9048E+01	6.8210E+03	6.7119E+01	8.3698E-01	5.8478E-07
487	0.0974	6.7635E+03	6.1273E+01	5.9196E+01	6.8405E+03	6.9448E+01	1.0205E+00	7.9131E-07
488	0.0976	6.7773E+03	6.1285E+01	5.9343E+01	6.8593E+03	7.1647E+01	1.2345E+00	1.0569E-06
489	0.0978	6.7912E+03	6.1297E+01	5.9488E+01	6.8773E+03	7.3803E+01	1.4796E+00	1.3878E-06

490	0.0980	6.8951E-03	6.1309E+01	5.7375E+01	5.4946E-03	7.6041E+01	1.7582E+00	1.8016E-06
491	0.0982	6.8190E-03	6.1321E+01	5.7441E+01	5.9111E-03	7.8294E+01	2.0728E+00	2.3173E-06
492	0.0984	6.8329E-03	6.1331E+01	5.7545E+01	6.2268E-03	8.0326E+01	2.4281E+00	2.9049E-06
493	0.0986	6.8468E-03	6.1344E+01	5.7620E+01	6.9617E-03	8.2171E+01	2.8203E+00	3.7115E-06
494	0.0988	6.8607E-03	6.1356E+01	5.7710E+01	6.9558E-03	8.4139E+01	3.2581E+00	4.6311E-06
495	0.0990	6.8746E-03	6.1367E+01	5.7730E+01	6.9492E-03	8.6295E+01	3.7418E+00	5.7355E-06
496	0.0992	6.8884E-03	6.1378E+01	5.7869E+01	6.9317E-03	8.8163E+01	4.2737E+00	7.0454E-06
497	0.0994	6.9023E-03	6.1388E+01	5.7936E+01	6.9135E-03	8.9946E+01	4.8562E+00	8.5917E-06
498	0.0996	6.9162E-03	6.1399E+01	5.8022E+01	7.0044E-03	9.1694E+01	5.4914E+00	1.0496E-05
499	0.0998	6.9301E-03	6.1410E+01	5.8097E+01	7.0146E-03	9.3354E+01	6.1813E+00	1.2536E-05
500	0.1000	6.9440E-03	6.1420E+01	5.8170E+01	7.0240E-03	9.4937E+01	6.9279E+00	1.4941E-05
501	0.1002	6.9579E-03	6.1430E+01	5.8262E+01	7.9325E-03	9.6414E+01	7.7331E+00	1.7819E-05
502	0.1004	6.9718E-03	6.1440E+01	5.8313E+01	7.9403E-03	9.7854E+01	8.5985E+00	2.1041E-05
503	0.1006	6.9857E-03	6.1450E+01	5.8382E+01	7.9473E-03	9.9140E+01	9.5258E+00	2.4816E-05
504	0.1008	6.9996E-03	6.1460E+01	5.8490E+01	7.0536E-03	1.0043E+02	1.0518E+01	2.9046E-05
505	0.1010	7.0134E-03	6.1469E+01	5.8517E+01	7.0588E-03	1.0159E+02	1.1578E+01	3.3808E-05
506	0.1012	7.0273E-03	6.1478E+01	5.8581E+01	7.0638E-03	1.0265E+02	1.2698E+01	3.9328E-05
507	0.1014	7.0412E-03	6.1488E+01	5.8647E+01	7.0672E-03	1.0362E+02	1.3875E+01	4.5859E-05
508	0.1016	7.0551E-03	6.1497E+01	5.8711E+01	7.0702E-03	1.0459E+02	1.5129E+01	5.2376E-05
509	0.1018	7.0690E-03	6.1506E+01	5.8771E+01	7.0724E-03	1.0559E+02	1.6448E+01	6.0043E-05
510	0.1020	7.0829E-03	6.1515E+01	5.8838E+01	7.0739E-03	1.0594E+02	1.7835E+01	6.8674E-05
511	0.1022	7.0968E-03	6.1523E+01	5.8894E+01	7.0745E-03	1.0655E+02	1.9290E+01	7.8252E-05
512	0.1024	7.1107E-03	6.1532E+01	5.8953E+01	7.0744E-03	1.0703E+02	2.0811E+01	8.8802E-05
513	0.1026	7.1246E-03	6.1540E+01	5.9010E+01	7.0735E-03	1.0749E+02	2.2399E+01	1.0069E-04
514	0.1028	7.1384E-03	6.1549E+01	5.9067E+01	7.0718E-03	1.0771E+02	2.4053E+01	1.1317E-04
515	0.1030	7.1523E-03	6.1557E+01	5.9122E+01	7.0693E-03	1.0799E+02	2.5771E+01	1.2742E-04
516	0.1032	7.1662E-03	6.1565E+01	5.9177E+01	7.0661E-03	1.0799E+02	2.7554E+01	1.4356E-04
517	0.1034	7.1801E-03	6.1573E+01	5.9230E+01	7.0622E-03	1.0800E+02	2.9398E+01	1.6059E-04
518	0.1036	7.1940E-03	6.1581E+01	5.9281E+01	7.0575E-03	1.0800E+02	3.1304E+01	1.7861E-04
519	0.1038	7.2079E-03	6.1589E+01	5.9334E+01	7.0520E-03	1.0800E+02	3.3268E+01	1.9865E-04
520	0.1040	7.2218E-03	6.1596E+01	5.9385E+01	7.0458E-03	1.0800E+02	3.5288E+01	2.2052E-04
521	0.1042	7.2356E-03	6.1604E+01	5.9435E+01	7.0389E-03	1.0800E+02	3.7363E+01	2.4433E-04
522	0.1044	7.2495E-03	6.1611E+01	5.9483E+01	7.0312E-03	1.0800E+02	3.9490E+01	2.6996E-04
523	0.1046	7.2634E-03	6.1618E+01	5.9531E+01	7.0228E-03	1.0800E+02	4.1668E+01	2.9742E-04
524	0.1048	7.2773E-03	6.1625E+01	5.9578E+01	7.0138E-03	1.0800E+02	4.3888E+01	3.2712E-04
525	0.1050	7.2912E-03	6.1633E+01	5.9626E+01	7.0040E-03	1.0800E+02	4.6153E+01	3.5935E-04
526	0.1052	7.3051E-03	6.1639E+01	5.9669E+01	6.9935E-03	1.0800E+02	4.8457E+01	3.9372E-04
527	0.1054	7.3190E-03	6.1646E+01	5.9713E+01	6.9823E-03	1.0800E+02	5.0797E+01	4.3044E-04
528	0.1056	7.3329E-03	6.1653E+01	5.9756E+01	6.9705E-03	1.0800E+02	5.3169E+01	4.6931E-04
529	0.1058	7.3468E-03	6.1660E+01	5.9798E+01	6.9580E-03	1.0800E+02	5.5570E+01	5.1034E-04
530	0.1060	7.3606E-03	6.1666E+01	5.9840E+01	6.9448E-03	1.0800E+02	5.7998E+01	5.5357E-04
531	0.1062	7.3745E-03	6.1673E+01	5.9881E+01	6.9310E-03	1.0800E+02	6.0439E+01	5.9898E-04
532	0.1064	7.3884E-03	6.1679E+01	5.9921E+01	6.9165E-03	1.0800E+02	6.2889E+01	6.4659E-04
533	0.1066	7.4023E-03	6.1685E+01	5.9960E+01	6.9014E-03	1.0800E+02	6.5338E+01	7.0870E-04
534	0.1068	7.4162E-03	6.1691E+01	5.9999E+01	6.8857E-03	1.0800E+02	6.7788E+01	7.5557E-04
535	0.1070	7.4301E-03	6.1697E+01	6.0037E+01	6.8696E-03	1.0800E+02	7.0328E+01	8.2570E-04
536	0.1072	7.4440E-03	6.1703E+01	6.0076E+01	6.8529E-03	1.0800E+02	7.2805E+01	8.8921E-04
537	0.1074	7.4579E-03	6.1709E+01	6.0110E+01	6.8351E-03	1.0800E+02	7.5254E+01	9.5617E-04
538	0.1076	7.4718E-03	6.1715E+01	6.0145E+01	6.8170E-03	1.0800E+02	7.7733E+01	1.0247E-03
539	0.1078	7.4856E-03	6.1721E+01	6.0180E+01	6.7984E-03	1.0800E+02	8.0170E+01	1.1008E-03
540	0.1080	7.4995E-03	6.1726E+01	6.0214E+01	6.7792E-03	1.0800E+02	8.2586E+01	1.1767E-03
541	0.1082	7.5134E-03	6.1732E+01	6.0248E+01	6.7595E-03	1.0800E+02	8.4976E+01	1.2614E-03
542	0.1084	7.5273E-03	6.1737E+01	6.0281E+01	6.7393E-03	1.0800E+02	8.7332E+01	1.3448E-03
543	0.1086	7.5412E-03	6.1743E+01	6.0313E+01	6.7188E-03	1.0800E+02	8.9652E+01	1.4365E-03
544	0.1088	7.5551E-03	6.1748E+01	6.0345E+01	6.6978E-03	1.0800E+02	9.1929E+01	1.5290E-03
545	0.1090	7.5690E-03	6.1753E+01	6.0376E+01	6.6757E-03	1.0800E+02	9.4159E+01	1.6264E-03
546	0.1092	7.5828E-03	6.1758E+01	6.0406E+01	6.6535E-03	1.0800E+02	9.6338E+01	1.7248E-03
547	0.1094	7.5967E-03	6.1763E+01	6.0436E+01	6.6309E-03	1.0800E+02	9.8462E+01	1.8343E-03
548	0.1096	7.6106E-03	6.1768E+01	6.0465E+01	6.6079E-03	1.0800E+02	1.0053E+02	1.9465E-03
549	0.1098	7.6245E-03	6.1773E+01	6.0494E+01	6.5844E-03	1.0800E+02	1.0253E+02	2.0589E-03
550	0.1100	7.6384E-03	6.1778E+01	6.0522E+01	6.5605E-03	1.0800E+02	1.0447E+02	2.1777E-03
551	0.1102	7.6523E-03	6.1783E+01	6.0549E+01	6.5362E-03	1.0800E+02	1.0634E+02	2.3017E-03
552	0.1104	7.6662E-03	6.1788E+01	6.0576E+01	6.5115E-03	1.0800E+02	1.0813E+02	2.4241E-03
553	0.1106	7.6801E-03	6.1792E+01	6.0602E+01	6.4865E-03	1.0800E+02	1.0986E+02	2.5539E-03
554	0.1108	7.6940E-03	6.1797E+01	6.0628E+01	6.4611E-03	1.0800E+02	1.1151E+02	2.6940E-03
555	0.1110	7.7078E-03	6.1801E+01	6.0654E+01	6.4354E-03	1.0800E+02	1.1309E+02	2.8365E-03
556	0.1112	7.7217E-03	6.1806E+01	6.0678E+01	6.4093E-03	1.0800E+02	1.1459E+02	2.9813E-03
557	0.1114	7.7356E-03	6.1810E+01	6.0703E+01	6.3830E-03	1.0800E+02	1.1601E+02	3.1305E-03
558	0.1116	7.7495E-03	6.1814E+01	6.0727E+01	6.3564E-03	1.0800E+02	1.1735E+02	3.2819E-03
559	0.1118	7.7634E-03	6.1818E+01	6.0750E+01	6.3294E-03	1.0800E+02	1.1861E+02	3.4417E-03
560	0.1120	7.7773E-03	6.1823E+01	6.0773E+01	6.3023E-03	1.0800E+02	1.1979E+02	3.6038E-03
561	0.1122	7.7912E-03	6.1827E+01	6.0795E+01	6.2749E-03	1.0800E+02	1.2089E+02	3.7698E-03
562	0.1124	7.8051E-03	6.1831E+01	6.0818E+01	6.2472E-03	1.0800E+02	1.2191E+02	3.9409E-03
563	0.1126	7.8189E-03	6.1835E+01	6.0839E+01	6.2194E-03	1.0800E+02	1.2286E+02	4.1164E-03
564	0.1128	7.8328E-03	6.1839E+01	6.0860E+01	6.1914E-03	1.0800E+02	1.2372E+02	4.2927E-03
565	0.1130	7.8467E-03	6.1842E+01	6.0881E+01	6.1632E-03	1.0800E+02	1.2451E+02	4.4750E-03
566	0.1132	7.8606E-03	6.1846E+01	6.0901E+01	6.1348E-03	1.0800E+02	1.2521E+02	4.6611E-03
567	0.1134	7.8745E-03	6.1850E+01	6.0921E+01	6.1063E-03	1.0800E+02	1.2585E+02	4.8509E-03
568	0.1136	7.8884E-03	6.1854E+01	6.0941E+01	6.0776E-03	1.0800E+02	1.2641E+02	5.0444E-03
569	0.1138	7.9023E-03	6.1857E+01	6.0960E+01	6.0489E-03	1.0800E+02	1.2689E+02	5.2415E-03
570	0.1140	7.9162E-03	6.1861E+01	6.0979E+01	6.0200E-03	1.0800E+02	1.2731E+02	5.4420E-03
571	0.1142	7.9300E-03	6.1864E+01	6.0997E+01	5.9911E-03	1.0800E+02	1.2765E+02	5.6458E-03
572	0.1144	7.9439E-03	6.1868E+01	6.1015E+01	5.9621E-03	1.0800E+02	1.2793E+02	5.8528E-03
573	0.1146	7.9578E-03	6.1871E+01	6.1033E+01	5.9331E-03	1.0800E+02	1.2814E+02	6.0629E-03
574	0.1148	7.9717E-03	6.1874E+01	6.1050E+01	5.9041E-03	1.0800E+02	1.2829E+02	6.2759E-03
575	0.1150	7.9856E-03	6.1878E+01	6.1067E+01	5.8750E-03	1.0800E+02	1.2838E+02	6.4917E-03
576	0.1152	7.9995E-03	6.1881E+01	6.1084E+01	5.8460E-03	1.0800E+02	1.2840E+02	6.7102E-03
577	0.1154	8.0134E-03	6.1884E+01	6.1100E+01	5.8169E-03	1.0800E+02	1.2837E+02	6.9312E-03
578	0.1156	8.0273E-03	6.1887E+01	6.1116E+01	5.7879E-03	1.0800E+02	1.2829E+02	7.1546E-03
579	0.1158	8.0412E-03	6.1890E+01	6.1132E+01	5.7590E-03	1.0800E+02	1.2815E+02	7.3801E-03
580	0.1160	8.0550E-03	6.1894E+01	6.1147E+01	5.7301E-03	1.0800E+02	1.2797E+02	7.6077E-03
581	0.1162	8.0689E-03	6.1897E+01	6.1163E+01	5.7014E-03	1.0800E+02	1.2774E+02	7.8372E-03

APPENDIX D

SAMPLE NOZZLE FLOW CALCULATION

Repeating the standard equation for compressible flow through a square-edged orifice (16),

$$Q = (Cd)(Y)(A_o)\sqrt{\frac{2\Delta P}{\rho}} \qquad (4.17)$$

where:

Q = flow

Cd = coefficient of discharge

Y = expansion factor

A = orifice area

ΔP = pressure drop across orifice

ρ = density

To determine a typical flow through an open sensing nozzle, values were taken as follows:

Cd = 0.67

ΔP = 5psi = 720 psf

$A_o = 2.18 \times 10^{-6}$ sq ft

ρ = 0.0955 lb/cu ft

$$Y = 0.94^{*}$$

Substituting into equation (4.17),

$$Q = (0.67)(0.94)(2.18 \times 10^{-6}) \sqrt{\frac{(2)(720)(32.2)}{0.0955}} (60)$$

$$= 0.0574 \text{ cu ft/min}$$

Converting to atmospheric pressure,

$$Q = (0.0574)\left(\frac{19.7}{14.7}\right) = 0.077 \text{ scfm}$$

Under the same conditions as calculated above, flow was measured at 0.078 scfm.

In order to meet the conditions of the project definition as given in Chapter I, 320 such nozzles would be needed, resulting in a total sensing air consumption of approximately 25 scfm.

---

*See Reference (16)

LITERATURE CITED

(1) Max M. Beasley, "Mechanical Development in Tufting Machinery," ASME Paper No. 66-TEX-2, Presented at the Textile Engineering Conference, Charlotte, N. C., April 19-20, 1966.

(2) Paul Ruttkay, "Eight Ways to Read Punched Tape," Control Engineering, March, 1961, pp. 152-153.

(3) H. P. Grant and R. E. Kronauer, "Fundamentals of Hot Wire Anemometry," Presented at the Symposium on Measurement in Unsteady Flow at the ASME Hydraulic Division Conference, Worchester, Mass., May 21-23, 1962.

(4) Norman A. Anderson, "Pneumatic Control Mechanisms," Instruments & Control Systems, February, 1963, p. 113.

(5) Allen C. Morse, Electrohydraulic Servomechanisms, McGraw-Hill Book Company, Inc., New York, N. Y., 1963, p. 30

(6) P. L. Abbey, et al., Fluid Amplifier State of the Art - Volume I, Research and Development - Fluid Amplifiers and Logic, NASA Report No. NASA-CR-101, General Electric Co., Oct., 1964.

(7) R. E. Bowles, "State of the Art of Pure Fluid Systems," Presented at the Symposium on Fluid Jet Control Devices at the Winter Annual Meeting of the ASME, New York, N. Y., November 28, 1962.

(8) Thomas G. Wetheral and Larry C. Atha, "Flueric Controls, A Description of Available Components and Current Applications," ASME Paper No. 65-WA/AUT-21, Presented at the Winter Annual Meeting, Chicago, Ill., November 7-11, 1965.

(9) H. L. Fox and O. Lew Wood, "The Development of Basic Devices and the Need for Theory," Control Engineering, September, 1964, pp. 75-81.

(10) W. A. Gray and H. Stern, "Fluid Amplifiers - Capabilities and Applications," Control Engineering, February, 1964, pp. 57-64.

(11) J. Modrey and W. C. Aubrey, Micro-Pneumatic Breadboards, Union College, Schenectady, N. Y., May, 1965.

(12) John J. Eige, "Multiple-Ball Pneumatic Amplifiers," Proceedings of the Fluid Amplification Symposium - Volume II, Diamond Ordnance Fuze Laboratories, Washington, D. C., May, 1964, pp. 273-287.

(13) John J. Blackburn, Gerhard Reethof, and J. Lowen Shearer, Fluid Power Control, The M.I.T. Press, Massachusetts Institute of Technology, 1960, pp. 215-216, 238-239, 263-268, 297-303.

(14) Albert G. Guy, Elements of Physical Metallurgy, Addison-Wesley Publishing Company, Inc., Reading, Mass., 1960, pp. 343-344.

(15) Gordon J. Van Wylen, Thermodynamics, John Wiley & Sons, Inc., New York, N. Y., 1961, pp. 189, 351.

(16) Victor L. Streeter, Fluid Mechanics, McGraw-Hill Book Company, Inc., New York, N. Y., 1958, pp. 99, 101-102, 182-182, 318-321.

(17) Reid F. Stearns, Russell R. Johnson, Robert M. Jackson, and Charles A. Larson, Flow Measurement with Orifice Meters, D. Van Nostrand Company, Inc., New York, N.Y., 1951, p. 192.

(18) C. B. Shuder and R. C. Binder, "Response of Pneumatic Transmission Lines to Step Inputs," Transactions - ASME, Series D, December, 1959, pp. 578-584.

(19) J. O. Hougen, O. R. Martin, and R. A. Walsh, "Dynamics of Pneumatic Transmission Lines," Control Engineering, September, 1963, pp. 114-117.

(20) L. Helm, "Determination of Pneumatic Capacities of Variable Volume," ACTA Technica, v 22 n 1-2, 1958, pp. 53-60.

(21) C. P. Rohman and F. C. Grogan, "On the Dynamics of Pneumatic Transmission Lines," Trans. ASME, May, 1957, pp. 853-874.

(22) Max Jakob, Heat Transfer, Volume I, John Wiley & Sons, Inc., New York, N. Y., 1949, pp. 270-283.

(23) H. Levy and E. A. Baggott, Numerical Solutions of Differential Equations, Dover Publications, Inc., New York, N. Y., 1950, pp. 96-110.

(24) Paul M. Derusso, Rob J. Roy, and Charles M. Close, State Variables for Engineers, John Wiley & Sons, Inc., New York, N. Y., 1965, pp. 313-344.

(25) R. W. Warren and S. J. Peperone, "Fluid Amplification - Basic Principles," Report No. TR-1039, Diamond Ordnance Fuze Laboratories, Washington, D. C., October, 1962, pp. 11-20.

(26) R. W. Warren, "Wall Effect and Binary Devices," Proceedings of the Fluid Amplification Symposium - Volume I, Diamond Ordnance Fuze Laboratories, Washington, D. C., October, 1962, pp. 11-20.

(27) J. N. Shinn and W. A. Boothe, "Connecting Elements into Circuits and Systems," Control Engineering, September, 1964, pp. 86-93.

(28) Silas Katz and Robert J. Dockery, "Fluid Amplification - Staging of Proportional and Bistable Fluid Amplifiers," Report No. TR-1165, Harry Diamond Laboratories, Washington, D. C., August 30, 1963.

(29) W. A. Boothe, "Performance Evaluation of a High-Pressure-Recovery Bistable Fluid Amplifier," Presented at the Symposium on Fluid Jet Control Devices at the Winter Meeting of the ASME, New York, N Y., November 28, 1962.

(30) Raymond N Auger, "Turbulence Amplifier Design and Application," Proceedings of the Fluid Amplification Symposium - Volume I, Diamond Ordnance Fuze Laboratories, Washington, D. C., October, 1962, pp. 357-366.

(31) Fluid Logic Fundamentals and the Turbulence Amplifier, by the Howie Corporation, Norristown, Pa.

(32) Ben A. Stsap, "Experimental Study of a Proportional Vortex Fluid Amplifier," Proceedings of the Fluid Amplification Symposium-Volume II, Diamond Ordnance Fuze Laboratories, Washington, D. C., May, 1964, pp. 85-108.

(33) Endre A. Mayer and Paul Maker, "Control Characteristics of Vortex Valves," Proceedings of the Fluid Amplification Symposium - Volume II, Diamond Ordnance Fuze Laboratories, Washington, D. C., May, 1964, pp. 61-83.

VITA

Stanley Frederick Petry was born in Columbus, Georgia, on June 19, 1930. In June, 1947, he graduated from Saint Bernard High School in Saint Bernard, Alabama. He entered Georgia Institute of Technology during the same month and graduated in June, 1952, receiving the degree of Bachelor of Mechanical Engineering (Co-operative Plan).

In February, 1955, following two years of service in the United States Army at Aberdeen Proving Grounds, Maryland, he was employed by E. I. duPont de Nemours and Company at Savannah River Plant in Aiken, South Carolina, where he remained until he returned to Georgia Tech in September, 1963. Awarded a National Defense Educational Act Fellowship, he completed the requirements for the Master of Science degree in March, 1965, and continued to pursue the Doctorate in the School of Mechanical Engineering.

Mr. Petry was married in 1952 to the former Witona Ann Swindle. They have a daughter, Laura Ellen, and a son, Eric Stanley.